RESEARCH REPORT

HEALTH EFFECTS INSTITUTE

Number 128
January 2005

Neurogenic Responses in Rat Lungs After Nose-Only Exposure to Diesel Exhaust

Mark L Witten, Simon S Wong, Nina N Sun, Ingegerd Keith, Chol-Bum Kweon, David E Foster, James J Schauer, and Duane L Sherrill

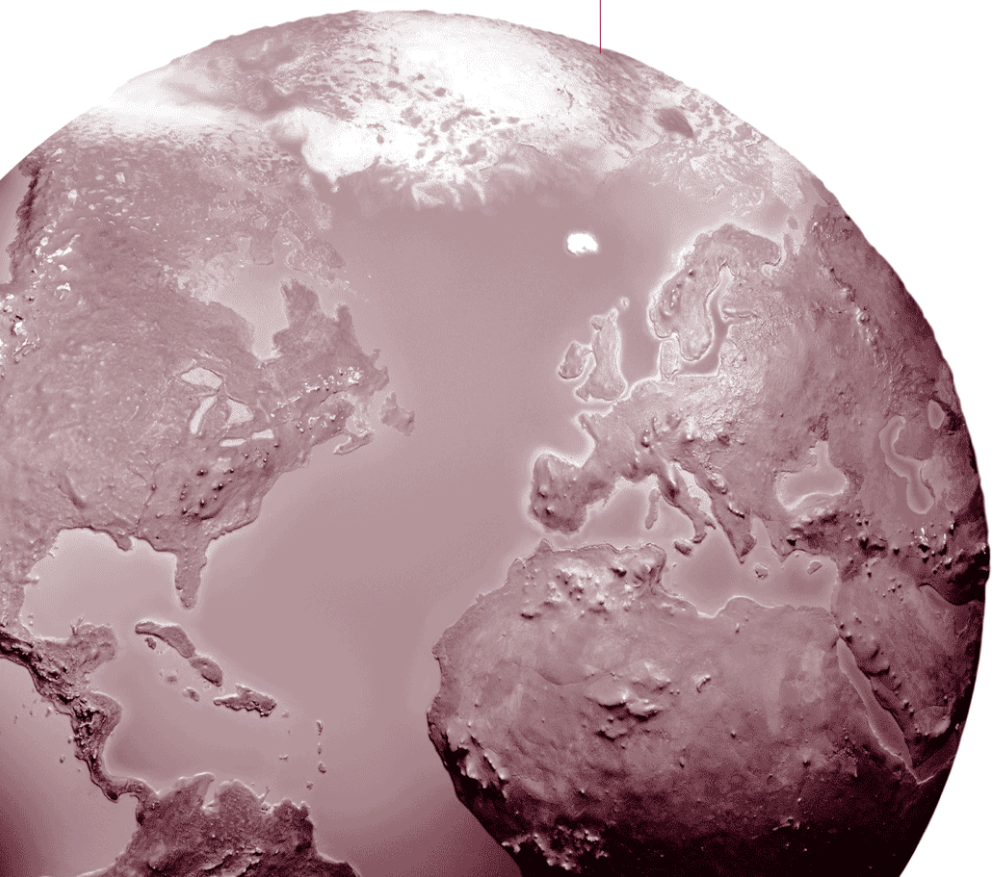

HEALTH
EFFECTS
INSTITUTE

The Health Effects Institute was chartered in 1980 as an independent and unbiased research organization to provide high quality, impartial, and relevant science on the health effects of emissions from motor vehicles, fuels, and other environmental sources. All results are provided to industry and government sponsors, other key decisionmakers, the scientific community, and the public. HEI funds research on all major pollutants, including air toxics, diesel exhaust, nitrogen oxides, ozone, and particulate matter. The Institute periodically engages in special review and evaluation of key questions in science that are highly relevant to the regulatory process. To date, HEI has supported more than 220 projects at institutions in North America, Europe, and Asia and has published over 160 Research Reports and Special Reports.

Typically, HEI receives half of its core funds from the US Environmental Protection Agency and half from 28 worldwide manufacturers and marketers of motor vehicles and engines who do business in the United States. Other public and private organizations periodically support special projects or certain research programs. Regardless of funding sources, HEI exercises complete autonomy in setting its research priorities and in reaching its conclusions.

An independent Board of Directors governs HEI. The Institute's Health Research Committee develops HEI's five-year Strategic Plan and initiates and oversees HEI-funded research. The Health Review Committee independently reviews all HEI research and provides a Commentary on the work's scientific quality and regulatory relevance. Both Committees draw distinguished scientists who are independent of sponsors and bring wide-ranging multidisciplinary expertise.

The results of each project and its Commentary are communicated widely through HEI's home page, Annual Conference, publications, and presentations to professional societies, legislative bodies, and public agencies.

HEI STATEMENT
Synopsis of Research Report 128

Neurogenic Responses of Rat Lung to Diesel Exhaust

Air pollution, including gases and particulate matter emitted from motor vehicles, has been associated with increases in both morbidity and mortality, but the underlying mechanisms responsible for these effects are not well understood. Insight into such mechanisms will aid in the understanding of human risk associated with air pollution.

In 1998, HEI issued Request for Preliminary Applications 98-6, entitled "Health Effects of Air Pollution". In response, Dr Witten and colleagues proposed to investigate the inflammatory effects of diesel exhaust exposure on rat airways. The investigators focused on the role of neurogenic inflammation, an inflammatory response defined by the release of neuropeptides, such as substance P (SP), from sensory nerve fibers known as *C fibers* located within the lung tissue. Neurogenic inflammation has been implicated in responses to inhaled irritants such as ozone and cigarette smoke and has been implied to play a role in asthma. HEI funded Dr Witten's study because they thought it would provide valuable information on the pathogenic mechanisms involved in respiratory responses to diesel exhaust.

APPROACH

The investigators exposed female rats (8 weeks old) to two concentrations of whole diesel exhaust emissions (35 and 630 µg/m^3 particulate matter) from a heavy-duty 1990s Cummins research engine. Exposures were conducted over 3 weeks (4 hr/day, 5 days/week); neurogenic and other inflammatory markers were measured immediately after the end of exposure. Half of the rats in each exposure group were pretreated with capsaicin, a neurotoxin that depletes sensory C fibers of neuropeptides and thereby inhibits the neurogenic inflammatory pathway. Control groups were exposed to air. Cigarette smoke exposure (~400 µg/m^3, 4 hr/day for 7 days) provided a positive control. The investigators measured endpoints of neurogenic inflammation: SP protein and gene expression, density of the SP receptor neurokinin-1 (NK1), and activity of neutral endopeptidase (NEP), the enzyme that breaks down SP. They also assessed leakage of blood plasma into lung tissue and other inflammatory markers, such as levels of the cytokines interleukin (IL)-1β, IL-6, IL-10, IL-12, and tumor necrosis factor α, numbers of inflammatory cells in lung tissue, and cellular lung pathology.

Witten collaborated with researchers from the University of Wisconsin to develop the diesel exhaust exposure system. Before animal exposures started, they evaluated a number of engine operation modes using the California Air Resources Board 8-mode test system for gaseous, particulate, and metal emissions. The investigators selected California Air Resources Board mode 6 for the animal experiments.

RESULTS AND INTERPRETATION

The authors are among the first to investigate neurogenic inflammation in the lungs of rats exposed to whole diesel exhaust. After exposure to both concentrations of diesel exhaust, consistently higher levels of plasma leakage and lower activity of the enzyme NEP were observed. Changes in levels of SP and its receptor NK1 were less consistent, however, and few changes were observed in cytokine levels. These results confirm previous findings of mild inflammatory responses after exposure to diesel exhaust.

The role of neurogenic inflammation remains unclear, however. Neurogenic inflammation has been convincingly demonstrated after exposure to ozone, sulfur dioxide, hydrogen sulfide, cigarette smoke, and wood smoke. In those studies, inflammatory responses were eliminated after animals had been treated neonatally with capsaicin. In the Witten study, rats were treated with capsaicin as young adults. Witten and colleagues showed that

Continued

This Statement, prepared by the Health Effects Institute, summarizes a research project funded by HEI and conducted by Dr Mark L Witten at the University of Arizona, Tucson AZ. The following Research Report contains both the detailed Investigators' Report and a Critique on the study prepared by the Institute's Health Review Committee.

capsaicin treatment caused a complete absence of SP in lung tissue, but it had little effect on the inflammatory response to diesel exhaust. Thus, the results do not support a role for C fibers in the airway inflammatory response to diesel exhaust. The results of the current study may also have been complicated by neuropeptide release from sources other than C fibers (such as the airway ganglia, mast cells, and eosinophils). The investigators did find evidence for neurogenic inflammation after exposure to cigarette smoke, which was in part reversed by capsaicin treatment.

When testing emissions at different engine operating conditions, the investigators found that elemental carbon dominated at medium to heavy loads, while organic carbon dominated emissions at lighter loads. Levels of sulfate, calcium, iron, magnesium, and particle numbers differed among operating conditions. They found some differences in particle composition between the lower and the higher level of diesel exhaust during the animal exposures, but their contribution to the inflammatory effects, if any, remains unclear. Additional research will be needed to investigate further the inflammatory mechanisms and the role of C fibers in airway responses to diesel exhaust and to identify which components of the diesel exhaust mixture may contribute to the inflammatory effects.

Library of Congress Catalog Number for the HEI Report Series: WA 754 R432.
The paper in this publication meets the minimum standard requirements of the ANSI Standard Z39.48-1984 (Permanence of Paper) effective with Report 21 in December 1988; and effective with Report 92 in 1999 the paper is recycled from at least 30% postconsumer waste with Reports 25, 26, 32, 51, 65 Parts IV, VIII, and IX, 91, 105, and 117 excepted. These excepted Reports are printed on acid-free coated paper.

HEALTH EFFECTS INSTITUTE

CONTENTS
Research Report 128

Neurogenic Responses in Rat Lungs After Nose-Only Exposure to Diesel Exhaust

Mark L Witten, Simon S Wong, Nina N Sun, Ingegerd Keith, Chol-Bum Kweon, David E Foster, James J Schauer, and Duane L Sherrill

Center for Toxicology & Southwest Environmental Health Sciences Center and Department of Pediatrics, University of Arizona, Tucson, Arizona; Department of Comparative Biosciences, School of Veterinary Medicine, University of Wisconsin, Madison, Wisconsin; Engine Research Center, University of Wisconsin, Madison, Wisconsin; Wisconsin College of Engineering and State Laboratory of Hygiene, University of Wisconsin, Madison, Wisconsin; and College of Public Health, University of Arizona, Tucson, Arizona

HEI STATEMENT

This Statement is a nontechnical summary of the Investigators' Report and the Health Review Committee's Critique.

INVESTIGATORS' REPORT

When an HEI-funded study is completed, the investigators submit a final report. The Investigators' Report is first examined by three ouside technical reviewers and a biostatistician. The report and the reviewers' comments are then evaluated by members of the HEI Health Review Committee, who had no role in selecting or managing the project. During the review process, the investigators have an opportunity to exchange comments with the Review Committee and, if necessary, revise the report.

Continued

CRITIQUE Health Review Committee

The Critique about the Investigators' Reports is prepared by the HEI Health Review Committee and staff. Its purpose is to place the studies into a broader scientific context, to point out strengths and limitations, and to discuss remaining uncertainties and implications of the findings for public health.

RELATED HEI PUBLICATIONS

Publishing history: This document was posted as a preprint on *www.healtheffects.org* and then finalized for print.

Citation for whole document:

Witten ML, Wong SS, Sun NN, Keith I, Kweon C-B, Foster DE, Schauer JJ, Sherrill DL. January 2005. Neurogenic Responses in Rat Lungs After Nose-Only Exposure to Diesel Exhaust. Research Report 128. Health Effects Institute, Boston MA.

When specifying a section of this report, cite it as a chapter of the whole document.

INVESTIGATORS' REPORT

Neurogenic Responses in Rat Lungs After Nose-Only Exposure to Diesel Exhaust

Mark L Witten, Simon S Wong, Nina N Sun, Ingegerd Keith, Chol-Bum Kweon, David E Foster, James J Schauer, and Duane L Sherrill

ABSTRACT

Using an in-line, real-time, in vivo exposure system, we investigated whether acute adverse effects of diesel exhaust (DE*) exposure involve neurogenic inflammation in the lungs via sensory nerve C fibers. A total of 168 female F344 rats (175 g, 8 weeks old) were randomly assigned to pretreatment with capsaicin or saline to deplete C-fiber neurotransmitters. In a 2 × 3 factorial design, groups of animals were then exposed nose-only to a low level of DE (LDE, 35.3 μg/m^3), a high level of DE (HDE, 632.9 μg/m^3), or sidestream cigarette smoke (CS, 0.4 mg/m^3). Two control groups were exposed whole body to filtered air in the animal room (fRA) or unfiltered air in the diesel engine room (eRA), respectively. DE was taken directly from a heavy-duty Cummins N14 research engine operated at 75% throttle (California Air Resources Board [CARB] 8, mode 6). Exposure to DE or air was 4 hours/day, 5 days/week, for 3 weeks. Exposure to CS was for 4 hours/day for 7 days.

Involvement of neurogenic inflammation in the response to DE or CS was assessed via comparison of plasma extravasation, a sensitive endpoint of neurogenic inflammation, between rats with and without capsaicin pretreatment. Lung injury was assessed via analysis of proinflammatory cytokines, respiratory permeability, and histopathology. Moreover, whether DE exposure affected the molecular mechanisms of neurogenic inflammation was analyzed through quantification of substance P (SP) and its primary neurokinin-1 (NK1) receptor at the gene and protein levels and through neutral endopeptidase (NEP) activity.

DE and CS exposure induced dose-dependent plasma extravasation, which may play an important role in initiating the associated lung inflammation and injury. Exposure of rats to DE affected the SP signaling pathway as indicated by overexpression of the NK1 receptor or reduction of SP in the lung tissue. DE exposure consistently inactivated tissue NEP, a key factor that switches neurogenic inflammation from its physiological and protective functions to a role that increases and perpetuates lung injury. The roles of these overlapping neurokininergic mechanisms in the initiation of DE-associated lung injury are plausible, and these changes may contribute to DE-associated respiratory disorders.

Capsaicin rats followed the same trends as those of saline animals when exposed to DE or CS: capsaicin rats did not have significantly different plasma extravasation in the airways or lung parenchyma compared to their corresponding controls. Histopathology evaluation likewise demonstrated the same degree of tissue changes, such as edema and alveolar macrophage collection, in capsaicin and saline rats after the same level of DE exposure.

In summary, our data suggest that neurokininergic mechanisms may have been involved in DE-induced inflammatory conditions in rat lung but that C fibers did not appear to be involved under these exposure conditions. We believe that time-course or protein knockdown/knockout animal studies are required to characterize further the role of neurokininergic mechanisms in DE-induced lung injury.

INTRODUCTION

Airborne fine particulate matter (PM < 2.5 μm in aerodynamic diameter, or $PM_{2.5}$) has been recognized as a major risk factor to human health for decades. Acute adverse effects from airborne PM have been demonstrated in epidemiology studies (Dockery et al 1992, 1994; Peters et al 1997).

* A list of abbreviations and other terms appears at the end of the Investigators' Report.

This Investigators' Report is one part of Health Effects Institute Research Report 128, which also includes a Critique by the Health Review Committee and an HEI Statement about the research project. Correspondence concerning the Investigators' Report may be addressed to Dr Mark L Witten, Department of Pediatrics, College of Medicine, Arizona Health Sciences Center, University of Arizona, 1501 N Campbell Ave, 3352 A, Tucson AZ 85724.

Although this document was produced with partial funding by the United States Environmental Protection Agency under Assistance Award R82811201 to the Health Effects Institute, it has not been subjected to the Agency's peer and administrative review and therefore may not necessarily reflect the views of the Agency, and no official endorsement by it should be inferred. The contents of this document also have not been reviewed by private party institutions, including those that support the Health Effects Institute; therefore, it may not reflect the views or policies of these parties, and no endorsement by them should be inferred.

Small short-term increases in PM levels have been associated with increased symptoms of certain pulmonary illnesses (ie, asthma, bronchitis, airway hyperresponsiveness) (Samet et al 2000). PM-associated morbidity and mortality are readily apparent in the young and old and in those with preexisting respiratory or cardiopulmonary disorders (Utell et al 1991). Mechanisms that explain the acute toxicity of ambient PM and the sensitive subpopulation phenomenon are not fully established, however. Ambient PM comes from diverse natural sources (sea spray, volcanic, earth erosion) and anthropogenic sources (industrial, urban, residential, environmental, traffic-related) and consists of complex aggregates of elemental and organic carbons, volatile organics, metals, sulfates, pesticides, pollen, microbial contaminants, and unknown materials, which are attached to an insoluble carbon core (Veronesi and Oortgiesen 2001). These complex aggregates have different physicochemical and biomedical characteristics that may be involved in pathogenic processes in the lungs.

Well-characterized PM-induced adverse health effects are manifested as irritation, inflammation, and functional impairment (Nikula et al 1995, 1997; Terashima et al 1997; Gordon et al 1998; Salvi et al 1999, 2000; Ghio et al 2000; Nel et al 2001). Airborne PM exposure can induce airway hyperresponsiveness and lung inflammation (impairment of airway scavenger cells, influx of macrophages and neutrophils, and damage of alveolar epithelial cells), but underlying mechanisms cannot quantitatively relate epidemiological data to actual levels of PM exposure. This uncertainty suggests that unknown approaches link or orchestrate known effects and mechanisms in lung responses to PM exposure. Experiments utilizing residual oil fly ash (Veronesi and Oortgiesen 2001) and other pollutants (Long et al 1999) may provide important clues for the mechanisms of lung responses by suggesting that afferent neural fibers (such as sensory C fibers) play a crucial role in mediating these mechanisms in lungs after exposure to airborne pollutants.

Reflexes generated by depletion of pulmonary C fibers are both protective and defensive (eg, apnea, laryngeal narrowing, bronchoconstriction, sneezing, coughing, aspiration, and expiration reflexes). The nervous system also modulates other lung defense strategies (such as mucociliary clearance, vasodilatation, increased vascular permeability, influx of inflammatory cells) and may play a role in healing after airway injury (Jimba et al 1995). The presence of these tachykinin-containing C fibers within the lungs of mammals has been demonstrated by radioimmunoassay and immunohistochemistry (Lundberg et al 1984; Hislop et al 1990; Killingsworth et al 1996; 1997). Examination of autopsy specimens of human lung has revealed SP-containing nerves in airways from bronchi to the alveolar ducts (Hislop et al 1990). Neurotransmitters (such as SP) released by lung C-fiber endings or by immunoinflammatory cells produce a cascade of cytokine-dominated pulmonary responses, including plasma leakage, collectively known as *neurogenic inflammation* (Okamoto et al 1993). The actions of sensory neurotransmitters are mediated through plasma membrane-bound neurokinin receptors, which have seven transmembrane domains and are coupled to G proteins (Rodger et al 1995). The sensory neurotransmitters are subject to enzymatic degradation and inactivation by NEP (also known as *metalloendopeptidase*, enzyme classification 3.4.24.11). NEP is a membrane-bound enzyme located mainly at the surface of airway epithelial cells but also present in airway smooth muscle cells, submucosal gland cells, and fibroblasts.

Current evidence has shown that C fibers are sensitive to many air pollutants, including ozone (Jimba et al 1995; Delaunois et al 1997), sulfur dioxide (Long et al 1999), nitric dioxide (Lucchini et al 1996; Joad et al 1997), and cigarette smoke (Bonham et al 1996; Joad et al 1995). Residual oil fly ash initiates inflammatory cytokine release by activation of capsaicin and acid receptors in a human bronchial cell line (Veronesi et al 1999, 2000).

SP, a neuropeptide that functions as a neurotransmitter, is released into the airways after exposure to house dustmites. Several investigations (Joos et al 1994; Lundberg 1995; Chu et al 2000) have found a significantly larger amount of SP in the bronchoalveolar lavage (BAL) fluid from subjects with asthma than from control subjects. SP concentrations measured in sputum induced by inhalation of hypertonic saline were significantly higher in patients with asthma than in healthy subjects (Tomaki et al 1995). The plasma levels of SP-like immunoreactive compounds also were significantly higher in patients with acute exacerbation of asthma than in healthy controls. Many inflammatory and structural cells of the airways (including inflammatory T cells, eosinophils, mast cells, macrophages, epithelial cells, fibroblasts, and even bronchial smooth muscle cells) are involved and become activated during asthma-like or other conditions. Most of the cells not only have NK1 receptors but also play an effector role by releasing proinflammatory mediators, cytotoxic mediators, and cytokines. Such release results in vascular leakage, hypersecretion of mucus, smooth muscle contraction, epithelial shedding, and bronchial hyperresponsiveness. It seems reasonable to speculate that airborne PM exposure may result in neurogenic inflammation. Due to its physicochemical complexity, however, PM toxicity may have a more common physicochemical mechanism. To this end, the afferent neural response to inhaled particles, as a key mechanism of the health effects of airborne particulate pollution, is the focus of this research.

In this study, DE was chosen because it represents a specific PM source and is a substantial contributor to total airborne fine particle pollution. In 2001, the US Environmental Protection Agency (EPA) specifically put DE particles on the list of 21 Mobile Source Air Toxics (MSATs) (EPA 2001). The listed MSATs are mostly airborne PM pollutants found in urban areas and highways and primarily derive from the combustion of fossil fuels in transportation and other equipment. Between 50% and 80% of emitted particles are small, 0.02 to 0.5 μm (EPA 1991), small enough to reach alveoli deep in the lungs. Moreover, DE is thought to pose a particularly high risk for the development of lung disease because DE contains numerous toxic chemicals (Bascom et al 1996). The daily average ambient concentrations of PM from DE have been reported to be 40 to 134 $\mu g/m^3$ for truck drivers, 4 to 192 $\mu g/m^3$ for railroad workers, and 8 to 42 $\mu g/m^3$ for near-road residency (World Health Organization [WHO] 1996). Exposure to these fine particles may adversely affect the respiratory system, which could directly and/or indirectly cause increased morbidity and mortality. To eliminate the possibility that physicochemical properties of DE particles are altered by being aged and resuspended before delivery, we utilized an on-line, real-time in vivo DE exposure system so that the studied animals were exposed to fresh particles.

Current US regulations consider only PM concentration (that is, the mass of all particles collected from diluted exhaust) and do not distinguish between more harmful particles and less harmful ones. Additional issues not currently addressed are whether the number of particles is actually being reduced with engine and combustion improvements and whether the distribution is only being shifted to a smaller size range. Therefore, great importance is being attributed to studies of DE particles in terms of both detailed chemical composition and size distributions. Moreover, approximately 30% of the fine PM in the atmosphere of urban areas has been reported to be organic aerosols (Gray et al 1986; Malm et al 1994; Christoforou et al 2000; Zheng et al 2002). Some of these organic compounds are known to be carcinogenic (International Agency for Research on Cancer Working Group 1980). Because organic compounds condense under ambient conditions, they must be considered in the detailed analyses of chemical composition of PM or DE (Hildemann et al 1989). To address this dynamic in our laboratory, a residence time chamber (RTC) was added to the exposure system. With this enhanced dilution system, the research engine could be run at conditions that varied load and speed. For the current study, one engine condition, mode 6, was used during the animal exposure studies. The mode 6 diesel engine setting was 75% of full load at 1200 rpm, the speed at which maximum engine torque was achieved. Mode 6 is characterized by a relative higher ratio of particles and lower level of organic compounds generated by diesel fuel and the lubricating oil among CARB 8 mode tests (Kweon et al 2002, 2003).

SPECIFIC AIMS

1. To determine whether neurogenic inflammation is involved in DE-induced lung injury;
2. to determine whether dysregulation of pulmonary neuropeptide SP due to DE exposure occurs at the gene and protein level;
3. to characterize the gene and protein expression of NK1 receptors in the lung after DE exposure; and
4. to determine whether NEP activity changes after DE exposure.

HYPOTHESES

- Exposure to DE for 3 weeks can cause pulmonary neurogenic inflammation, which is mediated by tachykinin SP (released from sensory nerve terminals and others) acting via NK1 receptors expressed on lung cells and accompanied by inactivity of NEP.
- The magnitude of neurogenic inflammation and subsequent lung injury may depend on the composition and physicochemical properties of DE as well as the concentration and duration of DE exposure.

METHODS AND STUDY DESIGN

EXPOSURE SETUP

Engine Bench Setup

For the experiments, a research single-cylinder direct-injection 4-cycle diesel engine (Figure 1) was adapted from an in-line six-cylinder engine (from the early 1990s N14 series, Cummins Inc, Columbus IN) with a low swirl, turbocharged, four-valve, centrally located direct-injection combustion system. The combustion chamber of the engine was a quiescent, shallow dish type that uses a unit injector (Cummins CELECT) (Table 1). This research engine used a commercial N14 cylinder head. Although the compression ratio of the research engine (13.1:1) was lower than that of the commercial engine (approximately

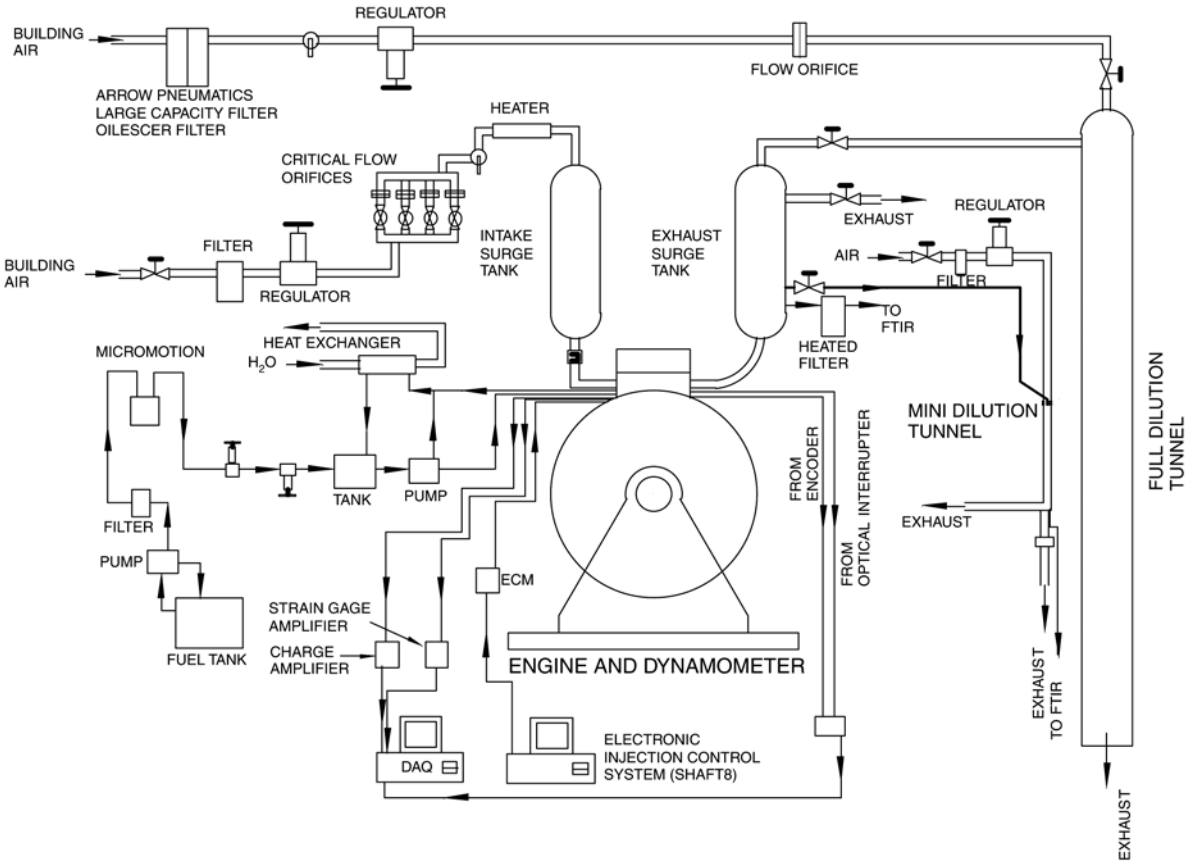

Figure 1. Research diesel engine (single-cylinder Cummins N14) bench layout. DAQ = data acquisition; FTIR = Fourier transform, infrared; ECM = enzyme control module.

Table 1. Specifications for Single-Cylinder Research Engine[a]

Cycle	4-stroke
Combustion chamber	Quiescent
Piston chamber	Shallow dish
Intake valves (*n*)	2
Exhaust valves (*n*)	2
Compression ratio	13.1:1
Swirl ratio	1.4
Displacement	2333 cc
Bore/stroke	139.7 mm / 152.4 mm
Combustion chamber diameter	97.8 mm
Connecting rod length	304.8 mm
Piston pin offset	None
Injection system	Unit injector, direct injection
Nozzle dimension	8 × 0.2 mm diameter
Length/diameter of holes (l/d)	4.1
Spray angle	152°

[a] Model N14, Cummins.

15:1), the research engine was turbocharged. Therefore, this single-cylinder research engine mimicked a typical heavy-duty on-highway diesel engine.

The exhaust gas sampling and analysis system used in this study is the heart of this research. The laboratory had a full-dilution tunnel system to collect PM samples from the engine. Gaseous emissions, such as nitrogen oxides, carbon monoxide, total hydrocarbon, and carbon dioxide, were measured using a raw engine exhaust emissions system (California Analytical Instruments). This gaseous emission system consisted of a model 300 heated flame ionization detector (HFID), total hydrocarbon analyzer, a model 400 heated chemiluminescent detector, a nitric oxide analyzer, and a model 300 infrared gas analyzer for carbon monoxide and carbon dioxide.

Augmented Full Dilution Tunnel System

In addition to the exhaust measurement systems described in the previous section, an augmented sampling system was designed and installed according to the EPA Fine Particle Chemical Speciation Network. Specifically,

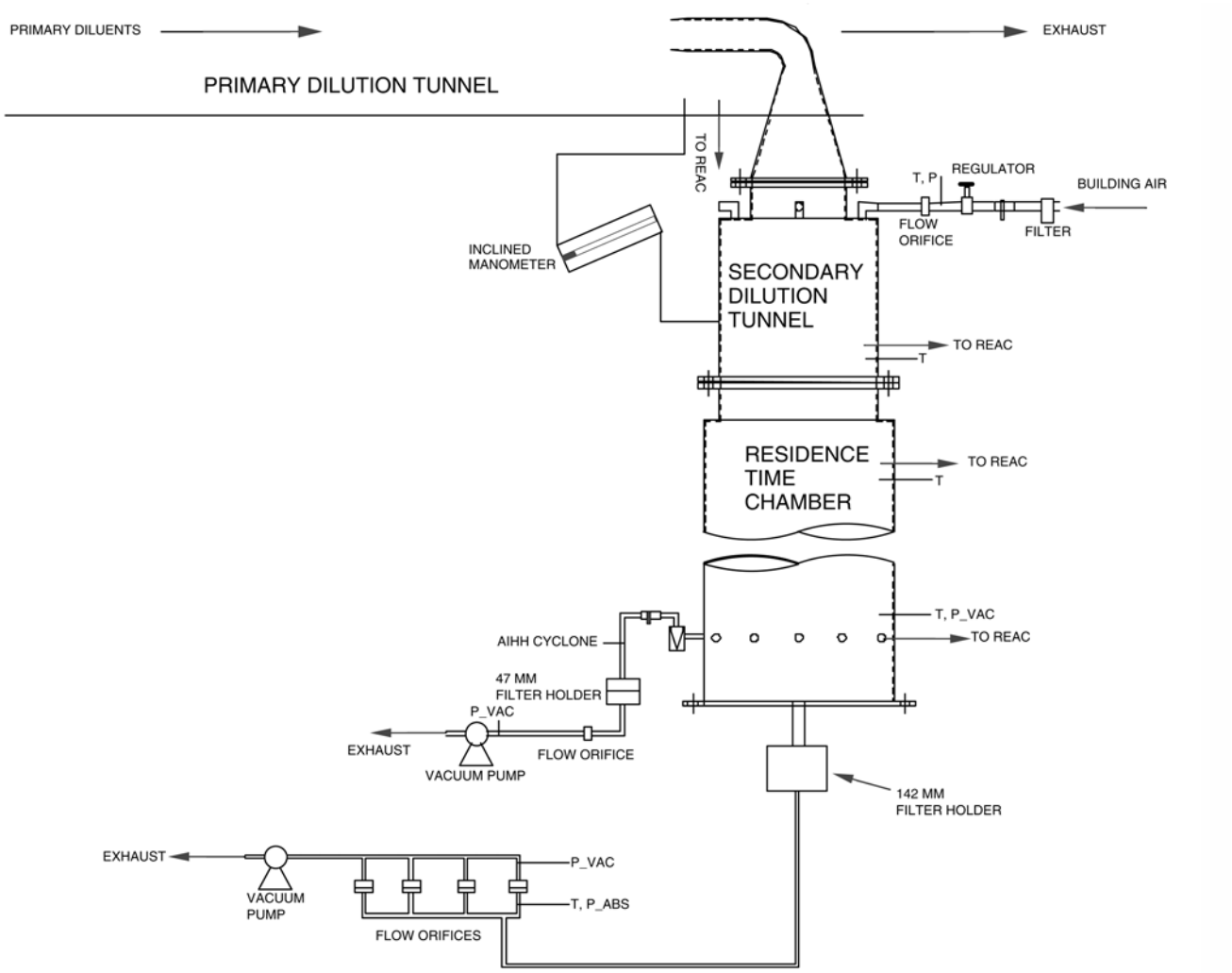

Figure 2. Augmented sampling system in the research diesel engine bench. REAC = gaseous emissions bench; T = temperature; P = pressure; P_{VAC} = vacuum pressure; P_{ABS} = absolute pressure; AIHL = Air and Industrial Hygiene Laboratory.

the secondary dilution tunnel of the typical full dilution tunnel was enhanced to allow detailed assessment of the individual chemical components of the PM. Design of the augmented sampling system was based on studies by Schauer and coworkers (1999a,b).

The augmented sampling system consisted of a primary dilution tunnel, secondary dilution tunnel, RTC, and subsystems: a 142-mm filter holder, two $PM_{2.5}$ cyclones, several 47-mm filter holders, and vacuum pumps (Figure 2). Because combusted diesel particles are naturally charged and thus can cause electrostatic deposition in the sampling system, the current sampling system was made with electrically nonchargeable materials (such as 304, 316, and 316L grades of stainless steel). Thermophoretic deposition is caused by asymmetric forces that arise from a temperature gradient. To minimize the temperature gradient inside the sampling line, its main body was made with a thin stainless steel tube (thickness, 0.16 cm; grade 304) and insulated. In addition, surface temperature of the RTC was controlled to be approximately the same as the inside gas temperature by using four rows of heated bands and respective temperature controllers. The sampling system inlet, which supplied the secondary dilution tunnel, was made thin and sharp to facilitate isokinetic sampling. The inlet's diameter was gradually increased to minimize inertial deposition of particles in bends of the pipe.

The RTC was designed to give a residence time between 30 and 60 seconds under isokinetic sampling. Based on previous work, we believe this to be sufficient time to allow all the condensation processes to take place and

equilibrium to be reached. A 142-mm filter holder with two functions was attached at the bottom of the RTC. First, the filter holder allowed a large range of sample flow rates, enabling us to control the residence time in the RTC while maintaining isokinetic flow from the primary dilution tunnel. Second, a large amount of sample, such as the soluble organic fraction, can be collected for analyses.

The augmented sampling system had extra sampling ports to collect different kinds of samples. The relative humidity of the diluted gases was measured with dry-bulb and wet-bulb thermometers installed in one of the available sampling ports. All the flow rates of air and diluents were controlled by critical flow orifices.

Detailed Chemical Composition Two types of sampling trains (Figure 3) were attached to the RTC and operated in parallel. All flow rates were controlled with critical flow orifices located downstream of the filter holders. The first component of each sampling train was an aluminum Teflon-coated $PM_{2.5}$ cyclone (Air and Industrial Hygiene Laboratory [AIHL]), which was operated at a flow rate of 24 L/min.

As shown in Figure 3 (top), the first sampling train consisted of a cyclone followed by three Teflon membrane filters (47-mm diameter; Gelman Teflo 2 µm pore size, Gelman Sciences, Ann Arbor MI) and one baked quartz fiber filter (47-mm diameter, Pallflex Tissuquartz 2500 QAO, Pall Corporation, East Hills NY). The first Teflon membrane filter was used for gravimetric determination of the PM and analyzed for sulfate ions by ion chromatography. The second was used for a duplicate PM concentration measurement, and the third was used for an analysis of trace metals by inductively coupled plasma mass spectrometry (ICPMS). The quartz fiber filter was used to measure elemental and organic carbon and analyzed with a carbon analyzer (Sunset Laboratories), operated according to the US National Institute of Occupational Safety & Health (NIOSH) method 5040.

The second sampling train (Figure 3, bottom) was composed of a cyclone followed by three baked quartz-fiber filters (operated in parallel) and a polyurethane foam cartridge (density = 0.022 g/cm^3, indentation load deflection = 30, 5.7 cm diameter, 7.6 cm length; Atlas Foam Products, Sylmar CA) in series. The cartridge was precleaned with solvent. The particle-phase organic compounds were collected on the three quartz-fiber filters; the foam cartridges downstream of those filters collected semivolatile organic compounds. The organic compounds collected on the filters and cartridges were analyzed by gas chromatography–mass spectrometry (GC-MS) as described by Schauer and colleagues (1999a,b).

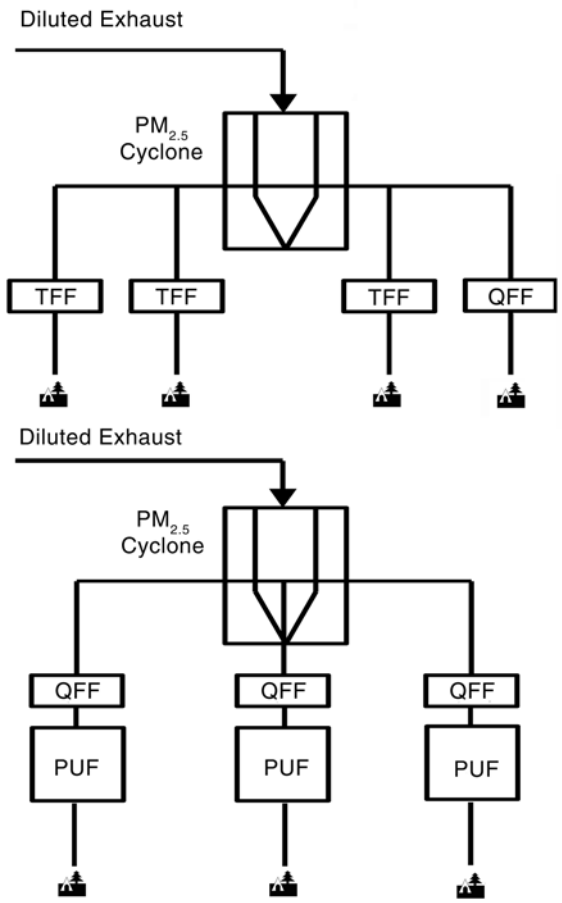

Figure 3. Sample trains of four (top) and three (bottom) filter holders with respective $PM_{2.5}$ cyclone (Air and Industrial Hygiene Laboratory). TFF = teflon filter; PUF = polyurethane foam; QFF = quartz fiber filter; and = critical flow orifice.

Particle Number Concentration and Size Distribution A scanning mobility particle sizer (SMPS; model 3936L10, TSI, Shoreview MN) was used to measure particle number concentrations and size distributions. The SMPS consists of an ^{85}Kr aerosol neutralizer (TSI model 3077) and ^{85}Kr bipolar charger to neutralize the charge on particles, a long differential mobility analyzer (TSI model 3081) to separate particles based on their electrical mobility, and a condensation particle counter (CPC; TSI model 3010) to count the number of particles. Calculation of particle volume concentrations assumed the particles were spherical.

Third Dilution Tunnel and Exposure Chamber For measurements to examine details of the engine operation and its combustion process, the samples obtained at the secondary dilution tunnel residence chamber were sufficient. For our DE exposure studies, particle concentrations at the

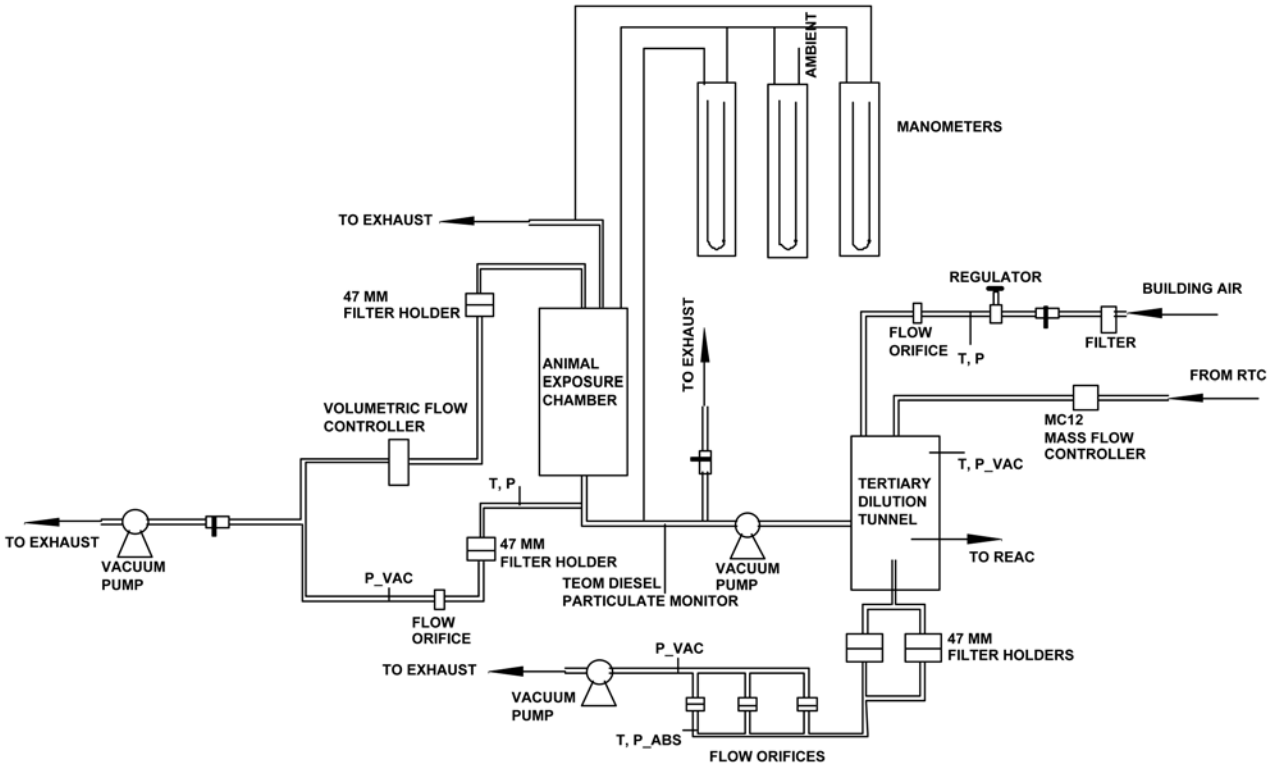

Figure 4. Third dilution tunnel with sampling filters, mass flow controller between the secondary dilution tunnel and third dilution tunnel, and animal exposure chamber. P_{VAC} = vacuum pressure; P_{ABS} = absolute pressure; T = temperature; P = pressure; REAC = gaseous emissions bench.

exit of the secondary dilution tunnel were still too high. Consequently, we installed a third dilution tunnel in which the sample was diluted further to reach concentrations desired for the animal exposure tests. The target particle concentrations for these tests were 65 and 650 $\mu g/m^3$, which represent moderate and high levels of human exposure in environmental and occupational microenvironments. These concentrations are on the same order as ambient conditions, ranging from approximately roadside to a heavily trafficked, confined region.

Accurate control over this exhaust stream was a significant challenge throughout the study. We accomplished this control via real-time monitoring of the flow rates and particle levels followed by a posteriori evaluation of filter samples taken from the sample line feeding the exposure chamber. This approach was necessary because concentrations in the sample stream were at, or slightly below, the measurement resolution of the real-time monitoring equipment. Consequently, we used the real-time monitoring equipment—a mass flow controller from the second dilution tunnel into the third dilution tunnel and a tapered-element oscillating microbalance (TEOM) for particle concentration—to monitor our operating conditions semiquantitatively in real-time. The more precise filter measurements were used to quantify the operating conditions fully after the experiments were completed.

In the tertiary dilution tunnel and animal exposure chamber (Figure 4), two filter holders were used to catch samples of the final exhaust gas before it entered the animal exposure chamber. One of the filters was used to assess mass loading of the exhaust stream going to the animal exposure chamber, and the other filter was used to assess elemental and organic partitioning of the PM. These data provided a consistency measure relative to the data taken from the secondary dilution tunnel and served to quantify particle loading of the sample stream being fed to the exposure chamber. The air regulator and mass flow controller were positioned before the tertiary dilution tunnel.

After leaving the tertiary dilution tunnel, the sample line was routed to the animal exposure chamber. The flow-balancing system ensured that pressure in the chamber was slightly above the atmospheric pressure and that sample pressure in the nose cone area was also slightly above the pressure in the nose cone bleed region. This flow-balancing system ensured that no external dilution of the gases was being breathed by the animals while not

stressing the animals' respiratory system through localized abnormal pressure. We monitored temperature within the exposure chamber with a digital readout thermometer and made filter measurements of the particle mass entering and leaving the chamber.

The exit filter measurement served two purposes. First, it enabled us to measure the particle concentration leaving the exposure chamber. Secondly, we ran this filter at a flow rate of 1 L/min, which was the desired flow rate through the chamber. The filter at the entrance of the exposure chamber was included to ensure no PM was lost in transit from the third dilution tunnel to the exposure chamber. Water manometers were used to monitor the pressure differences within the animal exposure chamber system.

Table 2. Summary of CARB 8 Modes

	Speed (rpm)	Load (%)	Remark
Mode 1 (M1)	1800	100	High rated speed
Mode 2 (M2)	1800	75	
Mode 3 (M3)	1800	50	
Mode 4 (M4)	1200	25	
Mode 5 (M5)	1200	100	Peak torque
Mode 6 (M6)	1200	75	
Mode 7 (M7)	1200	50	
Mode 8 (M8)	700	10	Low rated speed

Engine Operating Mode and Test Fuel

Experiments were conducted at operating mode 6 of the CARB 8 mode test matrix (Table 2). The CARB 8 modes range from light load at low speed to high load at high speed. The engine operating parameters used for this engine to achieve the CARB 8 modes of operation are given in Table 3. A wide range of engine operating conditions could be achieved by running the engine over the load and speed range encompassed by the CARB 8 mode test. The engine operating parameters can be adjusted in many ways to achieve the desired output mandated by the CARB 8 mode test conditions. For example, injection timing, the intake pressure and/or temperature, and fueling rate can be changed while still achieving the desired engine output. In this study, the engine was run at mode 6 of the CARB 8 mode test cycle: a 75% load condition at 1200 rpm, the speed at which maximum torque can be achieved. This mode was chosen because it is the most common high load condition used in engine tests in the laboratory of University of Wisconsin Engine Research Center (Madison WI) for the past several years.

The fuel was a commercial low sulfur diesel (#2, Mobil) purchased from a commercial gas station in Stoughton, Wisconsin (Table 4). In the United States, the lower limit of cetane number (CN) for #2 diesel fuel is about 40; this fuel was 39.1. The 0.9 difference could be an analytical error: even for the same fuel, the CN varies slightly depending on time of purchase and on the refinery. The aromatics content is also a typical value for #2 diesel fuel currently available from a gas station in United States. Figure 5 shows the pressure, heat release rate, and injection pressure profiles versus engine crank angle. These data are typical for an engine of

Table 3. Operating Conditions of CARB 8 Modes

	Mode 1	Mode 2	Mode 3	Mode 4	Mode 5	**Mode 6**	Mode 7	Mode 8
Intake pressure [kPa]	179.3	179.3	179.3	179.3	175.2	**179.3**	177.9	175.2
Intake temperature [°C]	49	48.3	48.3	48	48.3	**49**	48.1	48.7
Exhaust pressure [kPa]	174.1	188.5	184.4	157.9	150.7	**217.6**	187.9	161.7
Equivalence ratio, ϕ	0.69	0.50	0.34	0.21	0.82	**0.69**	0.41	0.09
Peak incylinder pressure	7.15	7.21	7.08	7.63	10.58	**7.85**	7.77	7.31
[MPa] @ aTDC[a]	13.25	14.0	7.25	8.5	10.75	**15.5**	13.25	3.75
Peak incylinder temperature	1958	1856	1588	1362	2212	**2140**	1728	1024
[K] @ aTDC	30.75	26.25	22.75	15.25	20.75	**28.75**	20.75	3.75
ISFC[b] [kg/ihp-hr]	0.172	0.147	0.14	0.132	0.168	**0.159**	0.144	0.232
IMEP[c] [kPa]	1086	924	677	517	1491	**1227**	866	139
SOI[d] [CA[e] aTDC]	−5	−5	−5	−2	−11	**−2**	−2	−6
Injection duration [CA]	25	20	13	10	27	**22**	15	3.5
Peak injection pressure [MPa]	121	113	106	62	96	**80**	70	42

[a] aTCD = after top dead center. [b] ISFC = indicated specific fuel comsumption. [c] IMEP = indicated mean effective pressure.
[d] SOI = start of injection. [e] CA = crank angle.

this type. They show that an initial rapid rise in energy release rate, known as the *premixed-burning fraction*, is followed by a mixing-dominated energy release zone, known as the *diffusion burning portion* of combustion.

We also tested ultralow sulfur diesel (sulfur = 14 ppm, aromatics = 22.1 weight%, CN = 52.9) and Fischer-Tropsch diesel (sulfur < 1 ppm, aromatics < 1 weight%, CN = 74) fuels (Figure 6). The ultralow sulfur diesel fuel is mandated to be commercially available by September 2006 for use in on-highway truck and bus engines for the model year 2007. These fuels were not used for the animal exposures, however. Data on these tests will be published elsewhere.

Table 4. Test Fuel Properties

Density, 15°C	865 kg/m^3
Specific gravity, 16/16°C	0.8684
Viscosity @ 40°C	2.595 mm^2/s
Flash point	70°C
Cetane number	39.1
Sulfur	352 ppm
Gross heating value	43506 kJ/kg
SFC[a] aromatics	49.2 wt%
Mono-aromatics	29.6 wt%
PNAs[b]	19.6 wt%
Hydrogen/carbon ratio	1.689

[a] SFC = supercritical fluid chromatography.

[b] PNAs = polynuclear aromatics.

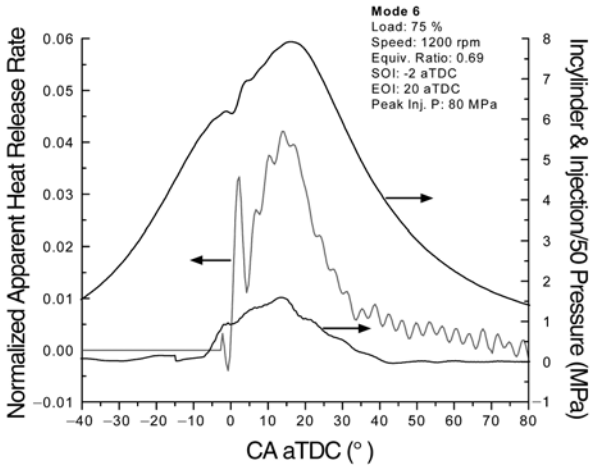

Figure 5. Pressure, normalized apparent heat release rate, and injection pressure versus engine crank angle. Mode 6 of CARB 8 mode test. CA aTDC = crank angle after top dead center; MPa = mega Pascal; SOI = start of injection; EOI = end of injection.

General Emissions and Particle Composition

The specific emissions (such as nonmethane hydrocarbon plus oxides of nitrogen, carbon monoxide, and PM emitted from the research diesel engine under the CARB 8 modes) are presented in Figure 7. The data shown are averaged over three different measurements in time except for the PM, which was measured at two different sampling ports simultaneously and averaged. All of these data are shown so that the emissions from mode 6 can be compared to the overall emissions from the engine under other operating conditions.

DE particles consist mainly of agglomerated solid carbonaceous material, volatile organics, sulfur compounds, and

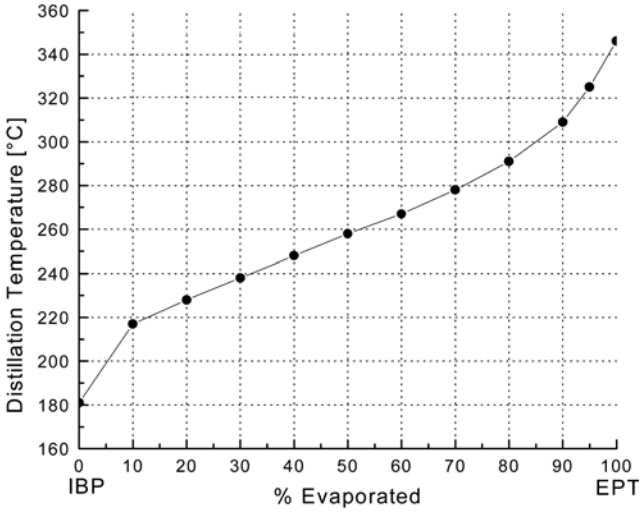

Figure 6. Distillation temperature curve of the ultralow sulfur diesel fuel. IBP = initial boiling point; EPT = endpoint temperature.

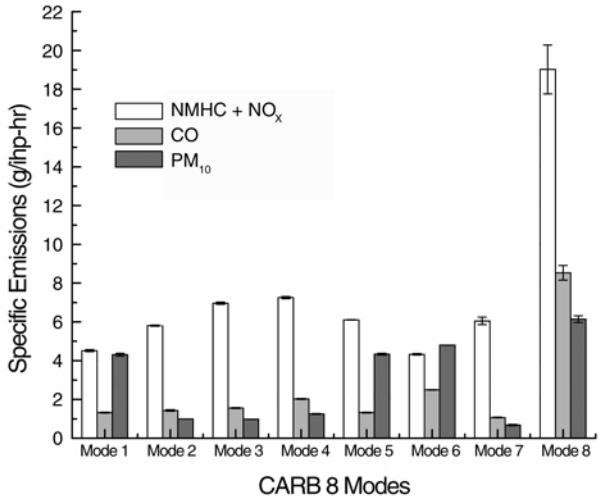

Figure 7. Specific emissions for the research engine under the CARB 8 modes. NMHC = nonmethane hydrocarbon. Data expressed as mean (SEM).

ash. In the current study, DE particle samples were analyzed for elemental carbon, organic carbon, and sulfates. Although the amount of metal compounds in particles is small, their health effect may be measurable. This is the major reason we included metal compounds in our study. The specific PM concentrations were averaged over the entire test period for each DE concentration (Figure 8). These samples were collected at the RTC and corrected for the dilution ratio. RTC1 and RTC2 are different sampling locations. The results show good agreement between mass and reconstructed mass, which indicates that the overall engine operating conditions were consistent for the exposure test periods.

At the level of overall dilution for the test engine, the slightest inaccuracy in flow control translated to a large deviation from the target level for DE particles. Filters were utilized so that accurate particle loading in the animal exposure chamber could be measured, but evaluation of the filter was completed after the exposures. In an effort to have real-time monitoring, a diesel particle monitor (model 1105; Rupprecht & Patachnick Co, Albany NY) was used. The minimum particle level at which the monitor operated reliably was 200 μg/m^3, so targeting the particle level to 65 μg/m^3 in real time could only be approximated. This diesel monitor was important to the experiment, however, because it gave us real-time assessment of the approximate level of particles in the flow system routing to the animal exposure chamber.

In an effort to maintain the target particle concentration level of 650 μg/m^3 at the animal exposure chamber, the dilution ratio was changed at the RTC, along with other variables, while the engine operating condition remained constant. The sample particle weight was measured daily after the test and the PM concentration at the exposure chamber inlet was controlled daily to approximate the target concentration for the 15 test days.

The exposure tests were performed for two DE concentration levels. In this test, several measurements were made along the sampling system. First, samples were collected from the RTC for analyses of sulfate ions, trace metals, elemental and organic carbon, PM concentration, volatile organic compounds, and semivolatile organic compounds. Second, carbon and PM concentration measurements were made at the tertiary dilution tunnel. Finally, PM concentrations were measured at the inlet and outlet of the exposure chamber.

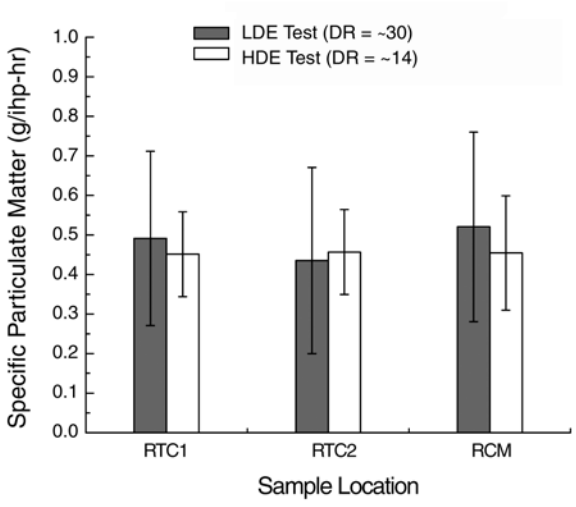

Figure 8. Sum of elemental carbon, organic carbon and sulfate particles. These were measured individually on different filters at mode 6 (75% load at 1200 rpm). DR = dilution ratio; RCM = reconstructed mass. Data expressed as mean (SEM).

ANIMALS, PRETREATMENT AND EXPOSURES

Animals

A total of 168 female F344 rats (8 weeks old; weighing ~175 g) were utilized for this study. All rats were housed in the American Association of Animal Laboratory and Care (AAALAC)-approved animal facility at the University of Wisconsin-Madison, College of Veterinary Medicine. In this species, SP-immunoreactive nerves have been demonstrated in the airways from the pharynx down to the peripheral bronchioles and the alveolar septa (Krause et al 1993; Okamoto et al 1993; Jimba et al 1995). The rats, two per cage, were on a 12/12 light/dark cycle with food and water ad libitum. The rats were randomly assigned to 7 groups, half the rats in each group receiving capsaicin pretreatment (Table 5).

Table 5. Animal Allocation

Exposure[a]	Pretreatment		Total Animals
	Saline	Capsaicin	
First-Round Exposure			
fRA	12	12	24
LDE[b]	12	12	24
eRA	12	12	24
Second-Round Exposure			
fRA	12	12	24
HDE[c]	12	12	24
CS[d]	12	12	24
eRA	12	12	24

[a] Exposures to LDE and HDE were nose only and to fRA and eRA were whole body; both had the following regimen: 4 hr/day × 5 days/wk × 3 wk. Exposures to CS were nose only with the following regimen: 4 hr/day × 7 continuous days.

[b] LDE mean mass concentration: 35.3 μg/m^3.

[c] HDE mean mass concentration: 632.9 μg/m^3.

[d] CS mean mass concentration: 400 μg/m^3.

Pretreatment

The rats were anesthetized intramuscularly with ketamine hydrochloride (HCl) (50 mg/kg; Research Biochemicals International, Natick MA), xylazine (8 mg/kg; Fort Dodge Laboratories, Fort Dodge IA), and acepromazine maleate (1 mg/kg; Fort Dodge Laboratories). Rats were injected with capsaicin (40 mg/kg intraperitoneally, 98% purity, Sigma, St Louis MO) or saline in six injections over 2 days. During pretreatment, the rats that received capsaicin also were treated with intraperitoneal theophylline (2 mg/kg), and terbutaline (0.2 mg/kg) to counteract bronchoconstriction and excessive mucus secretion. Three to five days later (day 0 of the experiment), the animals were examined by the webbing test (Jancso et al 1967) to confirm further the efficacy of capsaicin pretreatment. The lung tissues of the capsaicin and saline rats were collected for SP measurement by enzyme immunoassay.

DE Exposure

The rats were exposed to filtered air in the animal room (fRA) or available air in the engine room (eRA) and LDE or HDE for 4 hours/day, 5 days/week for 3 weeks. The target exposure concentrations of DE (65 and 650 $\mu g/m^3$) were derived from the WHO-documented practical ambient DE particle levels (WHO 1996) as well as from the 24-hour EPA standard for $PM_{2.5}$ (EPA 1998). Nose-only exposure was chosen not only to model natural exposure patterns but to avoid any initial afferent response to intratracheal instillation.

CS Exposure

The method for CS exposure was established (Witten et al 1992) and modified in a murine model (Wang et al 2002). Standard research cigarettes (1R4, University of Kentucky Smoking & Health Effects Laboratory) were utilized in this study. The rats were exposed to CS for 4 hours/day for 7 days through a 24-port nose-only exposure chamber (Intox Products, Albuquerque NM) using a constant vacuum (15 L/min). The time-integrated mass of CS particles delivered to the rats was 2.0 mg/exposure averaged, at a concentration of 0.4 mg/m^3, as measured by a seven-stage multijet impactor (Intox Products). The chosen concentration of CS was based on measurements of indoor air concentrations (for example, 10 to 1000 $\mu g/m^3$ total suspended particulates measured in smoker-occupied residences and up to approximately 2000 µg respirable suspended particulates per m^3 in restaurants). A lower order of magnitude may reflect young children's realistic exposed environment. The CS particles collected by the cascade impactor were found to have a median mass aerodynamic diameter of 0.34 µm with a geometric standard deviation of 0.46. CS composition was not assessed in this study. We refer to previous literature (Witten et al 1992; Witschi et al 1997) for this information.

ENDPOINTS

Immediately after exposure, the rats were anesthetized intramuscularly with ketamine HCl (50 mg/kg; Parke-Davis, Morris Plains NJ), xylazine (8 mg/kg; Mobay Corp, Shawnee KS), and acepromazine maleate (1 mg/kg; Fermenta Animal Health Co, Kansas City MO). Half were analyzed for plasma extravasation and half for respiratory permeability. After completion of these measurements, the diaphragmatic lung lobe and the right side upper lobe were removed from half the rats (3 of each group) for histopathology and immunohistochemical analysis at the Veterinary Pathology Laboratory at the University of Wisconsin. The remaining lung tissues of these 6 rats as well as whole lung tissues of the other 6 rats were flash frozen in liquid nitrogen and transported to the University of Arizona. There they were analyzed for gene and protein expression of SP, NK1 receptor, and proinflammatory cytokines.

Plasma Extravasation Measurement

Briefly, the right jugular vein of selected rats (N = 6/group) was cannulated and a bolus of 100 µCi/kg technetium-labeled albumin (^{99m}Tc-albumin) was administered. Two minutes later, a blood sample of 0.3 mL was taken from the cannula for estimation of blood radioactivity and packed cell volume. At 10 minutes after ^{99m}Tc-albumin administration, the abdominal and thoracic cavities were opened, and a clamp was placed on the thoracic vena cava. The abdominal vena cava was severed and a blood sample collected again for estimation of blood radioactivity and packed cell volume. An infusion of 20 mL of isotonic saline (5 mL/min) was performed to expel residual intravascular ^{99m}Tc-albumin. The lung was removed, and the trachea and lower left lung lobe was dissected free, gently blotted dry on filter paper, and weighed. The radioactivity was measured in a gamma counter (model 44-62, Ludlum Measurements, Sweetwater TX). The specific leakage of plasma (µL/g wet weight lung tissue) was calculated by dividing the tissue radioactivity by the product of the ^{99m}Tc-albumin plasma radioactivity and the weight of each tissue sample to obtain the volume of extravascular plasma in 1 g of tissue.

Microvascular Permeability Measurement

Six rats/group were implanted with an endotracheal tube and given a 0.1-mL bolus of 100 µCi technetium-labeled diethylenetriamine pentaacetate (^{99m}TcDTPA, M_r = 492 amu, physical half-life of 6.02 hours) with 5 to 7 tidal volume air flushes to disperse the ^{99m}TcDTPA throughout the lungs. Pulmonary epithelial clearance of ^{99m}TcDTPA was recorded for 10 minutes after instillation. Gamma radiation was measured with a portable probe (model 44-62, Ludlum) placed over the lungs and connected to a gamma

counter (model 2000, Ludlum). The range of the scintillation probe is 0 to 500,000 counts/minute. Pulmonary epithelial clearance of ^{99m}TcDTPA was established over a 10-minute count after instillation of ^{99m}TcDTPA into the lungs. A K value (percentage clearance of ^{99m}TcDTPA/min) was calculated through a first-order pharmacokinetic model and corrected for residual background radiation and radioactive decay.

SP and NK1 Receptor mRNA Measurements

Lung tissue samples (75 mg) were homogenized in the presence of guanidinium isothiocyanate. Total RNA was isolated using an RNAqueous-4 polymerase chain reaction (PCR) kit (Ambion, Austin TX). Residual DNA was digested by thorough treatment with 5 U of deoxyribonuclease I at 37°C for 45 minutes followed by inactivation with 1/10 volume of inactivation reagent. First strand complementary DNA (cDNA) was synthesized from 2 µg total RNA in a volume of 20 µL containing 1× reverse transcriptase buffer with 0.5 mM each deoxyribonucleoside triphosphatase, 0.5 U/µL ribonuclease (RNase) inhibitor (Ambion), 5 µM oligo(deoxythymidine)$_{15}$ primer, and 4 U reverse transcriptase (Omniscript, Qiagen, Valencia CA). For no-template control samples, RNA was replaced by H_2O. A negative control reaction omitting the reverse transcriptase was also performed for each DNAse-treated RNA sample. All samples were reverse transcribed under the same conditions and from the same reverse transcription master mix in order to minimize differences in efficiency.

A series of standards were prepared by performing tenfold serial dilutions of full-length NK1 receptors and β-preprotachykinin-I (β-PPT-I) cDNAs (from Dr Leeman) in the range of 5 million copies to two copies per reaction. All plasmid samples were treated with RNAse A prior to quantitation (in order to minimize contamination with bacterial RNAse from the plasmid purification procedure) and subsequently quantified using a combination of absorbance at 260 nm and gel electrophoresis. Glyceraldehyde-3-phosphate dehydrogenase (GAPDH) messenger RNA (mRNA) levels were analyzed as a positive control for cDNA synthesis, and a known amount of rat GAPDH and primers were custom manufactured by Maxim Biotech (South San Francisco CA).

Real-time quantitative mRNA was assessed with a real-time PCR assay kit (SYBR-Green, Applied Biosystems, Foster City CA) using an ICycler PCR machine (Bio-Rad, Richmond CA). The potential benefits of using SYBR-Green I dye to monitor PCR product formation continuously have been demonstrated by other investigators (Wittwer et al 1997; Morrison et al 1998). NK1 receptors, β-PPT-I and GAPDH mRNA were amplified in separate tubes, and the increase in fluorescence was measured in real time. Sense and antisense primers are listed in Table 6. Each sample was analyzed in triplicate along with standards and no-template controls. The reaction contained 100 ng cDNA, 0.3 µM primers, 10 mM Tris (hydroxymethyl) aminomethane hydrochloride (Tris-HCl), 50 mM potassium chloride (KCl), 2.5 mM magnesium chloride ($MgCl_2$), 0.2 mM deoxyribonucleoside triphosphatase, and 2.5 U DNA polymerase (HotStarTaq, Qiagen, Valencia CA) in a final volume of 25 µL. After denaturation at 95°C for 15 minutes, the cDNA products were amplified for 45 cycles. Each cycle consisted of a three-step procedure: denaturation at 94°C for 15 seconds, annealing at 60°C for 30 seconds, and extension at 72°C for 45 seconds.

Acquisition of fluorescent signal from the samples was carried out at the end of the elongation step. Because SYBR-Green I binds to any double-stranded DNA, the specific product from nonspecific products and primer dimers were confirmed immediately after amplification by melting analysis. The PCR products were heated to 95°C for 1 minute, annealed at 65°C (annealing temperature + 10°C), and then slowly heated from 65°C to 95°C at 0.3°C increments to obtain the melting curve. The PCR products were subjected to analysis by electrophoresis on a 2% agarose gel to confirm the efficiency of melting curve analysis. A similar setup was used for negative controls except that reverse transcriptase was omitted and no PCR products were detected under these conditions.

Table 6. Primer Sets

Target Gene	Primer/Probe	Sequence	Length (Base Pairs)
NK1 Receptor	Forward	5′-GCCAAGCGCAAGGTGGTCAAA-3′	102
	Reverse	5′-TGGGTTGATGTAGGGCAGGAGGA-3′	
β-PPT	Forward	5′-AAATCCAACATGAAAATCCTCGTG-3′	221
	Reverse	5′-CCGTTTGCCCATTAATCCAAAG-3′	
GAPDH	Forward	5′-AAGGTCATCCCAGAGGCTGAA-3′	111
	Reverse	5′-TACTTGGCAAGGTTTCTCCAG-3′	

All SYBR-Green PCR data were obtained using PCR software (ICycler, Bio-Rad). Direct detection of PCR products was monitored by measuring the increase in fluorescence caused by the binding of SYBR-Green I dye to double-stranded DNA. These measurements resulted in an amplification plot of the fluorescence signal versus cycle number.

Threshold cycle was defined as the fractional cycle number at which the fluorescence passes the fixed threshold. A plot of the log of initial target copy number for a set of standards versus the calculated threshold cycle value resulted in a straight line. Quantitation of the amount of target in unknown samples was accomplished by measuring the threshold cycle and using the standard curve to determine starting copy number. Standard curves were generated for each primer set and each PCR run using serial dilutions of rat NK1 receptors and β-PPT-I cDNA. All the samples were tested in duplicate with the reference gene GAPDH, a housekeeping gene for normalization of data. A ratio of specific mRNA to GAPDH amplification was then calculated to correct for any differences in efficiency at reverse transcription.

Enzyme Immunoassay for SP

SP in the lung tissue was quantitatively determined using a commercial enzyme immunoassay kit (Cayman Chemical, Ann Arbor MI) based on the competition between free SP, derived from the unknown sample, and an SP tracer (SP linked to an acetylcholinesterase [AChE] molecule) for a limited number of SP-specific rabbit antiserum binding sites. Briefly, the nonspecific binding sites on the 96-well microplate, precoated with mouse monoclonal antirabbit IgG (the capture antibody), were saturated with a blocking solution supplied by the manufacturer. AChE tracer, SP antiserum, and either standard SP or unknown samples were added sequentially and incubated at 4°C for 18 hours. After washing with buffer to remove any unbound reagents, an aqueous solution containing acetylthiocholine, the substrate for AChE, and 5,5′-dithiobis-(2-nitrobenzoic acid) (DTNB) was added to each well. AChE hydrolyzed acetylthiocholine into thiocholine, which reacts with DTNB to produce 5-thio-2-nitrobenzoic acid. This product has an intense yellow color with a characteristic absorbance at 412 nm. The absorbance was determined using an automated microplate reader (model Elx808, Bio-Tek Instruments, Winooski VT). All samples were run in duplicate.

Intensity of the color developed is inversely proportional to the amount of free SP present in the well during the incubation (Takeyama et al 1990). The sensitivity of the assay was determined by serial dilution and was found to be about 17 pg SP/mL. The cross reactivity of SP-related peptides in the assay was as follows: SP, 100%; SP (2–11), 93%; SP (4–11), 97%; SP (7–11), 30%; SP (8–11), < 0.01%; SP (1–4), < 0.01%; neurokinin A, 2.7%; and neurokinin B, 0.04%. The amount of SP in the lung tissue was expressed in femtomoles per minute per milligram protein. The total SP was defined as the sum of SP released into the lung during challenges and the residual SP in the tissue. Protein concentration in the lung tissue extract was determined by a dye binding method involving colloidal gold. Bovine serum albumin was used as the standard.

NEP Measurement

The lung tissues from the rats were washed with physiologic saline and stored at −70°C for later analysis. A cell-free extract of each lung tissue was homogenized in 10 mL of tissue protein extraction reagent (T-PER, Pierce Chemical, Rockford IL). The residue was removed from the extract by centrifuge at 12,000g for 10 minutes at 4°C. The supernatants were used for enzyme analysis. Cell-free NEP activity in each tissue lysate was measured spectrophotometrically by a coupled assay as reported by Van der Velden and colleagues (1999) and Papandreou and colleagues (1998) with minor modifications. Briefly, 5 µL of cell-free extract were incubated with 1 mM succinyl-Ala-Ala-Phe-*p*-nitroanilide (Suc-Ala-Ala-Phe-pNA) (Bachem Bioscience, King of Prussia PA) as a substrate in 0.1 M Tris-HCl (pH 7.6) in the presence of 1 µL (0.14 U/µL) porcine kidney aminopeptidase-N (AP-N, Sigma). The reaction (total volume: 200 µL) was measured in duplicate in a 96-well microtiter plate. In this coupled activity assay, NEP cleaves Suc-Ala-Ala-Phe-pNA between Ala and Phe, yielding Phe-pNA. AP-N subsequently cleaves Phe-pNA, generating pNA as the final product. The increase in specific absorbance at 405 nm (as a result of the accumulation of free pNA) was determined after 30 minutes incubated at 37°C using a plate reader (Bio-Tek Instruments). Cell-free (substrate alone or substrate with AP-N) and substrate-free blanks were run in parallel. Protein concentration was determined using a coomassie plus protein assay (Pierce, Rockford IL) with bovine serum albumin as a standard.

Determination of Cytokine mRNA

Cytokine gene expressions in the rat lungs were estimated using a multiplex PCR kit (BioSource International, Camarillo CA). The assay was performed according to instructions provided with the kit. The conditions used for PCR were the following: after 15 minutes of initial denaturation at 96°C, 1 minute at 96°C, and 4 minutes at 56°C for two cycles, followed by 1 minute at 94°C and 2.5 minutes at 57°C for 33 cycles. Final extension was carried out for 10 minutes at 70°C. Amplification products were separated

on a 2% agarose gel, stained with ethidium bromide, transilluminated with UV light, and photographed. The negatives were then analyzed by using gel video systems (Bio-Rad). The areas of the peaks for mRNA for each cytokine were used to calculate the percentage of cytokine mRNA relative to the amount of mRNA for GAPDH.

The relative concentrations of mRNAs encoding for interleukin (IL) 1β, IL-6, IL-10, IL-12, and tumor necrosis factor α (TNF-α) in lung tissue were estimated by reverse transcriptase (RT)-PCR using a modification of the method of Smith (2000). Poly(A)$^+$ RNA was then isolated using polystyrene latex-oligo(dt) beads (Qiagen). One hundred nanograms of poly(A)$^+$ RNA underwent reverse transcription in the presence of random hexamers using 200 U of Moloney murine leukemia virus RT, RNAse H minus, point mutant [MMLVRT(H$^-$)] (Promega, Madison WI). PCR strategies were based on those reported by Dr Yamamura of the Department of Pharmacology at the University of Arizona. These strategies allowed comparison of cytokine mRNA in different samples. For PCR, cell cDNA was combined with 2.5 U of *Taq* polymerase (Promega), 0.02 mM deoxyribonucleoside phosphatase, 1 µg of each primer, and buffer. Reactions were placed in a thermal cycler (Robocycler 40, Stratagene, La Jolla CA) using 95°C denaturation, 58°C annealing, and 72°C extension temperatures, with the first three of a total of 30 cycles having extended denaturation and annealing times. About 10% to 20% of each amplification reaction was then electrophoresed on ethidium bromide–stained agarose gels and viewed under UV illumination. For quantification, the indicated PCR amplifications were performed in the presence of ^{32}P end–labeled positive-standard primers. After separation on agarose gel, the amplified fragment was excised, and the amount of radiolabel incorporated was determined by scintillation counting.

The sensitivity and linearity of such cellular RT-PCR amplifications using limiting dilutions of RNA generated from in vitro cell transcription of the gene coding region is acceptable for quantitative comparisons (Smith et al 2000). The amplifications were performed under conditions that were in the linear range of amplifications for each gene. To assure that similar amounts of input RNA were reverse transcribed, RNA was quantified by DNA dipstick (Invitrogen, San Diego CA). Additionally, PCR amplification of the housekeeping gene, GAPDH, was performed on 5% of the total cDNA reaction per sample to assure that similar amounts of input RNA and similar efficiencies of reverse transcription were being compared. To assure the identity of the PCR-amplified fragments, the size of each amplified gene fragment was compared with those of DNA standards (Promega) that were electrophoresed on the same ethidium bromide–stained agarose gels. In addition, PCR-amplified fragments were subjected to direct DNA sequencing, and their sequencing was confirmed as previously described.

Cytokine Quantification

All cytokines (IL-1β, IL-6, IL-10, IL-12, and TNF-α) in supernatant from lung tissue were quantified using an enzyme-linked immunoabsorbent assay (ELISA) as directed by the kit supplier (R&D Systems, Minneapolis MN). Rat recombinant cytokine standards were used in every assay. ELISA plates were then analyzed on an automated microplate reader (model Elx808, Bio-Tek). All samples were run in duplicate.

Immunohistochemical Analysis and Pathology Examination

One sagittal, 1-mm-thick slice was collected from the diaphragmatic lung lobe and the right side upper lobe from all laboratory rats and controls. These slices were immersed in Bouin fixative for 24 hours, then placed on an automatic tissue processor, and embedded in pairs in paraffin (ie, one pair per rat) using a short processing protocol and low melting point paraffin. Sections (5 µm) were dewaxed and processed histochemically with hematoxylin and eosin (H&E) for general pathology examination and with toluidine blue for selective evaluation of mast cells.

For immunohistochemical analyses, 5-µm sections from the same blocks were dewaxed, hydrated, and treated as follows. Sections were first treated with normal, nonimmune goat serum for 30 minutes (from the species of secondary antibody) to block any nonspecific background. The sections were then treated lightly with Triton X (0.2%, 5 minutes) to facilitate antibody access to the tissue antigen. Primary antiserum, raised in rabbit, was then applied overnight at 4°C (SP, 1:500) or for 4 hours at room temperature (calcitonin gene-related peptide, CGRP, Peninsula, 1:800). After rinses in phosphate-buffered saline, sections were treated with the histostain kit (Zymed Laboratories, South San Francisco CA). Briefly, this method included secondary biotinylated goat antirabbit serum followed by horseradish peroxidase–labeled streptavidin, and development in a diaminobenzidine solution to achieve a reddish brown reaction product. Alternatively, sections were treated overnight with monoclonal (mouse) antibody raised against NK1 (Chemicon, 1:500), followed by tetramethylrhodamine isothiocyanate–labeled goat antimouse (Zymed, 1:50), which yielded red fluorescence at the sites of immunoreactivity. Slides were rinsed, coverslipped, and observed with a microscope (Eclipse 6000, Nikon) equipped with objectives for both brightfield and fluorescence. Images were then captured using a digital camera attached to the microscope, imported to a personal computer, and printed on photograde paper.

STATISTICAL METHODS AND DATA ANALYSIS

A total of 168 female F344 rats were randomly assigned to one of seven groups: six in two 2 × 3 factorial designs and one as the positive control group (CS). One gender was chosen to increase efficiency of a sample size by avoiding gender deviation. Prior to experimental treatment, mean body weight per group was analyzed by analysis of variance (ANOVA) to identify any random deviations.

Two rounds of exposure experiments were performed independently for LDE and HDE exposure with their corresponding fRA and eRA controls. Data (n = 12 for fRA or eRA) generated in two-round exposures were tested for differences using ANOVA and were combined when no statistically significant differences were observed (ie, the two fRA groups were combined and the two eRA groups were combined). Each endpoint in the groups (capsaicin versus saline pretreatment and air versus LDE, HDE or CS with each pretreatment) was first examined using descriptive statistics and tested for homogeneity of variance using the Bartlett test. Based upon the results of this test, data were normalized using a $\log_{10}$ transformation. Comparisons of means among groups were made using ANOVA in this log-normal scale. Because the measures were independent variables, mean changes were evaluated when appropriate using post hoc linear contrasts with adjustment for multiple comparisons using both Bonferroni and Fisher protected least-significant difference (PLSD)–corrected significance levels. Additional statistical analyses were performed to evaluate dose–response relations (the strength of linear relations) among air, LDE, and HDE exposures for NEP activity, plasma extravasation, and respiratory permeability by calculating Pearson correlation coefficients after log-normal transformation. All tests were two-sided, and $P < 0.05$ was considered significant. Data were collected and analyzed on a personal computer (Statview IV, Abacus Concepts, Berkeley CA) and expressed as means ± SEM.

RESULTS

PARTICLE CHARACTERISTICS

The average particle concentration (± SEM) for the 15-day LDE exposure was 35.3 ± 4.9 μg/m^3. At this exposure, small mass changes in any engine operating variable could cause a deviation in the particle concentration. For the HDE exposure, average particle concentration was 632.9 ± 47.61 μg/m^3 (mean ± SEM, n = 11).

DE particles consist mainly of agglomerated solid carbonaceous material, volatile organics, sulfur compounds, and ash. In the current study, elemental carbon, organic carbon, and sulfates were analyzed for the samples collected (Figure 9). These samples were collected at the RTC and corrected for dilution ratio. RTC1 and RTC2 were different sampling locations. The results showed good correlation between mass and reconstructed mass, which indicates that the overall engine operating conditions were consistent for the exposure test periods.

Specific elemental, organic carbon, and sulfates measured at the RTC are shown for mode 6 in Figure 9. Again, these components were averaged over the entire test period (15 days) for each operating condition and corrected for the dilution ratio. Elemental carbon was clearly a dominant component of the diesel PM at high load. Samples collected on a Teflon filter each day of LDE and HDE exposure were used to measure 46 trace metal compounds. Seven of them are shown in Table 7. Amounts of sodium, magnesium, manganese, and lead did not change with the dilution ratio for LDE and HDE exposure, but the amounts of calcium, iron, and chromium in HDE particles were approximately 50% of the amounts in LDE particles.

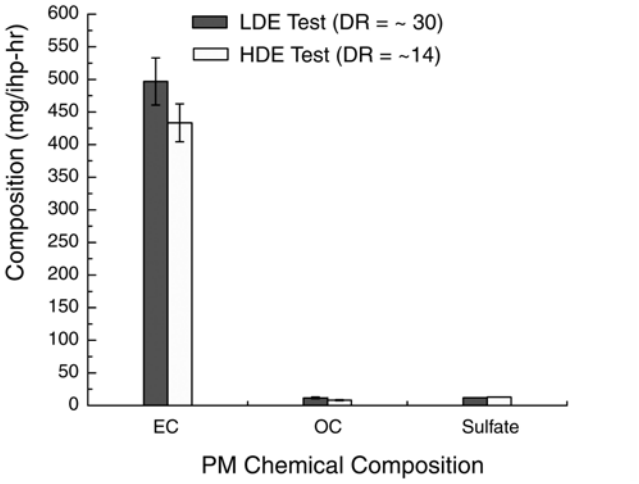

Figure 9. Mean elemental carbon (EC), organic carbon (OC), and sulfate concentrations in particles collected at RTC at mode 6 (75% load at 1200 rpm). Data expressed as mean (SEM). DR = dilution ratio.

Table 7. Trace Metals in DE Particles

	Concentration (ng/m^3)	
Trace Metals	LDE	HDE
Natrium	4.78 ± 0.32	4.07 ± 0.70
Magnesium	0.86 ± 0.32	0.60 ± 0.03
Calcium	10.66 ± 0.02	5.05 ± 0.48
Iron	6.44 ± 0.67	3.17 ± 0.22
Chromium	1.31 ± 0.12	0.68 ± 0.07
Manganese	0.22 ± 0.04	0.11 ± 0.02
Lead	0.97 ± 0.19	1.24 ± 0.08

The particle number and mass by size under all CARB 8 modes are shown in Figure 10. The particle size range measured with the SMPS was 7.234 to 294.27 nm. The results show only one representative measurement from each mode. The engine operating conditions significantly affected the particle size distributions in terms of both number and mass. The LDE exposure test showed slightly more than 50% of that of the HDE exposure test due to the higher dilution ratio. Currently, we are working to correct the effect of dilution ratio on the DE particle size distribution.

GASEOUS EMISSIONS

Regulated gaseous emissions (nitric oxide/nitrogen oxides, carbon dioxide, and total hydrocarbons) were measured at the exhaust pipe of the test engine and carbon dioxide emission was measured at the engine out, the RTC, and the tertiary dilution tunnel for use in the calculation of dilution ratios. As the DE mixed with a large amount of dilution air, the concentrations of gaseous emissions decreased significantly and no further chemical reactions of the regulated gaseous emissions occurred due to quenching. The concentrations of emitted gases at the exposure chamber were calculated using the information on dilution ratios and their engine-out concentrations. The results showed that concentrations of regulated gaseous emissions in the exposure chamber were approximately the same as their background concentrations (Table 8).

ORGANIC CONTENTS

Some emission concentrations of particle-phase and semivolatile organic compounds in the exposure chamber were resolved and identified for mode 6 (Table 9). Emission rates of ultratrace compounds were not measured in detail. The GC-MS method employed quantifies more than 100 organic compounds, which include *n*-alkanes, alkylcyclohexanes, hopanes, steranes, and polycyclic aromatic hydrocarbons (PAHs). Many of the 100 compounds were not detected and have not been reported in diesel engine emissions in previous research. The *n*-alkanes, hopanes, and steranes were observed to be the major classes of the particle-phase organic compounds, and *n*-alkanes were the major class of semivolatile organic compounds for the condition tested. Most of the particle-phase and semivolatile PAHs were below detection level except methyl-sub PAH (M_r 202 and 228). Samples were collected for detailed speciation, including metals. These results were not yet available at the time this report was written.

BIOPARAMETERS

SP

The level of β-PPT-I mRNA encoding SP in lung tissue after exposure to LDE or HDE showed no difference from air controls in either capsaicin or saline rats (Figure 11). After CS exposure, however, β-PPT-I mRNA levels in saline rats (but not capsaicin rats) were significantly higher. The level of SP in the lung tissue was significantly lower among saline-HDE rats, but not among saline-LDE rats or saline-CS rats (Table 10). In capsaicin rats, SP could not be detected in the lung tissue within most groups.

NK1 Receptors

Response patterns of the NK1 receptor gene after DE exposure were inconsistent (Figure 12). When compared

Table 8. Emissions of Regulated Gases in Exposure Chamber for HDE Exposure

Gas	Concentration (Mean ppm ± SD)
Nitric oxide	3.59 ± 0.71
Oxides of nitrogen	3.69 ± 0.73
Nitrogen dioxide	0.1 ± 0.043
Carbon monoxide	2.95 ± 0.54
Carbon dioxide	518.96 ± 97.47
Total hydrocarbon	0.031 ± 0.0068

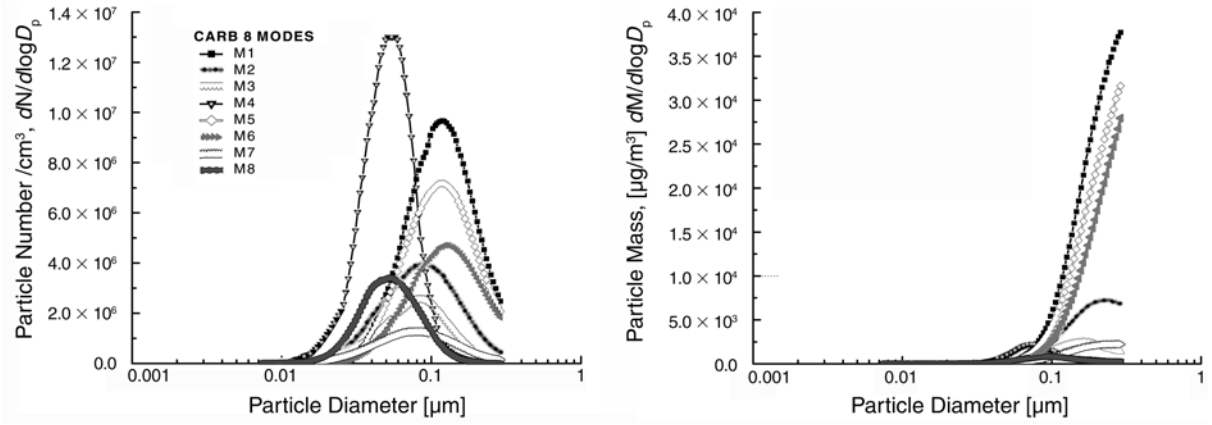

Figure 10. Particle number and mass by size under CARB 8 modes. Distributions are weighted by size and number.

Table 9. Emission Rates of Particle-Phase and Semivolatile Organic Compounds for Mode 6 in Exposure Chamber

Compounds	Emission Rates (ng/m^3) LDE	HDE
***n*-Alkanes**		
n-Tetracosane ($C_{24}H_{50}$)	0.102	0.226
n-Pentacosanes ($C_{25}H_{52}$)	0.133	0.285
n-Hexacosane ($C_{26}H_{54}$)	0.071	0.297
n-Heptacosane ($C_{27}H_{56}$)	0.046	0.332
Total class emission rate	0.352	1.140
Alcylcyclohexanes		
Tridecyclohexane	< 0.019	< 0.019
Pentadecylcyclohexane	< 0.019	< 0.019
Hexadecylcyclohexane	< 0.019	< 0.019
Heptadecylcyclohexane	< 0.019	< 0.019
Octadecylcylcohexane	< 0.019	< 0.019
Nonadecylcyclohexane	< 0.019	< 0.019
Total class emission rate	< 0.114	< 0.114
Hopanes		
22,29,30-trisnorneohopane	< 0.004	NM[a]
17β(H)-21α(H)-30-norhopane	< 0.004	0.202
17α(H)-21β(H)-hopane	< 0.004	0.322
22S,17α(H),21β(H)-30-homohopane	< 0.004	0.127
22R,17α(H),21β(H)-30-homohopane	< 0.004	0.131
22S,17α(H),21β(H)-30,31 bishomohopane	< 0.004	0.087
22R,17α(H),21β(H) 30,31 bishomohopane	< 0.004	0.426
Total class emission rate	< 0.028	1.295
Steranes		
20R, 5α (H),14β(H), 17β(H)-cholestane	< 0.010	0.146
20S, 5α (H),14β(H), 17β(H)-cholestane	< 0.010	0.137
20R, 5α (H),14α(H), 17α(H)-cholestane	< 0.010	0.303
20R, 5α (H),14β(H), 17β(H)-ergostane	< 0.010	0.091
20S, 5α (H),14β(H), 17β(H)-ergostane	< 0.010	0.097
20R, 5α (H),14β(H), 17β(H)-sitostane	< 0.010	0.095
20S, 5α (H),14β(H), 17β(H)-sitostane	< 0.010	0.064
Total class emission rate	< 0.070	0.933
PAHs		
Fluoranthene	< 0.004	< 0.004
Acephenanthrylene	< 0.004	< 0.004
Pyrene	< 0.004	< 0.004
(M_r 202)	< 0.004	0.146
Benzo[*ghi*]fluoranthene	< 0.004	< 0.004
Cyclopenta[*cd*]pyrene	< 0.004	< 0.004
Benz[*a*]anthracene	< 0.004	< 0.004
Chrysene/triphenylene	< 0.004	< 0.004
(M_r 228)	0.007	0.007
Benzo[*b*]fluoranthene	< 0.004	< 0.004
Benzo[*k*]fluoranthene	< 0.004	< 0.004
Benzo[*j*]fluoranthene	< 0.004	< 0.004
Benzo[*e*]pyrene	< 0.004	< 0.004
Benzo[*a*]pyrene	< 0.004	< 0.004
Perylene	< 0.004	< 0.004
Total class emission rate	< 0.063	0.205

[a] NM = not measured.

Table 10. SP in Lung Tissue After Saline or Capsaicin Treatment

Exposure (*n*)	SP (pg/g)[a] Saline	Capsaicin
fRA (12/12)	4.06 ± 0.75	0.07 ± 0.07
LDE (6/6)	2.23 ± 0.90	ND[b]
HDE (6/6)	0.44 ± 0.07[c]	ND
CS (6/6)	0.65 ± 0.18[c]	ND
eRA (12/12)	2.66 ± 0.79	0.06 ± 0.06

[a] Data expressed as mean ± SEM.

[b] ND = nondetectable.

[c] $P < 0.05$ compared to saline-fRA rats.

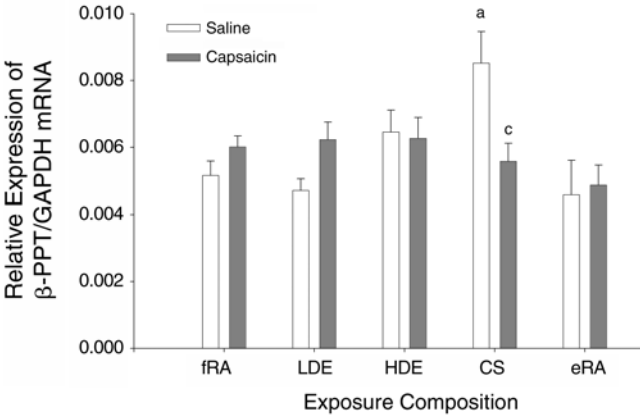

Figure 11. Expression of β-PPT-I encoding neurotransmitter SP in lung tissue after exposure. Data expressed as mean (SEM). [a] $P < 0.05$ compared to saline-fRA rats; [c] $P < 0.05$ compared to saline-CS rats.

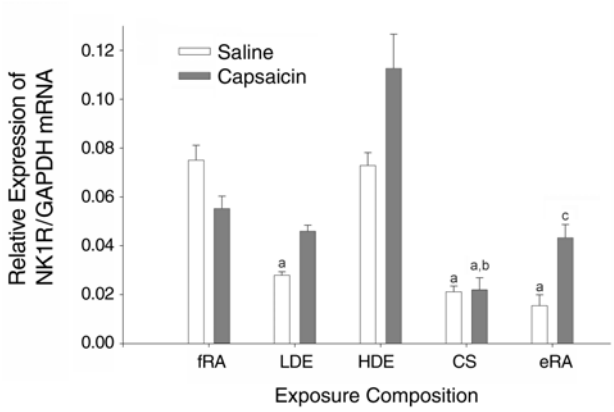

Figure 12. Gene expression of NK1 receptor (NK1R) in lung tissue after exposure. Data expressed as mean (SEM). [a] $P < 0.05$ compared to saline-fRA rats; [b] $P < 0.05$ compared to capsaicin-fRA rats; [c] $P < 0.05$ compared to saline-eRA rats.

with RA-exposed rats, saline-LDE rats showed significantly less NK1 receptor mRNA in the lung tissue, but saline-HDE rats showed the same levels. Capsaicin rats exposed to either level of DE showed no difference in NK1 receptor mRNA in lung tissues. The transcription rate of the NK1 receptor gene, in both capsaicin and saline rats, was significantly lower when rats had been exposed to CS. Interestingly, NK1 receptor mRNA was also lower among saline-CS animals than among saline-fRA animals.

NK1 receptor–like immunoreactivity appeared as punctate dots on the airway epithelium, resembling the pattern of synaptic varicosities (Figure 13A–F). In the capsaicin-HDE rats, immunoreacting receptor sites were larger and had a higher intensity than in the other groups (Figure 13E).

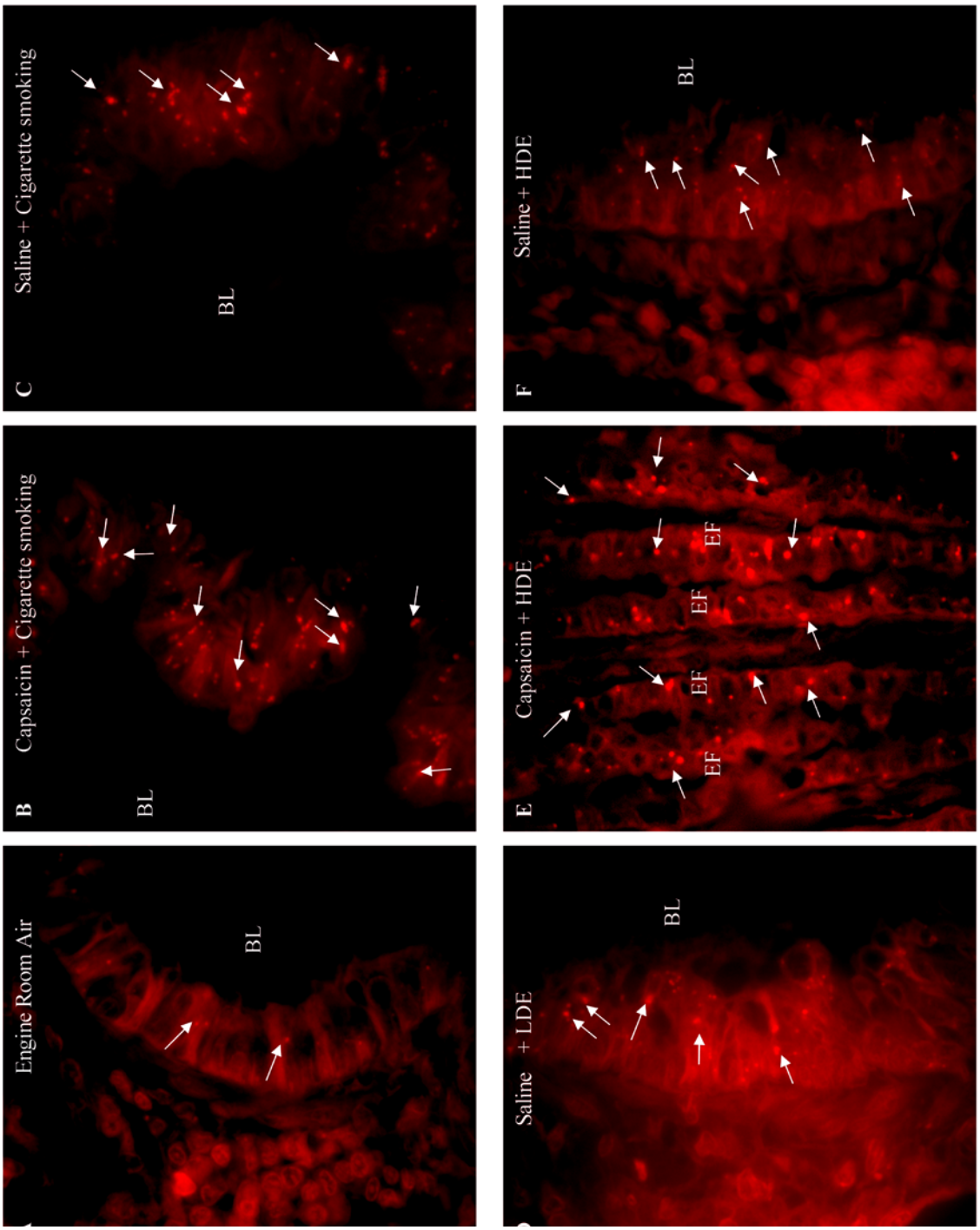

Figure 13. Immunohistochemical staining of NK1 receptor in lung tissue after exposure. NK1 receptor-like immunoreactivity, using Texas red-labeled secondary antibody, appeared as punctate dots (arrows) on the airway epithelium, resembling the pattern of synaptic varicosities (***A–F***). Note the qualitative difference in the capsaicin-HDE rats: the immunoreacting receptor sites are larger and have a higher intensity than in the other groups. BL = bronchial lumen; EF = epithelial fold.

The specific pattern of immunoreactivity allowed us to quantitate the number of such sites per unit basement membrane length (Figure 14). The most interesting findings were that both capsaicin-HDE and saline-HDE rats had the same numbers of immunopositive sites as both groups of CS rats. All four groups had about twice as many immunoreactive sites as did LDE rats. The eRA groups were not examined in as much detail and require further analyses, but our current data suggest fewer immunoreactive sites with capsaicin pretreatment.

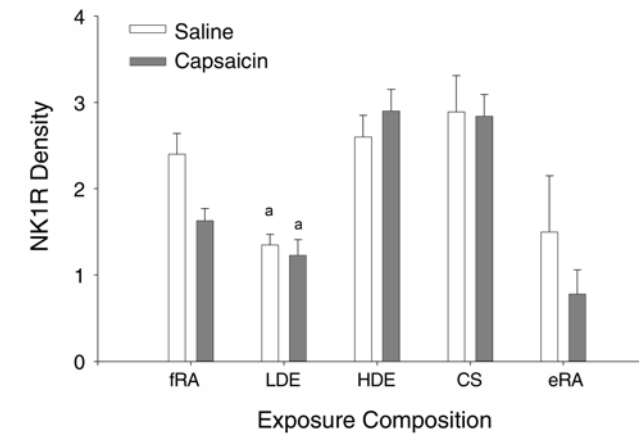

Figure 14. NK1 receptor (NK1R) density in lung tissue after exposure. Data expressed as mean (SEM). [a] $P < 0.05$ compared to saline-fRA rats.

NEP

NEP activity in the lungs of saline rats exposed to either level of DE was lower than in the saline-eRA controls ($P < 0.05$, Figure 15). NEP activity in capsaicin rats exposed to DE followed the same trend. After CS exposure, NEP activity was lower in saline rats but not capsaicin rats. After fRA or eRA exposure, NEP activity was not significantly different between capsaicin and saline groups.

Plasma Extravasation

Plasma extravasation, in both extrapulmonary and intrapulmonary airways, was measured by using ^{99m}Tc-albumin (Figure 16). In saline-DE rats, the levels of plasma extravasation were significantly higher dose-dependently in extrapulmonary ($r = 0.308$, $P = 0.0008$) and intrapulmonary ($r = 0.736$, $P < 0.001$) airways. The levels of plasma extravasation were also higher after exposure to CS. In capsaicin rats, all levels of plasma extravasation followed the same dose-dependent trend as those of the saline animals. Plasma extravasation tended to be greater in capsaicin animals compared with saline animals, but no significant difference was found within each pair with the exception of intrapulmonary measurements of eRA groups.

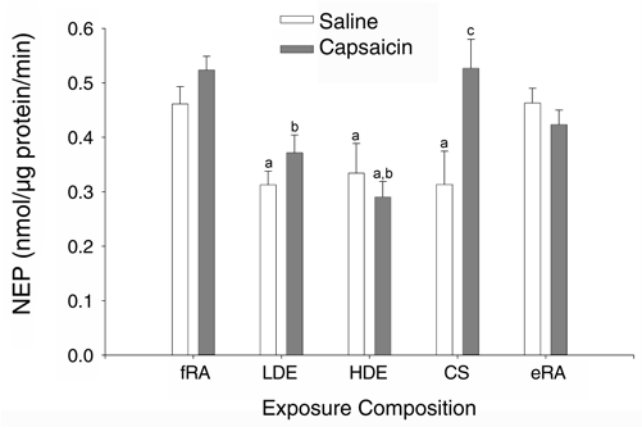

Figure 15. NEP activity in lung tissue after exposure. Data expressed as mean (SEM). [a] $P < 0.05$ compared to saline-fRA rats; [b] $P < 0.05$ compared to capsaicin-fRA rats; [c] $P < 0.05$ compared to saline-CS rats.

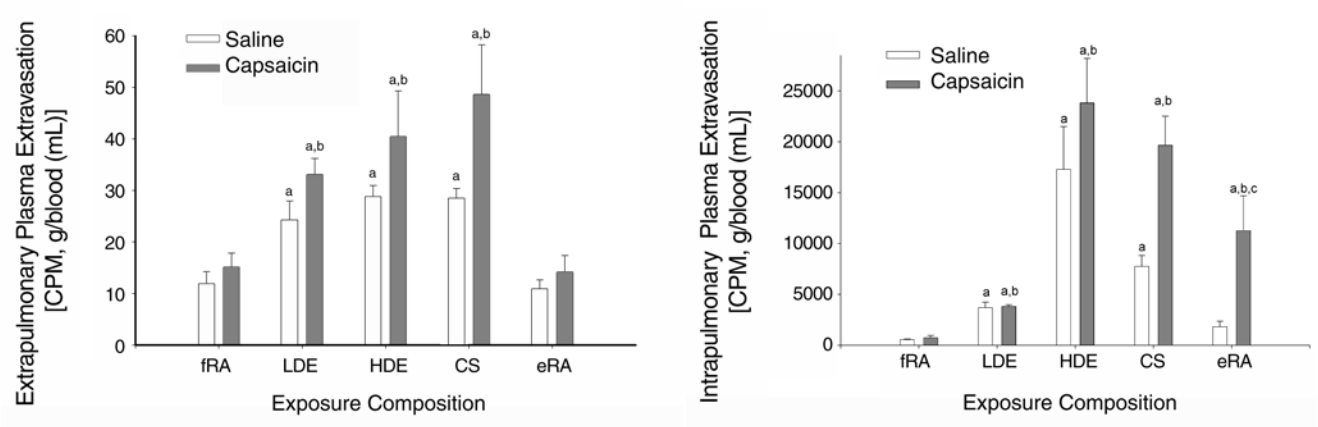

Figure 16. Plasma extravasation in airways after exposure: extrapulmonary airways and intrapulmonary airways. Data expressed as mean (SEM). [a] $P < 0.05$ compared to saline-fRA rats; [b] $P < 0.05$ compared to capsaicin-fRA rats; [c] $P < 0.05$ compared to saline-eRA rats.

Respiratory Permeability

In saline rats, DE exposure induced a significantly higher, dose-dependent respiratory permeability (r = 0.699, $P < 0.0001$) (Figure 17). In capsaicin-DE rats, respiratory permeability was not significantly different from controls (r = 0.23, P = 0.0602). Respiratory permeability was significantly higher in saline and capsaicin rats after exposure to CS compared with their fRA controls.

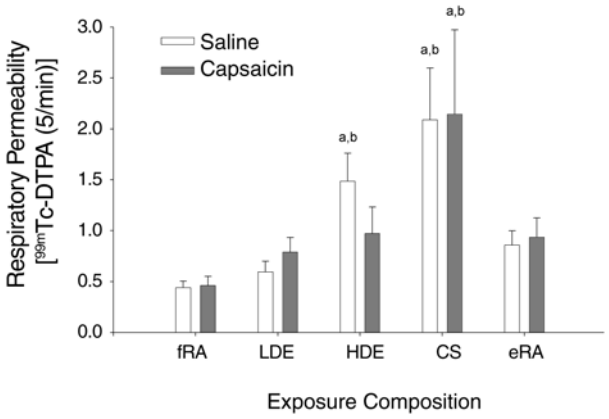

Figure 17. Respiratory permeability after exposure. Data expressed as mean (SEM). [a] $P < 0.05$ compared to saline-fRA rats; [b] $P < 0.05$ compared to capsaicin-fRA rats.

Cytokines

The concentrations of mRNA encoding for IL-1β, IL-6, IL-10, IL-12, and TNF-α in lung tissue relative to GAPDH mRNA were estimated by RT-PCR (Figure 18A–E). In saline and capsaicin rats exposed to LDE or CS, IL-1β mRNA levels were significantly higher than those of fRA controls (Figure 18A). IL-1β mRNA levels were also higher for saline-HDE rats but not for capsaicin-HDE rats. There was no difference in relative mRNA levels of IL-6 and IL-10 after DE or CS exposure (Figure 18B–C). The relative IL-12 mRNA level was no different than fRA controls in saline-DE rats but lower in saline-CS rats (Figure 18D). Relative IL-12 mRNA levels were significantly lower in capsaicin-HDE animals than in saline-fRA, capsaicin-fRA, and saline-HDE animals. TNF-α mRNA level was higher in saline-HDE rats, but not in saline-LDE animals (Figure 18E). In capsaicin rats, however, the relative TNF-α mRNA level was higher after LDE or CS exposure but not after HDE exposure (Figure 18E).

Lung tissue levels for total protein, IL-1β, IL-12, and TNF-α did not change after LDE or HDE exposure compared with controls (Table 11). However, IL-12 was significantly higher among saline animals exposed to CS. Moreover, in the capsaicin-CS group, total protein, IL-1β, and IL-12 were also higher when compared to the corresponding air controls.

Table 11. Total Protein, IL-1β, IL-12, and TNF-α in Lung Tissue of Rats Exposed to DE and CS

Exposure Groups	Total Protein (μg/g)[a]	Cytokines (pg/g)[a]		
		IL-1β	IL-12	TNF-α
fRA				
Saline	56.74 ± 7.95	1471.7 ± 157.0	108.0 ± 17.6	31.6 ± 8.3
Capsaicin	67.04 ± 6.06	1569.0 ± 176.4	108.2 ± 11.8	34.6 ± 7.3
LDE				
Saline	65.54 ± 3.12	1590.2 ± 342.5	122.7 ± 24.3	47.5 ± 11.9
Capsaicin	66.11 ± 6.57	1595.5 ± 306.7	121.5 ± 24.4	35.8 ± 9.0
HDE				
Saline	59.00 ± 6.16	1476.4 ± 222.3	105.8 ± 18.1	29.5 ± 6.5
Capsaicin	72.98 ± 9.73	1379.5 ± 127.9	98.8 ± 6.6	26.3 ± 5.8
CS				
Saline	53.38 ± 12.01	2799.7 ± 432.3	170.2 ± 26.4[b,c]	25.7 ± 5.7
Capsaicin	86.80 ± 6.67[b,d]	4086.5 ± 488.2[c]	219.7 ± 31.6[b,c]	33.5 ± 8.3
eRA				
Saline	61.31 ± 5.69	1575.8 ± 183.6	109.3 ± 13.6	29.6 ± 5.1
Capsaicin	66.79 ± 5.39	1649.8 ± 281.6	101.3 ± 12.4	31.0 ± 7.3

[a] Data expressed as mean ± SEM.

[b] $P < 0.05$ compared to saline-fRA rats.

[c] $P < 0.05$ compared to capsaicin-fRA rats.

[d] $P < 0.05$ compared to saline-CS rats.

Histopathology and Immunohistochemistry

Inflammatory-cell margination was observed along the venular endothelium in the lungs of saline rats exposed to HDE. Diapedesis was evident by perivascular cuffing (Figure 19D–F) with subsequent mononuclear cell migration and dispersal throughout the entire lung parenchyma and alveoli (Figure 18F). Alveolar edema was also observed in these animals (Figure 19F). Likewise, larger numbers of activated alveolar macrophages were observed throughout the lungs of HDE rats compared with other groups (Figure 19A–C). LDE rats had only occasional alveolar macrophages (Figure 19B) as did the fRA controls. These macrophages were easily identified by phagocytosed, small, black DE particles within the cytoplasm (Figure 19A, C). Surprisingly, several similar macrophages, although in small numbers, were also observed in saline-eRA control rats. After capsaicin and HDE exposure, half as many particle-laden alveolar macrophages were observed (45.1 cells per ×40 microscope field ± 7.7 SEM vs 18.9 ± 1.2; $P = 0.011$). There was no notable influx of polymorphonuclear leukocytes (PMNs) or eosinophils. In addition, HDE rats had an increased number of mast cells (staining purple with toluidine blue), mostly oriented toward thin-walled vessels and airway smooth muscle (Figure 20; Table 12).

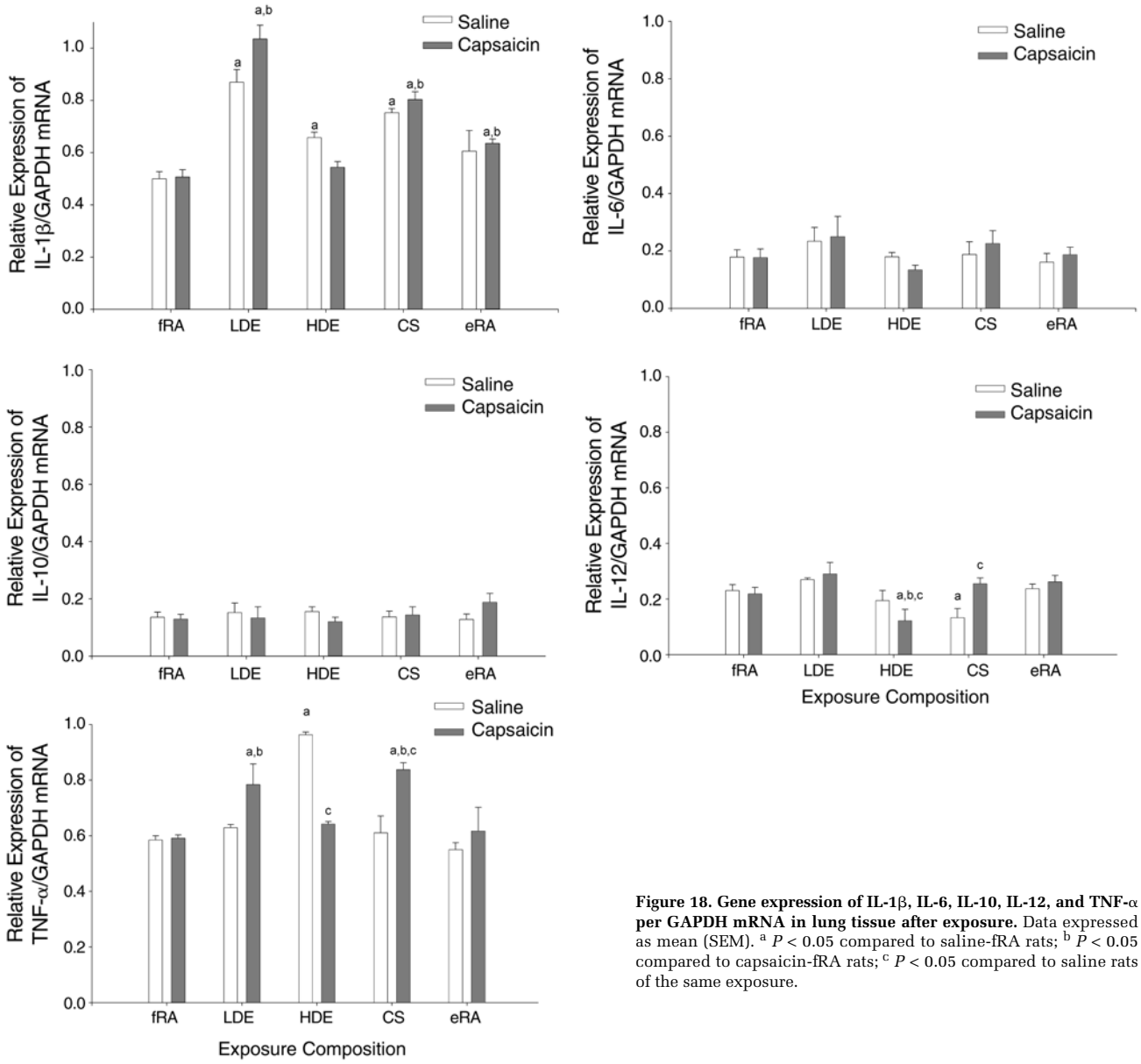

Figure 18. Gene expression of IL-1β, IL-6, IL-10, IL-12, and TNF-α per GAPDH mRNA in lung tissue after exposure. Data expressed as mean (SEM). [a] $P < 0.05$ compared to saline-fRA rats; [b] $P < 0.05$ compared to capsaicin-fRA rats; [c] $P < 0.05$ compared to saline rats of the same exposure.

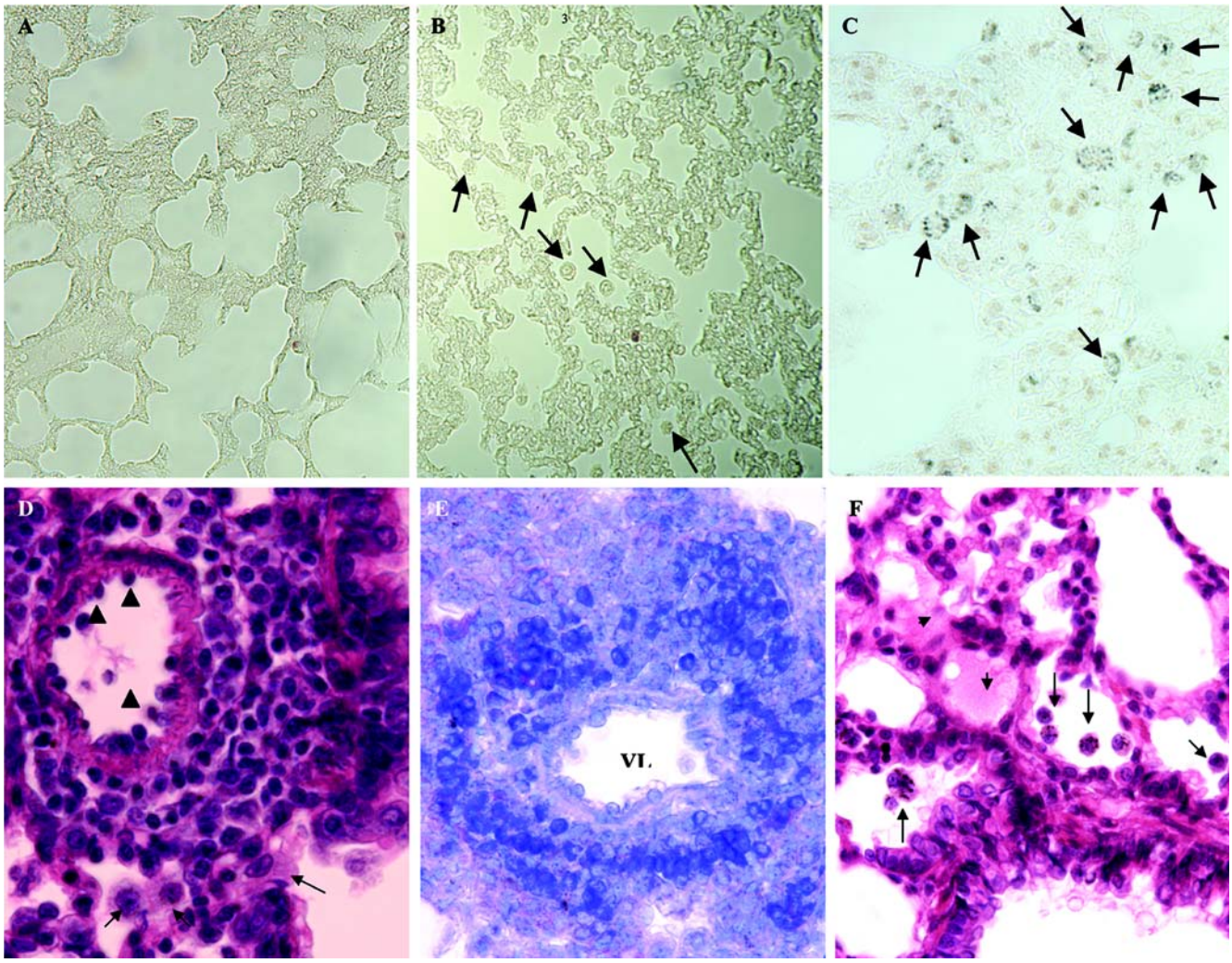

Figure 19. Inflammatory cells in lung tissue. Unstained, dewaxed paraffin sections show no macrophages in alveolar parenchyma after fRA exposure (***A***), very few alveolar macrophages (arrows) after LDE exposure (***B***), and a large number of alveolar macrophages (arrows) after HDE exposure (***C***). Note the accumulation of black DE particles in macrophages of lung after exposure to HDE (***C***). In H&E stained lung section from rats exposed to HDE (***D***), note margination of inflammatory cells (arrowheads) along the lumenal surface of the vascular endothelium and perivascular orientation (cuffing) of inflammatory cells. Activated alveolar macrophages are indicated with arrows. A similar image is shown with toluidine blue staining, which renders inflammatory cells blue (***E***). Lung parenchyma of rat after HDE exposure shows activated macrophages in alveolar spaces (***F***; arrows, H&E). VL = vessel lumen.

Moreover, sloughing of airway epithelial cells was observed in HDE and CS rats (Figure 21).

More C fibers were visible in saline rats than capsaicin rats as demonstrated by the presence of immunoreactivity for the typical markers SP and CGRP (Table 12; Figures 22 and 23). The fibers were localized in airway mucosa and vascular adventitia, and CGRP-immunoreactive fibers were observed in close proximity to alveolar macrophages, other alveolar cells, and possibly the surfactant-producing type II alveolar epithelial cells (Figure 24). Capsaicin pretreatment almost completely depleted SP and CGRP from C fibers, however, rendering these fibers impossible to identify (Table 12). Density of SP-immunoreactive nerve fibers was difficult to assess accurately due to inconsistencies in intensity of the immunoreactivity compounds. There was an impression of lower density in several capsaicin-HDE rats compared with saline-HDE rats (Figure 25D,E), but the finding was not consistent across all animals. The basophils

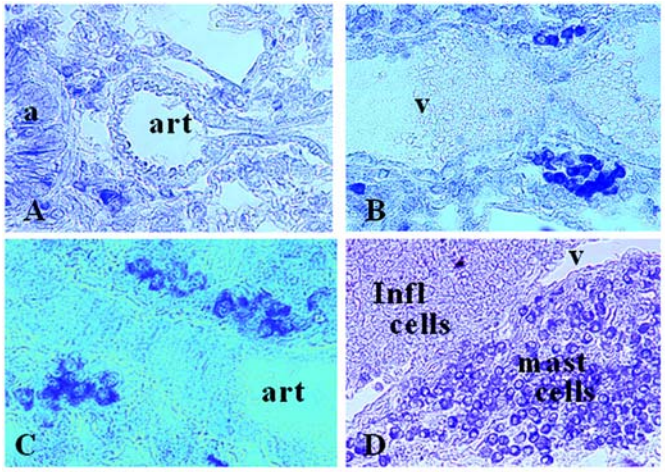

Figure 20. Inflammatory cells and mast cells in lung tissue after exposure. Invasion of young inflammatory cells and mast cells is demonstrated with toluidine blue stain rendering general inflammatory cells blue and mast cells purple due to metachromasia. ***A***. In a capsaicin-eRA rat, a few cells are visible to the left of the artery. ***B***. In saline-LDE rat, note the low level of mast cells on both sides of vein. ***C***. A capsaicin-HDE rat. ***D***. A saline-HDE rat. Note the massive invasion of young inflammatory cells and mast cells. V, vein; art, artery; a, airway.

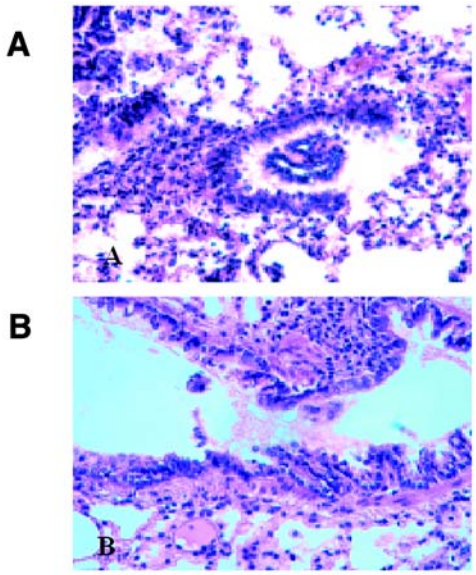

Figure 21. Sloughing of airway epithelial cells after exposure. ***A.*** Lung from saline-HDE rat shows a terminal bronchiole opening into the alveolar parenchyma. A section of folded epithelium in its lumen is lodged peripherally to its site of sloughing. ***B.*** Lung from saline-CS rat shows mild loss of bronchiolar epithelium indicated by epithelial debris in lumen. H&E stain.

Table 12. Number of Cells and C-Fiber Profiles in Lung Tissue of Rats Exposed to DE or CS[a]

Exposure Goups	SP Fibers	CGRP Fibers	Inflammatory Cells[b]	Mast Cells	NEB[c]	NEC[d]
fRA						
Saline	6.5 ± 1.2	7.4 ± 1.1	2.0 ± 1.4	3.6 ± 2.1	0.4 ± 0.4	0.1 ± 0.1
Capsaicin	0.8 ± 0.2	3.0 ± 2.8	10.2 ± 2.1	9.7± 3.4	0.3 ± 0.1	0.1 ± 0
LDE						
Saline	2.1 ± 1.6	8.8 ± 9.6	1.4 ± 0.3	0.1 ± 0.1	0.4 ± 0.3	0.2 ± 0.2
Capsaicin	1.4 ± 1.5	1.3 ± 1.4	0.3 ± 0.2	0.2 ± 0.2	0.3 ± 0.3	0.1 ± 0.2
HDE						
Saline	0.9 ± 0.6	7.3 ± 4.1	47.2 ± 27.1[e]	12.5 ± 6.1[e]	0.4 ± 0.3	0.1 ± 0.2
Capsaicin	0.5 ± 0.6	1.1 ± 1.0	12.5 ± 7.9	2.8 ± 2.5	0.4 ± 0.2	0.2 ± 0.1
CS						
Saline	0.9 ± 0.4	15.0 ± 0.8	ND[f]	ND	0.7 ± 0.1	0.2 ± 0
Capsaicin	0.8 ± 0.6	10.8 ± 0.9	ND	ND	0.5 ± 0.1	0.2 ± 0.1
eRA						
Saline	6.3 ± 0.6	1.4 ± 0.5	1.1 ± 0.4	0.8 ± 0.4	0.4 ± 0.1	0.2 ± 0.1
Capsaicin	0.6 ± 0.5	8.0 ± 0.6	5.5 ± 5.8	6.0 ± 2.8	0.3 ± 0.2	0.1 ± 0.1

[a] Data expressed as mean ± SEM. $N = 3–4$ per group. Based on average number of cell or nerve profiles per 10 to 15 microscopic fields for each rat lung using 40× objective. Inflammatory cells and mast cells were identified with toluidine blue (blue and purple, respectively). CGRP and SP fibers were identified using immunocytochemical techniques.

[b] Macrophages, PMN, and basophils.

[c] NEB = clustered neuroendocrine cells containing CGRP.

[d] NEC = solitary neuroendocrine cells.

[e] $P < 0.05$ compared to saline-fRA rats.

[f] ND = not done.

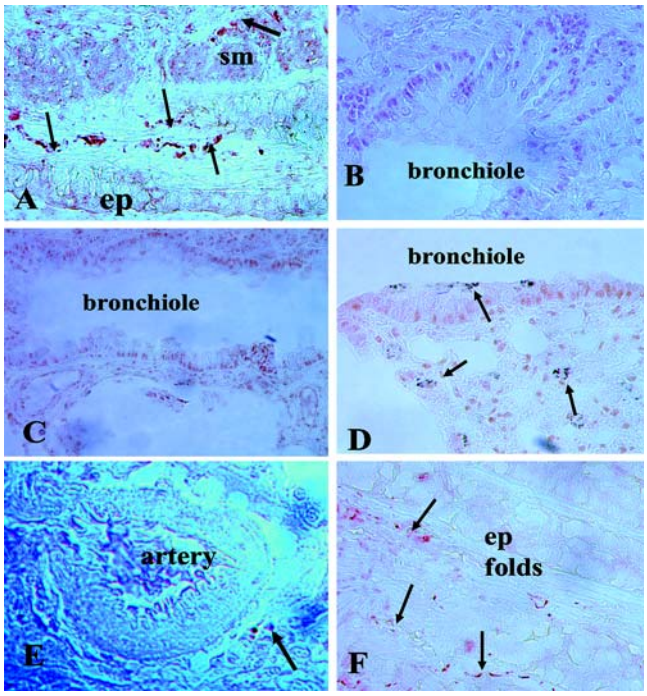

Figure 22. SP-containing C fibers in lung tissue after exposure. Immunoreactivity is visible as a reddish reaction product. ***A.*** Tissue after saline-fRA exposure. Note rich innervation (arrows) in the airway mucosa and smooth muscle (sm). ***B.*** Tissue after capsaicin-HDE exposure. ***C.*** Tissue after saline-LDE exposure. ***D.*** Tissue after saline-HDE exposure. Note how the alveolar macrophages are laden with DE particles (black dots). ***E.*** Tissue after capsaicin-CS. SP immunoreactivity is minimal; note the two brown dots to the right of the artery. ***F.*** Sample taken after saline-CS exposure shows SP fibers. Note the thin appearance compared to fibers in A, suggesting recent sprouting, and the near absence of labeled fibers in B, C, and E. ep, airway epithelium; sm, smooth muscle.

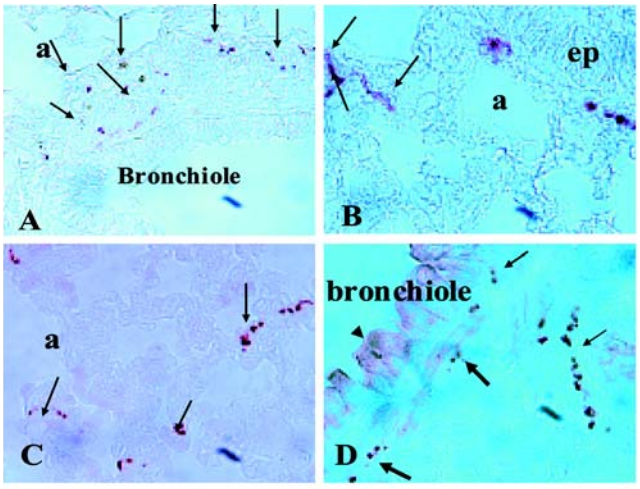

Figure 23. CGRP containing C fibers (reddish brown). Note widespread fibers in airway mucosa **(*A*)** and alveolar parenchyma **(*B*)** after saline-eRA exposure. ***C.*** Also note the liberal distribution of fibers in alveolar septa after saline-LDE. ***D.*** Rich innervation is evident around bronchiolar airways after saline-CS, and immunoreactivity is visible in the airway epithelium, suggesting CS-induced CGRP release and flooding. a, alveolus; ep, airway epithelium.

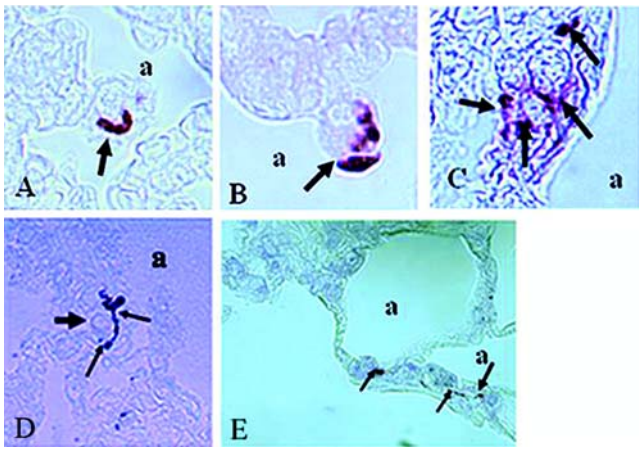

Figure 24. CGRP containing C-fiber innervating lung cells. ***A***. After saline-LDE exposure, part of a CGRP fiber is visible in close proximity to an alveolar macrophage that is free in the alveolar lumen. Note the proximity of the nerve fiber to the macrophage nucleus. ***B***. A similar image is evident in the lung from a saline-CS rat. ***C–E***. CGRP innervation of alveolar cells from rats exposed to saline-eRA (***C***) and saline-LDE (***D***). Two innervated alveolar cells from a saline-HDE rat (***E***) resemble surfactant-producing alveolar type II cells (arrows). a = alveolar lumen.

stained with toluidine blue were frequently in close proximity with individual CGRP-immunopositive nerve fibers (Figure 25C). Moreover, these cells were most likely monocytes in the process of being transformed into activated macrophages. This hypothesis is supported by the unique finding of an alveolar macrophage, free in the alveolar space, showing overlap with a segment of a CGRP-positive nerve fiber in one LDE rat (Figure 25D).

Immunohistochemistry also showed flooding of bronchioles with CGRP, a neuropeptide colocalized with SP in C fibers in a vessel lumen (Figure 26A), most likely remaining from its release from airway epithelial neuroendocrine cells (Figure 26B,D–F) upon capsaicin's effect on vanilloid receptors. Similar sites were noted on vascular medial smooth muscle. Clusters of neuroendocrine cells were found in the bronchi and bronchioles as well as in the alveoli (Figure 26F). Immunoreactive nerve fibers were present in the airway smooth muscle (Figure 26D,E) and in the alveolar parenchyma (Figure 26C). There appeared to be a higher number of these fibers in the alveolar parenchyma of HDE rats.

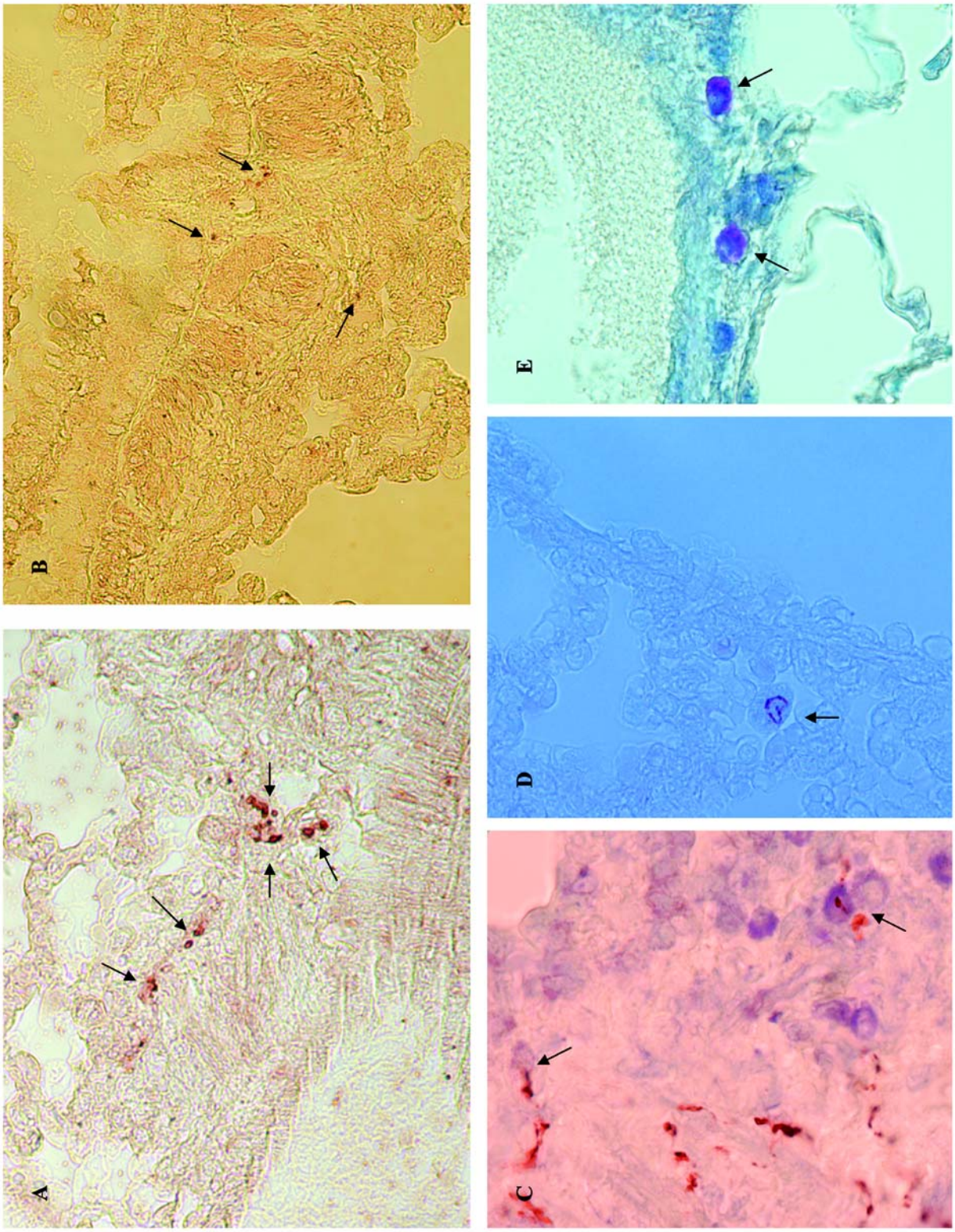

Figure 25. Density of SP immunoreactive fibers and colocated CGRP immunoreactive fibers in lung tissue. An impression of reduced density in several capsaicin-HDE rats (***B***) contrasts with tissue from saline-HDE rats (***A***). ***C***. These basophils stained with toluidine blue were frequently contacted by individual nerve fibers that immunoreacted with antiserum to CGRP. ***D***. An alveolar macrophage from an LDE rat overlays with a segment of CGRP-positive nerve fiber. ***E***. Rats exposed to HDE had an increased number of mast cells (stained purple with TB in this micrograph), mostly oriented toward thin-walled vessels and airway smooth muscle.

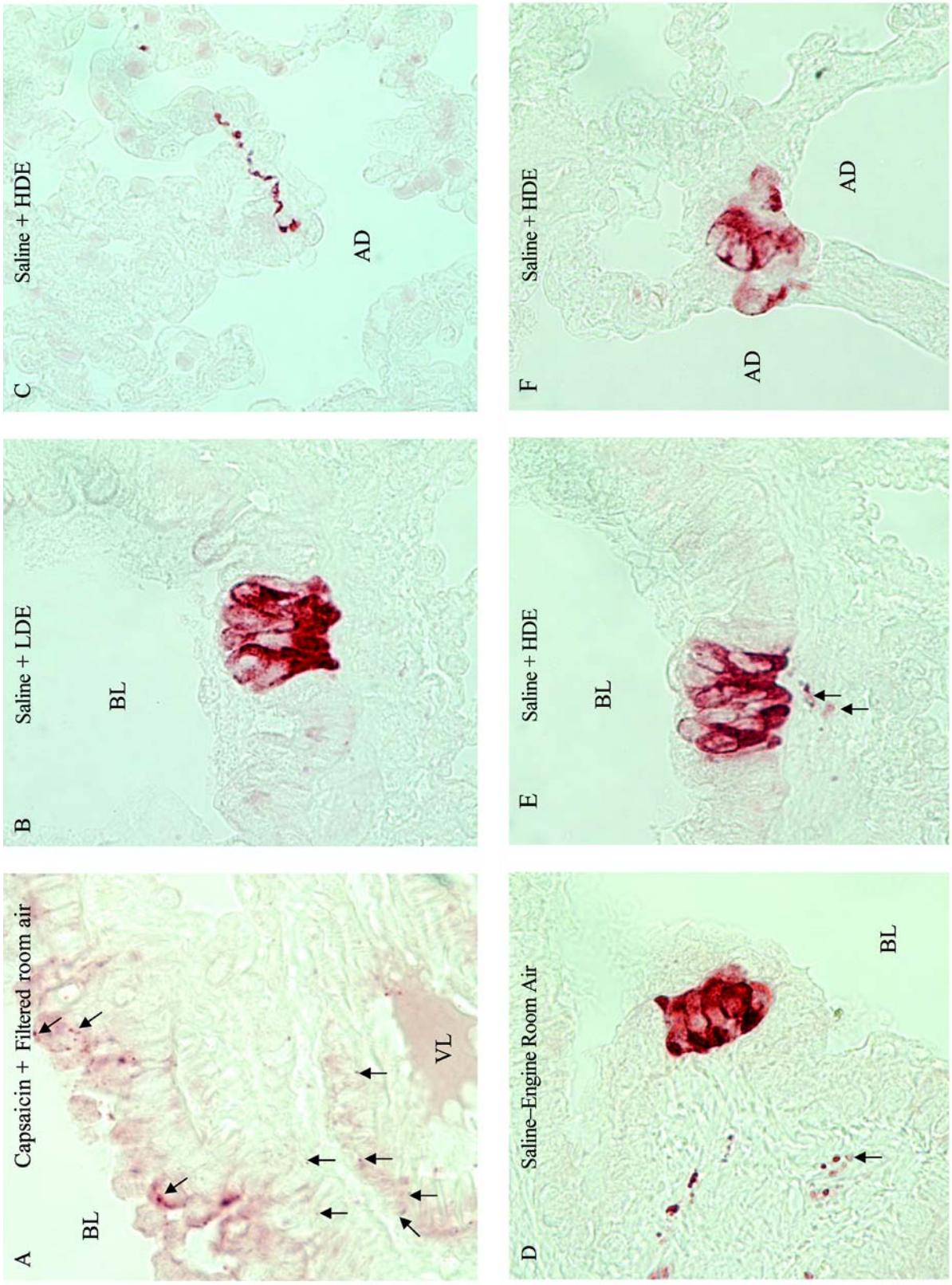

Figure 26. CGRP-like immunoreactivity (brown label) in lung tissue. (***A***) Note CGRP-like immunoreactivity blanketing the bronchiolar epithelium in this specimen from a capsaicin-fRA rat. Arrows indicate immunoreactive spots that resemble receptor sites on the domes of Clara cells in the airway epithelium; these cells were also found on the airway and vascular smooth muscle. Some diffuse immunoreaction is also visible in the vascular lumen (VL). CGRP-positive clustered neuroendocrine cells and associated sensory C fibers (arrows) are visible in the airway mucosa from an LDE rat (***B***), an eRA rat (***D***), and an HDE rat (***E***). Alveolar nerve fiber (***C***) and neuroendocrine cells (***F***) appear to be more numerous in the HDE groups. AD = alveolar duct; BL = bronchiolar lumen; VL = vascular lumen; Vehicle = saline.

DISCUSSION, CONCLUSIONS, AND IMPLICATIONS OF FINDINGS

DE EXPOSURE SYSTEM

Overall, our data demonstrate that the chemical composition of particles depends on engine operating conditions. There was a dramatic shift in the ratio of elemental to organic carbon and in the sulfate ions and trace metals of interest when the engine was operated at different loads and speeds. Similarly, there was a shift in the particle size range but it had no impact on the mass loading. We evaluated one operating condition (mode 6) in this study. The following conclusions were made from the diesel engine/animal exposure system.

- The enhanced full dilution tunnel system that was designed and tested for this study provided a thorough mixing in the RTC. Samples from different sampling locations had basically the same chemical composition.
- Elemental carbon increased linearly as the equivalence ratio (ϕ) increased. Above medium loads, elemental carbon was the dominant component of the DE mass. In contrast, organic carbon decreased linearly as the equivalence ratio increased and was dominant at light loads. The sulfates increased with an increase in the equivalence ratio. Only one operating condition, mode 6, was used for the exposure tests.
- The metal compounds of interest were observed in order from largest to smallest mass loading: calcium, iron, magnesium, lead, and manganese, for the modes studied. The calcium was measured in amounts significantly higher than the other metals of interest. With an increase in the equivalence ratio, all metals of interest exhibited a minimum for mode 7 at 1200 rpm and for mode 2 at 1800 rpm. Higher calcium, iron, and magnesium were observed at higher engine loads.
- At a specific engine speed and injection timing, the median particle size shifted linearly to a larger particle size as the equivalence ratio increased. The median particle number concentration decreased as the equivalence ratio decreased. Again, only one operating condition, mode 6, was used for the animal exposures.
- As the engine speed was changed from 1200 rpm to 1800 rpm, the elemental carbon and sulfates increased significantly, while the increase in the organic carbon was negligible. The metal compounds of interest also increased as the engine speed increased (particularly, iron, calcium, and lead). Both the median particle size and number concentration increased as the engine speed increased. Even though many particle characteristics change with engine operating conditions, only mode 6 was tested.

This system is good for in vivo animal exposure because fresh particles and compositions are the focus of emissions controls. Several characteristics may be compared to approaches used previously: (1) resuspended environmental particles (Vincent et al 1997; Bouthillier et al 1998; Adamson et al 1999; Kodavanti et al 1999); (2) concentrated present-day ambient particles (Sioutas et al 1995; Gordon et al 1998, 1999); (3) model particles created by reconstituting binary or tertiary mixtures (Jakab et al 1996; Kleinman et al 1999); and (4) individual chemical components identified on certain industrial PM, such as transition metals (Dreher et al 1997; Gavett et al 1997). Our diesel engine emission/animal exposure system at the University of Wisconsin gave us continuous measurements of the chemical and physical properties of DE in a real-time mode. Consequently, we did not have to resuspend the DE particles and no aging phenomenon of DE particles occurred that might have changed the observed health effects. Finally, our diesel engine emission/animal exposure system allowed us to change the diesel engine parameters (ie, engine throttle), which our research demonstrates causes significant changes in resulting particle/gas ratio).

Our results showed that the chemical composition, particle number concentrations, and size distributions of PM depended highly on the engine operating conditions. Elemental carbon was dominant at mode 6. Mass and reconstructed mass concentrations (elemental and organic carbons plus sulfates) averaged over the entire test period showed good agreement for LDE and HDE emission tests as well as measurements for elemental carbon, organic carbon, and sulfates for each emission test. The targeted particle concentrations were attained at the exposure chamber.

NEUROGENIC RESPONSES IN LUNGS

Acute exposure to moderately high concentrations of PM has many deleterious effects on the respiratory system, including decreases in pulmonary function, cough, chest tightness, airway inflammation, airway hyperreactivity, increases in bronchial epithelial permeability, and exacerbation of current symptoms of cardiorespiratory disease (Gilmour et al 1996, 2001). These adverse health effects also occur at current EPA guideline concentrations for airborne fine particles. Therefore, it is reasonable to speculate that DE may not only directly deplete the bronchopulmonary C fiber reflex but also may affect sensory neurotransmitter signaling of SP and its primary NK1 receptor. Little is known about neurogenic inflammation relating to DE exposure, however. To determine whether neurogenic inflammation is associated with DE-induced lung inflammation and injury, we

designed a 2 × 3 factorial design (capsaicin vs saline pretreatment to deplete sensory neurotransmitters of C fibers and room air vs 2 concentrations of DE) with a positive control (CS).

Previous studies have shown that exposure of rats to DE, with or without capsaicin pretreatment, causes dose-dependent, neurogenic inflammation as measured by plasma extravasation, lung permeability, and alveolar edema (Bowden et al 1996a; Bozic et al 1996). In the current study, we demonstrated that DE exposure affected sensory neurokinin signaling with alterations of genes and protein levels for SP and NK1 receptor expression and with reduction of NEP activity. This finding indicates the possibility of an unconditional afferent neural response after continuous environmental pollutant exposure.

The transcription rates for β-PPT-I encoding SP and protein expression for SP in lung tissue were examined by real-time quantitative RT-PCR, enzyme immunoassay, and immunohistochemistry. SP is not only contained in a distinct subpopulation of primary afferent nerves characterized by sensitivity to capsaicin but is also expressed in immunoinflammatory and other cells. More recent studies have indicated that non-neural cells may be a major source for neurokinins both in animals and humans. SP is derived from each of four transcripts (ie, α-, β-, γ-, and δ-PPT-I), which are alternately spliced from the β-PPT-I gene, while other related peptides are derived from selected transcripts. This derivation pattern suggests that SP may have a higher probability of being produced whenever the β-PPT-I gene is expressed after depletion. However, we did not find any changes in expression of β-PPT-I mRNA in lung tissue after exposure of saline rats to either DE concentration. Possibly SP is expressed at the posttranscription levels in the lungs. But in this experimental design, we could not rule out that the β-PPT-I gene was activated so early that feedback mechanisms may have masked any change at the end of the 3-week DE exposure series. In contrast, CS exposure for 7 days increased the β-PPT-I mRNA encoding SP in lung tissue. Although differences may arise from different constituents and properties of CS, the exposure regimen may be an important factor for this observation. Interestingly, the saline rats exposed to HDE or CS showed significantly less lung tissue SP. Thus continuous exposure to HDE for 3 weeks or CS for 1 week appeared to have depleted this neurotransmitter during the acute response. If this explanation is appropriate, the stored neurotransmitters in bronchopulmonary C-fiber endings may have been depleted due to repeated challenge.

Because a variety of lung cells are targeted through SP's primary receptor, NK1 receptor, we also examined gene and protein expression of the NK1 receptor in lung tissues by real-time quantitative RT-PCR and immunohistochemistry techniques. NK1 receptor mRNA levels in the lungs were lower when exposed to LDE, whereas no change occurred when exposed to HDE. This finding suggests that exposure of normal rats to DE may activate the NK1 receptor at the gene level with paracrine and/or autocrine signaling mechanisms. Considering that NK1 is part of a pathway in signal transduction within a complex network involving cytokines, hormones, and other inflammatory mediators, this study may partially explain the molecular connection between sensory neurotransmitters and tissue cells in which the NK1 receptor is expressed (Cascieri et al 1995). NK1 receptor gene expression after CS exposure was similar to its expression after LDE exposure. In contrast, an in situ hybridization study reported a twofold higher level of NK1 receptor mRNA in lung samples of smokers compared to nonsmokers (Bai et al 1995). Modulating the process of coupling the NK1 receptor to G-proteins may be a realistic posttranslational mechanism by which its signal transduction can be influenced. Immunohistochemical analysis using a NK1 receptor antibody indicated a qualitative difference in capsaicin rats exposed to HDE: immunoreacting receptor sites were larger and had a higher intensity than the other groups. The key finding was that capsaicin or saline rats exposed to HDE had the same numbers of immunopositive sites as did the capsaicin-CS animals. Consequently, this observation suggests that overexpression of the NK1 receptor could increase sensitivity of the respiratory system to DE exposure (Reynolds et al 1997).

One of the most important findings of this study is that exposure of healthy rats to DE, even at the particle level of 35.3 $\mu g/m^3$, consistently inactivated NEP in lung tissue. The alterations of NEP activity, we speculate, may have been due to any of three causes: inactivation of NEP by oxidants; loss of NEP from cell surfaces through endocytosis and/or proteolytic clipping; decreased NEP transcription through protein kinase C activation. Supporting evidence came from our pathology analysis, which showed slough of epithelial cells in the bronchioles of DE-exposed animals. NEP is known to be a membrane-bound enzyme, located mainly at the surface of airway epithelial cells, but is also present in airway smooth muscle cells, submucosal gland cells, and fibroblasts. Previous research has demonstrated that removal of the airway epithelium substantially increases the airway responses to SP (Lilly et al 1993). In our studies involving acute smoke exposure and 21-aminosteroid, the airway epithelial lining showed conspicuous lesions consistent in their severity to airways subjected to fire smoke (Wang et al 1999). Because of the high concentration of NEP in the epithelium, therefore, it

is not surprising that membrane damage or epithelial sloughing causes substantial loss of NEP and leads to an unconditional sensory response evoked by endogenous SP after DE exposure. Therefore, NEP is critical to modulating the activity of endogenously released SP and hence of neurogenic inflammation in the development of lung injury and dysfunction. On the basis of these observations, the reduction of NEP activity may be regarded as a factor that switches neurokininergic airway responses from their physiological and protective functions to a possible detrimental role that increases and perpetuates airway inflammation. This mechanism may also occur in other particle-induced lung injury and dysfunction, but further studies are needed to assess NEP decrease in this pathogenesis, based on the use of NEP inhibitors, thiorphan and phosphoramidon, and recombinant NEP.

In addition to the SP signaling system, we found CGRP-like immunoreactivity in airway C fibers and neuroendocrine cells. We even noted close proximity of immunoreactive CGRP fibers to several inflammatory cells in a rat treated with HDE. CGRP is a neuropeptide with proposed proinflammatory properties in allergen-sensitized rats (Fischer et al 1996). Lung CGRP is located in sensory C fibers originating from the nodose, trigeminal, and dorsal root ganglia as well as in neuroendocrine cells of the airway epithelium (Keith et al 1991), as observed in this study. In addition to its role in inflammation, CGRP is the most potent peptide vasodilator known to date and provides protection against hypoxic pulmonary hypertension (Tsien et al 1997). In contrast, CGRP's vasodilatory properties can be adverse in the brain where they contribute to migraine headaches (Durham and Russo 2000). CGRP is also involved in the complex process of pain signaling (Salmon et al 2001). CGRP's diverse actions may be ascribed to the existence of several different receptors (Qing et al 2001). CGRP-induced vasodilation together with SP's important role in plasma extravasation (Martling et al 1988) could independently or together promote inflammatory-cell diapedesis and population of pulmonary tissue as observed in this study. Moreover, in the present study, the finding that fewer alveolar macrophages were present in the lung tissue of rats whose CGRP was depleted with capsaicin also supports CGRP's proinflammatory role.

The observation that alveolar parenchyma of HDE rats appeared to have more CGRP fibers than their controls, and perhaps also more alveolar CGRP-containing neuroendocrine cells, supports the concept of vessel dilation and inflammation. Fischer and coworkers (1996) found a threefold to fourfold increase in SP, neurokinin A, and CGRP in airways and a 25% increase in sensory neurons positive for neurokinin A in the nodose ganglia after antigen challenge. They concluded that these changes were associated with allergic airway hyperreactivity. Likewise, Dakhama and colleagues (2002) linked CGRP with airway hyperreactivity. We expect similar effects in the neurokininergic responses to DE exposure. CGRP's role in DE-induced airway inflammation and hyperreactivity is unknown at this time, but its reported role in airway inflammation makes it an important candidate in our study.

While CGRP and SP are colocalized in the sensory (C fiber) afferents and neuritic processes of the airway mucosa (Martling et al 1988), only CGRP is present within the epithelial neuroendocrine cells. These cells are large CGRP factories that account for the majority of CGRP synthesized in the lung. Immunohistochemical evidence of airway flooding with CGRP after capsaicin treatment suggests substantial release from the neuroendocrine cells. Furthermore, the observation of possible CGRP receptor localization and binding on Clara cells of capsaicin rats suggests that CGRP modulates Clara cell secretion. CGRP is reported to exert protective effects on epithelia in several organs including the gastric mucosa. This issue was not a part of the present study, however, and should be followed up separately.

We found evidence of a high number of mast cells in lungs of HDE rats. Mast cell proteases are also known to induce inflammation. This can be accomplished by trypsin and mast cell tryptase cleaving proteinase-activated receptor 2 and thus inducing widespread neurogenic inflammation (Steinhoff et al 2000). This sequence could contribute to the proinflammatory effects of mast cells in inflammatory disease and supports continued attention to mast cells in DE-induced inflammation.

Neurogenic inflammation in airway or lung tissue, related dose-dependently to DE exposure, is characterized by plasma protein extravasation and edema. Depletion of bronchopulmonary C fibers leads to plasma leakage as a result of neurokinins acting on the NK1 receptors situated on the postcapillary venules. Upon depletion, the released neurotransmitters (such as SP and CGRP) may cross-talk through neurokinin receptors to many types of white blood cells in the lung as well as epithelial cells. Then, the proinflammatory chemokines, cytokines, and radicals synthesized by most types of these cells may also be affected. Local lung cells have been shown not only to possess NK1 receptors but also to contain mRNA and protein for SP upon activation by endogenous factors. Expression and release occur in a receptor-mediated fashion because cytokine levels are reduced by pretreatment with pharmacologic receptor antagonists. In this study, significantly higher transcription rates for IL-1β and TNF-α, two critical proinflammatory cytokines, were observed after DE

exposure, indicating that these cytokines were activated at the gene level. We did not observe significant changes of protein expression for most cytokines measured, however, suggesting that these cytokines were not involved at this time. Additional evidence includes inactivity of NEP, which boosts neurogenic inflammation. Histopathology data also indicated that activation of mast cells and alveolar macrophages was associated with SP or CGRP. One possible consequence to the lungs is that an individual may become more susceptible to respiratory infections if exposed to environmental pollutants. Further, such exposure may decrease respiratory function in a person whose airways are already damaged by respiratory diseases (such as asthma and chronic obstructive pulmonary disease [COPD]).

In order to confirm that C fibers are involved in DE-induced neurogenic inflammation, we utilized a model of capsaicin pretreatment in adult rats. In this protocol, capsaicin depleted C fibers rather than obliterated them. Capsaicin induces the release of SP and other neurotransmitters from sensory endings, causing plasma leakage *via* the activation of tachykinin NK1 receptor on endothelial cells (Payan 1989; Otsuka and Yoshioka 1993; Bowden et al 1996b). The plasma leakage, a phenomenon known as *neurogenic inflammation*, has been well characterized in rat airways. Measurements in capsaicin rats followed the same trend as those in saline animals when exposed to the same DE levels. Therefore, it appears that inflammation induced by DE exposure in our study can not be attributed to SP or other neuropeptides from bronchopulmonary C fiber endings from our study. We speculate that the reasons for these results may be as follows.

1. No single time point could be identified that characterized all endpoints. Each individual endpoint followed a specific time-course in response to molecular and cellular events. For example, significantly less SP was detected in lung tissue from HDE rats than from the controls, which may reflect augmented release of SP during exposure followed by degradation. This finding also suggests that, at the early period, NEP activity retained its function. Therefore, data generated from this cross-section study did not identify each significant change in the DE-induced neurogenic responses.
2. We cannot completely rule out the possibility that the animals may have recovered their C-fiber function during the 3-week study. Although utilized frequently in our previous studies, this protocol probably depleted C fibers, rather than obliterated them permanently. Consequently, it is not surprising that capsaicin rats exposed to DE or CS showed the same or slightly greater responses of neurogenic inflammation, respectively, as did those of saline animals. Immunohistochemical evaluation of SP supported this speculation. The density of SP-immunoreactive C fibers was difficult to assess due to inconsistencies in intensity of the immunoreactive compounds. In spite of impressive lower density in several capsaicin-HDE rats compared with saline-HDE rats, individual variability prevented any significant difference between the groups after a 3-week exposure. Therefore, a time-course study using a state-of-the-art method, such as transgenic and knockout animal models, may clarify this point in future studies.

To identify the chemical and physical characteristics of DE associated with neurotoxicity, efforts were made to determine the physical aspects and chemical composition of particles that induced inflammatory changes in this animal species. We speculated that DE-induced neurogenic inflammation might be attributed to the particle mass concentration. In this study, sizes and/or chemical components of the particles did not differ substantially between LDE and HDE. Our results are difficult to compare with previous studies of airborne particles, however, because of variation in the particle composition, particle measurement methods, and health endpoints.

CONCLUSIONS

In summary, using an in-line, real-time, in vivo exposure system with freshly generated DE, we investigated neurogenic inflammatory effects of DE in rats with intact C fibers and those with C fibers depleted by capsaicin pretreatment. Exposure of normal rats to DE caused dose-dependent plasma extravasation, which is utilized frequently as a sensitive endpoint of neurogenic inflammation, in both extrapulmonary and intrapulmonary airways. DE exposure also resulted in consistent inactivity of NEP, an increased rate of proinflammatory cytokine transcription (IL-1β and TNF-α), increased respiratory permeability, and altered histopathology. Moreover, inhalation of these emissions affected molecular neurokininergic mechanisms (from gene regulation to protein processing) for SP and its primary NK1 receptors. On the basis of these observations, a change in SP signaling, overexpression of NK1 receptors, and lower NEP activity appear to be key factors that switch neurogenic pulmonary responses from their physiologic and protective functions to a detrimental role that increases and perpetuates lung injury. The overlapping neurogenic mechanisms in the initiation of DE-induced lung injury are plausible. Consequently, these changes may contribute to DE-associated respiratory disorders.

Capsaicin rats followed the same trend as saline animals when exposed to DE in this study. Plasma extravasation in the airways and lung parenchyma of capsaicin-DE rats was not significantly different from controls, but there was a trend for higher plasma extravasation in the capsaicin-DE

rats. Histopathology evaluation likewise demonstrated slightly more tissue changes (such as edema and alveolar macrophage collection) among capsaicin compared with saline rats after the same level of DE exposure. In summary, our data suggest that neurokininergic mechanisms may be involved in DE-induced inflammatory conditions in the rat lungs. Bronchopulmonary C fibers did not appear to be involved at 3 weeks (although we cannot rule out that the animals recovered their C-fiber function during DE exposure). Consequently, it is not surprising that capsaicin rats showed the same response as saline animals when they were exposed either to DE or CS. At this point, we cannot confirm involvement of C fibers in DE-induced inflammation and injury.

Further studies are needed to clarify the role(s) and mechanism of neurogenic inflammation in the response to DE exposure. First, as the emission composition changes with the engine speed and load, more operating modes among CARB 8 modes should be evaluated. Second, more thorough and systematic experimental designs should follow this initial study. This study only examined an SP signaling profile at one time. A time-course study would be needed to clearly understand involvement of neurogenic inflammation determinants. In addition, intervention studies (using antagonists and gene knockdown or knockout models of NK1 receptors, or inhibitors and antibodies directed against NEP) are needed to confirm these data and further examine the mechanism of neurogenic inflammation. We had originally proposed to conduct time course and intervention studies and are planning to pursue these in the future. Third, the study should be extended to additional neuropeptides (such as CGRP and neurokinin A) in neurons and nonneuronal lung cells that may be involved in DE-induced pathology. Last, whether neurogenic inflammation is involved in a variety of DE-induced adverse effects in the lungs is difficult to determine with this limited cross-section study. Only after extensive systematic studies to clarify the role(s) and mechanism of neurogenic inflammation in DE-induced toxicity could we develop appropriate therapeutic and preventive strategies that might mitigate serious, widespread, and costly health problems associated with DE or other PM exposure.

REFERENCES

Adamson IYR, Vincent R, Bjarnason SG. 1999. Cell injury and interstitial inflammation in rat lung after inhalation of ozone and urban particulates. Am J Respir Cell Mol Biol 20:1067–1072.

Bai TR, Zhou D, Weir T, Walker B, Hegele R, Hayashi S, McKay K, Bondy GP, Fong T. 1995. Substance P (NK1)- and neurokinin A (NK2)-receptor gene expression in inflammatory airway diseases. Am J Physiol Lung Cell Mol Physiol 269:L309–L317.

Bascom R, Bromberg PA, Costa DA, Devlin R, Dockery DW, Frampton MW, Lambert W, Samet JM, Speizer FE, Utell M. 1996. Health effects of outdoor air pollution. Part 1. Committee on the Environmental and Occupational Health Assembly of the American Thoracic Society. Am J Respir Crit Care Med 153:3–50.

Bonham AC, Kott KS, Joad JP. 1996. Sidestream smoke exposure enhances rapidly adapting receptor responses to substance P in young guinea pigs. J Appl Physiol 81:1715–1722.

Bouthillier L, Vincent R, Goegan P, Adamson IYR, Bjarnason S, Stewart M, Guénette J, Potvin M, Kumarathasan P. 1998. Acute effects of inhaled urban particles and ozone: Lung morphology, macrophage activity, and plasma endothelin-1. Am J Pathol 153:1873–1884.

Bowden JJ, Baluk P, Lefevre PM, Schoeb TR, Lindsey JR, McDonald DM. 1996a. Sensory denervation by neonatal capsaicin treatment exacerbates Mycoplasma pulmonis infection in rat airways. Am J Physiol Lung Cell Mol Physiol 270:L393–L403.

Bowden JJ, Baluk P, Lefevre PM, Vigna SR, McDonald DM. 1996b. Substance P (NK1) receptor immunoreactivity on endothelial cells of the rat tracheal mucosa. Am J Physiol 270:L404–L414.

Bozic CR, Lu B, Hopken UE, Gerard C, Gerard NP. 1996. Neurogenic amplification of immune complex inflammation. Science 273:1722–1725.

Cascieri MA, Tung MF, Strader CD. 1995. Molecular characterization of a common binding site for small molecules within the transmembrane domain of G-protein coupled receptors. J Pharmacol Toxicol Methods 33:179–185.

Christoforou CS, Salmon LG, Hannigan MP, Solomon PA, Cass GR. 2000. Trends in fine particle concentration and chemical composition in southern California. J Air Waste Manage Assoc 50:43–53.

Chu HW, Kraft M, Krause JE, Rex MD, Martin RJ. 2000. Substance P and its receptor neurokinin 1 expression in asthmatic airways. J Allergy Clin Immunol 106:713–722.

Dakhama A, Kanehiro A, Mäkelä MJ, Loader JE, Larsen GL, Gelfand EW. 2002. Regulation of airway hyperresponsiveness by calcitonin gene-related peptide in

allergen sensitized and challenged mice. Am J Respir Crit Care Med 165:1137–1144.

Delaunois A, Segura P, Dessy-Doize C, Ansay M, Montano LM, Vargas MH, Gustin P. 1997. Ozone-induced stimulation of pulmonary sympathetic fibers: A protective mechanism against edema. Toxicol Appl Pharmacol 147:71–82.

Dockery DW, Pope CA III. 1994. Acute respiratory effects of particulate air pollution. Annu Rev Public Health 15:107–132.

Dockery DW, Schwartz J, Spengler JD. 1992. Air pollution and daily mortality: Associations with particulates and acid aerosols. Environ Res **59**:362–373.

Dreher KL, Jaskot RH, Lehmann JR, Richards JH, McGee JK, Ghio AJ, Costa DL. 1997. Soluble transition metals mediate residual oil fly ash induced acute lung injury. J Toxicol Environ Health 50:285–305.

Durham PL, Russo AF. 2000. Differential regulation of mitogen-activated protein kinase-responsive genes by the duration of a calcium signal. Mol Endocrinol 14:1570–1582.

Environmental Protection Agency (US). 1998. Revised Ozone and Particulate Matter (PM) National Ambient Air Quality Standards. EPA Air Quality Strategies and Standards Division, Washington DC.

Environmental Protection Agency (US). 1991. National Air Quality and Emissions Trends Report. EPA/450/R-92-001. Office of Air Quality Planning and Standards, Research Triangle Park NC.

Environmental Protection Agency (US). 2001. Control of Emissions of Hazardous Air Pollutants From Mobile Sources; Final Rule. 40 CFR, Parts 80 and 86. Fed Regist 66:17229–17273.

Fischer A, McGregor GP, Saria A, Philippin B, Kummer W. 1996. Induction of tachykinin gene and peptide expression in guinea pig nodose primary afferent neurons by allergic airway inflammation. J Clin Invest 98:2284–2291.

Gavett SH, Madison SL, Dreher KL, Winsett DW, McGee JK, Costa DL. 1997. Metal and sulfate composition of residual oil fly ash determines airway hyperreactivity and lung injury in rats. Environ Res 72:162–172.

Ghio AJ, Kim C, Devlin RB. 2000. Concentrated ambient air particles induce mild pulmonary inflammation in healthy human volunteers. Am J Respir Crit Care Med 162:981–988.

Gilmour MI, Daniels M, McCrillis RC, Winsett D, Selgrade MJK. 2001. Air pollutant-enhanced respiratory disease in experimental animals. Environ Health Perspect 109(Suppl 4):619–622.

Gilmour PS, Brown DM, Lindsay TG, Beswick PH, MacNee W, Donaldson K. 1996. Adverse health effects of PM_{10} particles: Involvement of iron in generation of hydroxyl radical. Occup Environ Med 53:817–822.

Gordon T, Gerber H, Fang CP, Chen LC. 1999. A centrifugal particle concentrator for use in inhalation toxicology. Inhalation Toxicol 11:71–87.

Gordon T, Nadziejko C, Schlesinger R, Chen LC. 1998. Pulmonary and cardiovascular effects of acute exposure to concentrated ambient particulate matter in rats. Toxicol Lett 96–97:285–288.

Gray HA, Cass GR, Huntzicker JJ, Heyerdahl EK, Rau JA. 1986. Characteristics of atmospheric organic and elemental carbon particle concentrations in Los Angeles. Environ Sci Technol 20:580–589.

Hildemann LM, Cass G, Markowski GR. 1989. A dilution stack sampler for collection of organic aerosol emissions: Design, characterization and field tests. Aerosol Sci Technol 10:193–204.

Hislop AA, Wharton J, Allen KM, Polak JM, Haworth SG. 1990. Immunohistochemical localization of peptide-containing nerves in human airways: Age-related changes. Am J Respir Cell Mol Biol 3:191–198.

International Agency for Research on Cancer Working Group. 1980. An evaluation of chemicals and industrial processes associated with cancer in humans based on human and animal data: IARC Monographs volumes 1 to 20. Cancer Res 40:1–12.

Jakab GJ, Clarke RW, Hemenway DR, Longphre MV, Kleeberger SR, Frank R. 1996. Inhalation of acid coated carbon black particles impairs alveolar macrophage phagocytosis. Toxicol Lett 88:243–248.

Jancso N, Jancso-Gabor A, Szolcsanyi J. 1967. Direct evidence for neurogenic inflammation and its prevention by denervation and by pretreatment with capsaicin. Br J Pharmacol 31:138–151.

Jimba M, Skornik WA, Killingsworth CR, Long NC, Brain JD, Shore SA. 1995. Role of C fibers in physiological responses to ozone in rats. J Appl Physiol 78:1757–1763.

Joad JP, Bric JM, Pinkerton KE. 1995. Sidestream smoke effects on lung morphology and C-fibers in young guinea pigs. Toxicol Appl Pharmacol 131:289–296.

Joad JP, Kott KS, Bonham AC. 1997. Nitric oxide contributes to substance P-induced increases in lung rapidly adapting receptor activity in guinea-pigs. J Physiol (London) 503:635–643.

Joos GF, Germonpre PR, Kips JC, Peleman RA, Pauwels RA. 1994. Sensory neuropeptides and the human lower airways: present state and future directions. Eur Respir J 7:1161–1171.

Keith IM, Pelto-Huikko M, Schalling M, Hökfelt T. 1991. Calcitonin gene-related peptide and its mRNA in pulmonary neuroendocrine cells and ganglia. Histochemistry 96:311–315.

Killingsworth CR, Paulauskis JD, Shore SA. 1996. Substance P content and preprotachykinin gene-I mRNA expression in a rat model of chronic bronchitis. Am J Respir Cell Mol Biol 14:334–340.

Killingsworth CR, Shore SA, Alessandrini F, Dey RD, Paulauskis JD. 1997. Rat alveolar macrophages express preprotachykinin gene-I mRNA-encoding tachykinins. Am J Physiol Lung Cell Mol Physiol 273:L1073–L1081.

Kleinman MT, Mautz WJ, Bjarnason S. 1999. Adaptive and non-adaptive responses in rats exposed to ozone, alone and in mixtures, with acidic aerosols. Inhalation Toxicol 11:249–264.

Kodavanti UP, Jackson MC, Ledbetter AD, Richards JR, Gardner SY, Watkinson WP, Campen MJ, Costa DL. 1999. Lung injury from intratracheal and inhalation exposures to residual oil fly ash in a rat model of monocrotaline-induced pulmonary hypertension. J Toxicol Environ Health 57:543–563.

Krause JE, Bu J-Y, Takeda Y, Blount P, Raddatz R, Sachais BS, Chou KB, Takeda J, McCarson K, DiMaggio D. 1993. Structure, expression and second messenger-mediated regulation of the human and rat substance P receptors and their genes. Regul Pept 46:59–66.

Kweon CB, Foster DE, Schauer JJ, Okada S. 2002. Detailed Chemical Composition and Particle Size Assessment of Diesel Engine Exhaust. Society of Automotive Engineers Technical Paper 2002-01-2670. SAE Inc, Warrendale PA. Available from *www.sae.org*.

Kweon CB, Okada S, Bae M, Mieritz M, Schauer JJ, Foster DE. 2003. Effects of Engine Operating Conditions on Organic Compounds in Engine Exhaust of a Heavy-Duty Direct-Injection Diesel Engine. Society of Automotive Engineers Technical Paper 2003-01-0342. SAE Inc, Warrendale PA. Available from *www.sae.org*.

Lilly CM, Drazen JM, Shore SA. 1993. Peptidase modulation of airway effects of neuropeptides. Proc Soc Exp Biol Med 203:388–404.

Long NC, Abraham J, Kobzik L, Weller EA, Murthy GGK, Shore SA. 1999. Respiratory tract inflammation during the induction of chronic bronchitis in rats: Role of C-fibres. Eur Respir J 14:46–56.

Lucchini RE, Springall DR, Chitano P, Fabbri LM, Polak JM, Mapp CE. 1996. In vivo exposure to nitrogen dioxide (NO_2) induces a decrease in calcitonin gene-related peptide (CGRP) and tachykinin immunoreactivity in guinea-pig peripheral airways. Eur Respir J 9:1847–1851.

Lundberg JM. 1995. Tachykinins, sensory nerves, and asthma—An overview. Can J Physiol Pharmacol 73:908–914.

Lundberg JMT, Hokfelt T, Martling CRS, Saria A, Cuello C. 1984. Substance P-immunoreactive sensory nerves in the lower respiratory tract of various mammals including man. Cell Tissue Res 235:251–261.

Malm WC, Sisler JF, Huffman D, Eldred RA, Cahill TA. 1994. Spatial and seasonal trends in particle concentration and optical in the United States. J Geophys Res 99:1347–1370.

Martling C-R, Saria A, Fischer JA, Hökfelt T, Lundberg JM. 1988. Calcitonin gene-related peptide and the lung: Neuronal coexistence with substance P, release by capsaicin, and vasodilatory effect. Regul Pept 20:125–139.

Morrison TB, Weis JJ, Wittwer CT. 1998. Quantification of low-copy transcripts by continuous SYBR Green I monitoring during amplification. Biotechniques 24:954–958, 960, 962.

Nel AE, Diaz-Sanchez D, Li N. 2001. The role of particulate pollutants in pulmonary inflammation and asthma: Evidence for the involvement of organic chemicals and oxidative stress. Curr Opin Pulm Med 7:20–26.

Nikula KJ, Avila KJ, Griffith WC, Mauderly JL. 1997. Lung tissue responses and sites of particle retention differ between rats and cynomolgus monkeys exposed chronically to diesel exhaust and coal dust. Fundam Appl Toxicol 37:37–53.

Nikula KJ, Snipes MB, Barr EB, Griffith WC, Henderson RF, Mauderly JL. 1995. Comparative pulmonary toxicities and carcinogenicities of chronically inhaled diesel exhaust and carbon black in F344 rats. Fundam Appl Toxicol 25:80–94.

Okamoto Y, Shirotori K, Kudo K, Ishikawa K, Ito E, Togawa K, Saito I. 1993. Cytokine expression after the topical administration of substance P to human nasal mucosa: The role of substance P in nasal allergy. J Immunol 151:4391–4398.

Otsuka M, Yoshioka K. 1993. Neurotransmitter functions of mammalian tachykinins. Physiol Rev 73:229–308.

Papandreou CN, Usmani B, Geng Y, Bogenrieder T, Freeman R, Wilk S, Finstad CL, Reuter VE, Powell CT, Scheinberg D, Magill C, Scher HI, Albino AP, Nanus DM. 1998. Neutral endopeptidase 24.11 loss in metastatic human prostate cancer contributes to androgen-independent progression. Nat Med 4:50–57.

Payan DG. 1989. Neuropeptides and inflammation: The role of substance P. Annu Rev Med 40:341–352.

Peters A, Dockery DW, Heinrich J, Wichmann HE. 1997. Short-term effects of particulate air pollution on respiratory morbidity in asthmatic children. Eur Respir J 10:872–879.

Qing X, Svaren J, Keith IM. 2001. mRNA expression of novel CGRP1 receptors and their activity-modifying proteins in hypoxic rat lung. Am J Physiol Lung Cell Mol Physiol 280:L547–L554.

Reynolds PN, Holmes MD, Scicchitano R. 1997. Role of tachykinins in bronchial hyper-responsiveness. Clin Exp Pharmacol Physiol 24:273–280.

Rodger IW, Tousignant C, Young D, Savoie C, Chan CC. 1995. Neurokinin receptors subserving plasma extravasation in guinea pig airways. Can J Physiol Pharmacol 73:927–931.

Salmon AM, Damaj MI, Marubio LM, Epping-Jordan MP, Merlo-Pich E, Changeux JP. 2001. Altered neuroadaptation in opiate dependence and neurogenic inflammatory nociception in alpha CGRP-deficient mice. Nat Neurosci 4:357–358.

Salvi S, Blomberg A, Rudell B, Kelly F, Sandström T, Holgate ST, Frew A. 1999. Acute inflammatory responses in the airways and peripheral blood after short-term exposure to diesel exhaust in healthy human volunteers. Am J Respir Crit Care Med 159:702–709.

Salvi SS, Nordenhall C, Blomberg A, Rudell B, Pourazar J, Kelly FJ, Wilson S, Sandström T, Holgate ST, Frew AJ. 2000. Acute exposure to diesel exhaust increases IL-8 and GRO-α production in healthy human airways. Am J Respir Crit Care Med 161:550–557.

Samet JM, Zeger SL, Dominici F, Curriero F, Coursac I, Dockery DW, Schwartz J, Zanobetti A. 2000. The National Morbidity, Mortality, and Air Pollution Study, Part II: Morbidity and Mortality from Air Pollution in the United States. Research Report 94. Health Effects Institute, Cambridge MA.

Schauer JJ, Kleeman MJ, Cass GR, Simoneit BRT. 1999a. Measurement of emissions from air pollution sources. 1. C_1 through C_{29} organic compounds from meat charbroiling. Environ Sci Technol 33:1566–1577.

Schauer JJ, Kleeman MJ, Cass GR, Simoneit BRT. 1999b. Measurement of emissions from air pollution sources. 2. C_1 through C_{30} organic compounds from medium duty diesel trucks. Environ Sci Technol 33:1578–1587.

Sioutas C, Koutrakis P, Burton RM. 1995. A technique to expose animals to concentrated fine ambient aerosols. Environ Health Perspect 103:172–177.

Smith KR, Veranth JM, Hu AA, Lighty JS, Aust AE. 2000. Interleukin-8 levels in human lung epithelial cells are increased in response to coal fly ash and vary with the bioavailability of iron, as a function of particle size and source of coal. Chem Res Toxicol 13:118–125.

Steinhoff M, Vergnolle N, Young SH, Tognetto M, Amadesi S, Ennes HS, Trevisani M, Hollenberg MD, Wallace JL, Caughey GH, Mitchell SE, Williams LM, Geppetti P, Mayer EA, Bunnett NW. 2000. Agonists of proteinase-activated receptor 2 induce inflammation by a neurogenic mechanism. Nat Med 6:151–158.

Takeyama M, Mori K, Takayama F, Kondo K, Kitagawa K, Fujii N. 1990. Enzyme immunoassay of a substance P-like immunoreactive substance in human plasma and saliva. Chem Pharm Bull (Tokyo) 38:3494–3496.

Terashima T, Wiggs B, English D, Hogg JC, van Eeden SF. 1997. Phagocytosis of small carbon particles (PM_{10}) by alveolar macrophages stimulates the release of polymorphonuclear leukocytes from bone marrow. Am J Respir Crit Care Med 155:1441–1447.

Tomaki M, Ichinose M, Miura M, Hirayama Y, Yamauchi H, Nakajima N, Shirato K. 1995. Elevated substance P content in induced sputum from patients with asthma and

patients with chronic bronchitis. Am J Respir Crit Care Med 151:613–617.

Tsien A, Diaz-Sanchez D, Ma J, Saxon A. 1997. The organic component of diesel exhaust particles and phenanthrene, a major polyaromatic hydrocarbon constituent, enhances IgE production by IgE-secreting EBV-transformed human B cells in vitro. Toxicol Appl Pharmacol 142:256–263.

Utell MJ, Frampton MW, Morrow PE. 1991. Air pollution and asthma: Clinical studies with sulfuric acid aerosols. Allergy Proc 12:385–388.

van der Velden VHJ, Naber BAE, van Hal PTHW, Overbeek SE, Hoogsteden HC, Versnel MA. 1999. Peptidase activities in serum and bronchoalveolar lavage fluid from allergic asthmatics—Comparison with healthy non-smokers and smokers and effects of inhaled glucocorticoids. Clin Exp Allergy 29:813–823.

Veronesi B, Oortgiesen M. 2001. Neurogenic inflammation and particulate matter (PM) air pollutants. Neurotoxicology 22:795–810.

Veronesi B, Oortgiesen M, Carter JD, Devlin RB. 1999. Particulate matter initiates inflammatory cytokine release by activation of capsaicin and acid receptors in a human bronchial epithelial cell line. Toxicol Appl Pharmacol 154:106–115.

Veronesi B, Oortgiesen M, Roy J, Carter JD, Simon SA, Gavett SH. 2000. Vanilloid (capsaicin) receptors influence inflammatory sensitivity in response to particulate matter. Toxicol Appl Pharmacol 169:66–76.

Vincent R, Bjarnason SG, Adamson IYR, Hedgecock C, Kumarathasan P, Guénette J, Potvin M, Goegan P, Bouthillier L. 1997. Acute pulmonary toxicity of urban particulate matter and ozone. Am J Pathol 151:1563–1570.

Wang S, Lantz RC, Robledo RF, Breceda V, Hays AM, Witten ML. 1999. Early alterations of lung injury following acute smoke exposure and 21-aminosteroid treatment. Toxicol Pathol 27:334–341.

Wang S, Sun NN, Zhang J, Watson RR, Witten ML. 2002. Immunomodulatory effects of high dose α-tocopherol acetate on mice subjected to sidestream cigarette smoke. Toxicology 175:235–245.

Witschi H, Joad JP, Pinkerton KE. 1997. The toxicology of environmental tobacco smoke. Annu Rev Pharmacol Toxicol 37:29–52.

Witten ML, Joseph PM, Lantz RC, Lazarus DS, Jung WK, Hales CA. 1992. Chronic sidestream cigarette smoke exposure causes lung injury in rabbits. Indoor Environ 1:341–347.

Wittwer CT, Ririe KM, Andrew RV, David DA, Gundry RA, Balis UJ. 1997. The LightCycler: A microvolume multisample fluorimeter with rapid temperature control. Biotechniques 22:176–181.

World Health Organization. 1996. Diesel Fuel and Exhaust Emissions. WHO Environmental Health Criteria Series 171. WHO, Geneva, Switzerland.

Zheng M, Cass GR, Schauer JJ, Edgerton ES. 2002. Source apportionment of $PM_{2.5}$ in the southeastern United States using solvent-extractable organic compounds as tracers. Environ Sci Technol 36:2361–2371.

ABOUT THE AUTHORS

Mark L Witten is a research professor and director of the Joan B and Donald Diamond Lung Injury Laboratory in the Department of Pediatrics at the University of Arizona College of Medicine, Tucson, Arizona. He received his PhD degree with a double major in physiology and exercise physiology at Indiana University in 1983. Dr Witten has more than 20 years of scientific interest and involvement in the experimental studies of environmental pollutants (including cigarette smoke, acute smoke inhalation, JP-8 jet fuel, and currently DE particulates). He has published over 200 manuscripts, abstracts, and book chapters. As principal investigator, he assumed the overall responsibility for this research project.

Simon S Wong has provided 75% effort to design, execute, and write up the actual studies as well as data analyses of the bioendpoint experiments. Dr Wong received his MD in prevention medicine and MPH in environmental and occupational toxicology from China Medical University, Shenyang, China, in 1982 and 1988, respectively. He has more than 10 years of involvement in epidemiological and animal studies of air pollutants on health in China. Currently, he is an assistant professor in the Department of Pediatrics at the University of Arizona College of Medicine, Tucson, Arizona. His research focus is pulmonary afferent neural pathogenesis of environmental pollutants (such as diesel exhaust and cigarette smoke).

Nina N Sun currently is an assistant research scientist in the Department of Pediatrics at the University of Arizona

College of Medicine, Tucson, Arizona. She has provided 75% effort to be responsible for the molecular biology experiments for this study. Nina received her BD in Biochemistry at Peking University, Beijing, China in 1986. She completed a master's degree in molecular nutrition at the University of Arizona in Tucson in 1988. She was a research associate at the University of Texas Medical Branch in Galveston in 1998 and 1999 concentrating on molecular biology studies. She has more than 16 years of involvement in interdisciplinary research projects from the basic to applied sciences.

Ingegerd M Keith currently is a professor in the School of Veterinary Medicine at the University of Wisconsin-Madison. She received an MS in zoology in 1971 and a Medicine Kandidat degree in the human medicine MD training program in 1976, both at the University of Stockholm, Sweden. She obtained a PhD in cardiovascular research at the University of Wisconsin-Madison in 1980 with an emphasis on human pulmonary pathophysiology. Dr Keith has conducted independent research in her own laboratory over the last 21 years in the areas of pulmonary toxicology, hypertension and lung neuropeptide function. She was principal investigator for all activities at the University of Wisconsin including animal protocol approvals, DE exposures, and neuropeptide research.

Chol-Bum Kweon is a PhD candidate at the Engine Research Center of the University of Wisconsin-Madison under Professor David E Foster. He received his BE and MS in mechanical engineering at Yeungnam University, the Republic of Korea, in 1995 and at University of Wisconsin–Madison in 1999, respectively. While serving as a mechanic in the Korean Army, he gained substantial theoretical and practical experience in diesel engines, transmissions, electronic systems, and chassis. As a research assistant at the Engine Research Center, he has performed a significant number of experiments with small and heavy-duty direct-injection diesel engines, especially in terms of engine combustion, performance, emissions, and fuel composition. His current research is focused specifically on the detailed chemical speciation and sizing of diesel PM for various engine operating conditions and fuel composition and relating these parameters to combustion. For this current project, He designed and installed all the diesel engine hardware systems and performed the diesel engine exposure tests. His responsibility also included engine-related data analyses, postprocessing of particles samples, and writing a segment of the HEI report detailing the diesel engine emission/animal exposure system.

David E Foster is currently a professor of mechanical engineering at the University of Wisconsin in the Engine Research Center. He received his BS and MS in mechanical engineering at University of Wisconsin, and his PhD in mechanical engineering at the Massachusetts Institute of Technology. He has published over 60 technical publications in the Society of Automotive Engineers Transactions, Combustion and Flame, Combustion Science and Technology, and the American Society of Mechanical Engineers. Dr Foster has devoted 10% of his efforts to generating diesel exhaust particles and setting up the diesel engine in-line real-time exposure system in this study.

James J Schauer is currently an assistant professor at the University of Wisconsin in the College of Engineering and Wisconsin State Laboratory of Hygiene. He received a BS in chemical engineering at the Colorado School of Mines, an MS in environmental engineering at the University of California, and a PhD in environmental engineering at the California Institute of Technology. His research interests include development of measurement and analytical techniques to characterize source emissions and ambient pollutant concentrations, design of abatement strategies for regional and indoor air pollution problems, and development of process modifications and technologies for air pollution control. In this project, Dr Schauer was responsible for the diesel exhaust particle analyses.

Duane L Sherrill is currently a research professor and head of the biometrics core of the University of Arizona College of Public Health. He received a BS in mathematics at the Metropolitan State College in 1976 and an MS and PhD in biometrics at the University of Colorado Health Science Center in 1982 and 1987, respectively. His research interests include the development of measurement and analytical techniques for estimating the spatial relationships between lung function and diseases. In this project, Dr Sherrill was responsible for guidance of the statistical analysis.

OTHER PUBLICATIONS RESULTING FROM THIS RESEARCH

Wong SS, Sun NN, Keith I, Kweon CB, Foster DE, Schauer JJ, Witten ML. 2003. Tachykinin substance P signaling involved in diesel exhaust-induced bronchopulmonary neurogenic inflammation in rats. Arch Toxicol 77:638–650.

ABBREVIATIONS AND OTHER TERMS

^{99m}Tc-albumin	technetium-labeled albumin
^{99m}TcDTPA	technetium-labeled diethylenetriamine pentaacetate
AChE	acetylcholinesterase
Ala	alanine
ANOVA	analysis of variance
CARB	California Air Resources Board
cDNA	complementary DNA
CGRP	calcitonin-gene related peptide
CN	cetane number
CS	sidestream cigarette smoke
DE	diesel exhaust
EPA	Environmental Protection Agency (US)
eRA	engine room air
fRA	filtered room air
GAPDH	glyceraldehyde-3-phosphate dehydrogenase
GC-MS	gas chromatography–mass spectrometry
H&E	hematoxylin and eosin
HCl	hydrochloride
HDE	high level of DE (as particle mass)
IL	interleukin
LDE	low level of DE (as particle mass)
mRNA	messenger RNA
M_r	molecular weight
NEP	neutral endopeptidase
NK1	neurokinin-1
NO_2	nitrogen dioxide
PAH	polycyclic aromatic hydrocarbon
PCR	polymerase chain reaction
Phe	phenylalanine
PM	particulate matter
$PM_{2.5}$	PM smaller than 2.5 μm in aerodynamic diameter
PMN	polymorphonuclear leukocytes
β-PPT-I	β-preprotachykinin-I
RNase	ribonuclease
RT	reverse transcriptase
RTC	residence time chamber
SMPS	scanning mobility particle sizer
SO_2	sulfur dioxide
SP	substance P
TNF-α	tumor necrosis factor α
WHO	World Health Organization

CRITIQUE
Health Review Committee

Exposure to air pollution, in the form of gases and particulate matter, has been associated with increased morbidity and mortality in epidemiologic studies (Dockery and Pope 1994; American Thoracic Society 1996; Samet et al 2000; Health Effects Institute 2001) but the underlying mechanisms responsible for these effects are not well understood. Because motor vehicle emissions comprise a significant source of air pollutants, they are an important target for study and potential regulation. Understanding such mechanisms and which components of the pollutant mixture are the most toxic will play an important role in assessing human risk associated with air pollutants and the sources that emit them.

In 1998, HEI issued Request for Preliminary Applications (RFPA*) 98-6, "Health Effects of Air Pollution," inviting proposals from investigators studying the health risks of exposure to air pollution from motor vehicles and other sources, including those using conventional, reformulated, oxygenated, and diesel fuels. In response to RFPA 98-6, Dr Mark Witten and colleagues of the University of Arizona proposed to investigate whether exposing rats to diesel engine emissions would induce neurogenic inflammation in the airways. Neurogenic inflammation is defined by secretion of neuropeptides from C fibers (slow conducting unmyelinated sensory nerve fibers) and nonneural cells, and the resulting leakage of blood plasma into the tissue. Witten and colleagues proposed to measure levels of neuropeptides and other inflammatory markers in lungs of rats exposed to two levels of whole diesel exhaust (particle concentration 65 or 650 $\mu g/m^3$) for 3 weeks. They proposed to use young rats to provide relevance to respiratory responses in children. To investigate the involvement of C fibers, they also proposed to evaluate responses to whole diesel exhaust in rats pretreated with capsaicin, a neurotoxin used to eliminate C fibers. In addition, the investigators would use cigarette smoke as a positive control. The HEI Research Committee funded a one-year study because they thought it would provide interesting data on the pathogenic mechanisms for lung inflammation after exposure to diesel exhaust.†

The intent of this Critique is to aid HEI sponsors and the public by highlighting the strengths of the study, pointing out alternative interpretations of results, and placing the report in scientific perspective.

SCIENTIFIC BACKGROUND

Many epidemiologic studies have shown an association between air pollution and adverse respiratory effects such as lung and airway inflammation, irritation, and functional impairment (Dockery and Pope 1994; American Thoracic Society 1996; Samet et al 2000; Health Effects Institute 2001). Supporting evidence of respiratory inflammatory responses to air pollutant exposure has been provided by controlled exposure studies in animals and humans. Physiologic changes such as influx of macrophages and neutrophils into the lung, and damage to alveolar epithelial cells have been observed after exposure to ozone, nitrogen dioxide (NO_2), and diesel exhaust (Peden 1996; Nikula et al 1997; Krishna et al 1998; US Environmental Protection Agency 2002), but the mechanisms by which air pollutants induce pathobiological effects are not established. One hypothesis suggests that pollutant exposure may induce oxidative stress (Goldsmith et al 1998), which in turn leads to synthesis of proinflammatory cytokines such as tumor necrosis factor α (TNF-α). Other pathways of inflammation have also been suggested. For example, preliminary data from rats exposed to high concentrations of residual oil fly ash or hydrocarbons associated with particles indicate that afferent neural fibers in the airways may also play a role (Robledo and Witten 1999; Veronesi et al 1999).

Neurogenic inflammation was first defined as the plasma extravasation (leakage) from postcapillary venules resulting from stimulation of sensory nerve fibers, such as C fibers of the airways (Jancso et al 1967). The peripheral terminals of sensory C fibers, located within and underneath the epithelial tissue in the vagus and superior laryngeal nerves of the lung and airways, surround airway smooth muscle, submucosal glands and bronchial blood vessels. In response to irritants or inflammatory mediators, C fibers produce neuropeptides, including substance P (SP) and calcitonin gene-related peptide (CGRP). In addition to C fibers, other neuropeptide-producing cells include eosinophils, macrophages, lymphocytes, and dendritic cells (Joos et al 2000). Release of neuropeptides induces cough, airway constriction, increased mucous production and inflammatory effects including recruitment of inflammatory cells and plasma extravasation (Solway and Leff 1991). Acute neurogenic inflammation is thought to be a protective response;

* A list of abbreviations and other terms appears at the end of the Investigators' Report.

† Dr Witten's 1-year study, "Inflammatory Mechanisms with Exposure to Air Pollution Particles," began in June 2001. Total expenditures were $141,028. The draft Investigators' Report from Witten and colleagues was received for review in July 2002. A revised report received in January 2003, was accepted for publication in March 2003. During the review process, the HEI Health Review Committee and the investigators had the opportunity to exchange comments and to clarify issues in the Investigators' Report and in the Review Committee's Critique.

chronic stimulation of C fibers may have detrimental effects, however.

SP stimulates bronchial smooth muscle contraction, production of cytokines interleukin (IL)-1, IL-6 and TNF-α from human monocytes, and activation of mast cells, causing subsequent release of inflammatory mediators and cytokines (Lotz et al 1988). SP is coded for by the β-preprotachykinin gene-I (β-PPT-I), and its actions are mediated through activation of the plasma membrane-bound neurokinin-1 (NK1) receptor (Lundberg 1995). NK1 receptors are found on alveolar macrophages, neutrophils, and epithelial cells in lung tissue (Frossard and Advenier 1991). CGRP is a potent vasodilator thought to induce bronchial vessel dilation both in vivo and in vitro (Reslerova and Loutzenhiser 1998). Unlike SP, CGRP does not appear to promote contraction of bronchial smooth muscle. Airway enzymes, neutral endopeptidase (NEP) in particular, inactivate both neuropeptides (Di Maria et al 1998).

A common method to assess the role of neurogenic inflammation in rodents is to inject capsaicin, a neurotoxic agent derived from peppers, into neonatal animals (Jancso et al 1987). Capsaicin stimulates C-fiber production of neuropeptides at low doses in neonates (around 0.5 mg/kg), but eliminates or depletes C fibers at high doses (50 mg/kg and above). Some degeneration of B-type primary afferent neurons in sensory ganglia may also take place. As adults, neonatally treated rats have fewer sensory ganglia and suffer a depletion of fibers in peripheral and dorsal roots. The degree of fiber depletion and the type of fibers affected depends on the capsaicin dose administered (Jancso et al 1987). Systemic injection of capsaicin in adults is less effective in destroying C fibers and some recovery of sensory fibers may occur over time (Russell and Burchiel 1984).

A neurogenic inflammatory response to cigarette smoke has been well documented (Lei et al 1995; Joad et al 1996). Lundberg and colleagues (1988) reported that the gaseous phase of cigarette smoke (rather than the particulate phase) is responsible for irritation and plasma extravasation. Cigarette smoke has also been shown to decrease activity of NEP and thus could lead to increased levels of SP. An even greater decrease in NEP was observed when capsaicin treatment preceded cigarette smoke exposure (Kuo and Lu 1995). C-fiber stimulation by cigarette smoke exposure may also contribute to allergen-evoked asthma by increasing airway hypersensitivity. These effects were not observed in capsaicin-treated rats with depleted C fibers (Lundberg et al 1991).

Studies using controlled exposure to air pollutant gases or mixtures have provided evidence that neurogenic inflammation can contribute to the inflammatory response to inhaled irritants. Lai and Kou (1998) demonstrated C-fiber sensitivity to the gaseous phase of wood smoke. Killingsworth and colleagues (1996) found the SP content in the tracheas of rats exposed to sulfur dioxide to be three times that of the controls. In humans, short-term exposure to ozone caused epithelial shedding and increased release of SP into the airways (Krishna et al 1997). In addition, C-fiber sensitivity to NO_2, toluene diisocyanate, sulfur dioxide (SO_2) and ammonium has been shown (Mapp et al 1990; Lucchini et al 1996; Wang et al 1996).

More recently, evidence has emerged indicating that particulate matter may also contribute to neurogenic inflammation. Veronesi and colleagues (1999) observed an increase in inflammatory cytokines in bronchial epithelial cells exposed to residual oil fly ash in vitro. This effect was not seen in capsaicin-pretreated cells exposed to residual oil fly ash (Veronesi et al 1999). In addition, increased levels of the inflammatory cytokine IL-6 have been observed in mice exposed to residual oil fly ash via intratracheal instillation and specifically in those mice with significantly higher levels of capsaicin-sensitive receptors on airway neurons (Veronesi et al 2000).

Witten and colleagues planned to examine neurogenic inflammatory mediators in response to diesel engine emissions, which contain particles as well as semivolatile organic compounds and irritant gases such as NO_2. Repeated exposure to diesel exhaust has been shown to cause airway inflammation (US Environmental Protection Agency 2002) and diesel exhaust particles (delivered to the nose) have been hypothesized to enhance the allergic response in allergic human participants (Diaz-Sanchez et al 1996). Witten and colleagues proposed to study young rats to provide relevance to respiratory responses in children. Children may be more susceptible to the effects of air pollutants, and the growing asthma epidemic in children is a concern (Peden 2002). Because children have a higher number of SP-immunoreactive nerves in the airways (Lilly et al 1993), the possible role of neurogenic inflammation in children's asthma deserves special attention (Hislop et al 1990). Barnes has stated that the role of neurogenic inflammation in airway inflammatory diseases, such as asthma and chronic obstructive pulmonary disease (COPD), is still uncertain because little direct evidence supports the involvement of sensory neuropeptides in human airways (Barnes 2001).

TECHNICAL EVALUATION

APPROACH

Witten and colleagues hypothesized that acute lung and airway inflammatory responses to diesel exhaust exposure are mediated by neuropeptides released from sensory nerves and other nonneural cells. The investigators exposed rats to air or two concentrations of whole diesel exhaust from a heavy duty diesel engine for 3 weeks (4 hours/day, 5 days/week). At the end of the exposure period, they examined biological parameters associated with neurogenic inflammation. One control group remained undisturbed in the animal room and breathed filtered air. Another group of rats breathed ambient air in the engine room. These rats were subject to the same noise and temperature differences as the diesel-exhaust exposed groups. As a positive control, a separate group of rats was exposed to sidestream cigarette smoke (4 hours/day for 7 days). Half of the rats in each exposure group were pretreated with capsaicin, so that biologic responses to diesel exhaust and cigarette smoke could be studied in animals with depleted neuropeptide-producing C fibers.

SPECIFIC AIMS

The investigators pursued the several specific aims in order to determine

1. whether neurogenic inflammation is involved in lung injury after diesel exhaust exposure;
2. whether diesel exhaust exposure changes the genetic expression or protein levels of SP;
3. whether diesel exhaust exposure changes expression of the NK1 receptor; and
4. whether diesel exhaust exposure changes the activity of NEP.

The investigators evaluated additional inflammatory endpoints such as plasma leakage, cytokine production, and general lung pathology.

STUDY DESIGN AND METHODS

Exposure System

The investigators collaborated with Drs David Foster and James Schauer of the University of Wisconsin to set up a diesel engine exposure system. The investigators used a Cummins research engine similar to an early 1990s N14 heavy-duty diesel engine, and commercial Mobil #2 low-sulfur diesel fuel. They modified the system by adding a third dilution tunnel to generate the desired exposure levels. They used a tapered element oscillating microbalance for continual monitoring of the mass of particulate emissions. They used filters at the end of the secondary dilution tunnel residence chamber to collect exhaust samples for analysis of particulate matter mass, composition, number, and size distribution, elemental and organic carbon, sulfate ions, volatile organic compounds, semivolatile organic compounds and trace metals. In preliminary studies, the investigators analyzed emissions from a number of engine operating conditions using the 8-mode California Air Resources Board (CARB) test cycle and low sulfur fuel. They chose mode 6 (a 75% load condition with a speed of 1200 rpm at peak torque) for the animal experiments because it was the most common high load condition used for tests at the University of Wisconsin Engine Research Center during the past several years.

Animal Exposures

Animals were exposed at the University of Wisconsin. Investigators randomly assigned female F344 rats (8–9 weeks old) to treatment groups. Capsaicin (40 mg/kg) or saline was injected intraperitoneally under anesthesia in 6 injections over 2 days. Theophylline (2 mg/kg) and terbutaline (0.2 mg/kg) were administered during capsaicin treatment to treat acute bronchospasm. Subsequently, rats were exposed nose-only to whole diesel exhaust at two concentrations (35 $\mu g/m^3$ or 630 $\mu g/m^3$ particulate matter) for 4 hours/day, 5 days/week, for 3 weeks. There were two control groups: one breathed filtered air in the animal facilities; the other breathed ambient air in the engine room. A separate group of rats was exposed nose-only to sidestream cigarette smoke for 4 hours/day for 7 days at a particulate concentration of 400 $\mu g/m^3$ (yielding an average cumulative exposure of 2.0 mg). The investigators chose this particle concentration because it is within the range of commonly observed indoor levels in smokers' homes or restaurants where smoking is allowed. The investigators chose a 7-day exposure to cigarette smoke because they thought it would be sufficient to observe neurogenic inflammation. Each exposure group included 24 animals (12 capsaicin-treated and 12 saline-treated).

Endpoints Measured

Witten and colleagues analyzed the following inflammatory markers involved in neurogenic inflammation in both saline-treated and capsaicin-treated rats:

- SP: messenger RNA (mRNA) levels were measured in lung tissue homogenate by polymerase chain reaction (PCR), and protein levels in lung tissue were measured using enzyme immunoassay.

- NEP: enzyme activity was measured in lung tissue.
- NK1 receptor: density was measured in lung tissue homogenate by PCR.
- Plasma extravasation (leakage from blood to lung tissue): radioactivity was assessed in lungs 10 minutes after injecting technetium-labeled albumin into the jugular vein of anesthetized animals.
- Respiratory permeability (exchange from gas to blood in the lung): 10 minutes after a radioactive compound was introduced into the trachea of anesthetized animals, clearance was measured after 5 to 7 tidal volumes of air had been flushed into the lungs.
- Cytokines: TNF-α, IL1-β, IL-6, IL-10, and IL-12 protein levels were measured using enzyme-linked immunosorbent assay (ELISA).
- Histopathology: Identification and distribution of C fibers, evidence for CGRP-containing neurons and NK1 receptors, presence of inflammatory cells, and sloughing (dislodging) of epithelial cells was examined in 5-µm lung tissue sections using specific staining methods.

Of 12 rats per group, 6 were analyzed for plasma extravasation and 6 for respiratory permeability. In 6 rats (3 from the plasma extravasation group and 3 from the respiratory permeability group), slices of the diaphragmatic lung lobe and the right side upper lobe were taken for histopathologic and immunohistochemical analysis. The tissue samples were processed histochemically with hematoxylin and eosin for general pathology examination, and toluidine blue for mast cell evaluation. After they blocked nonspecific binding, investigators treated tissue samples with an antiserum specific for CGRP or antibodies specific for NK1 receptor. They then stained the samples with a secondary fluorescent antibody and examined them under a microscope for brightfield and fluorescence. These experiments were performed at the School of Veterinary Medicine at the University of Wisconsin in the laboratory of Dr Ingegerd Keith. The remaining lung tissue from these rats and from the other 6 rats in each group was transported to the University of Arizona and analyzed for gene and protein expression of SP, NK1 receptor, and proinflammatory cytokines.

Statistical Analyses

Based on descriptive statistics and results of the Bartlett test for homogeneity of variance, data were normalized using a $\log_{10}$ transformation. The log normal scale was used to make comparisons of mean endpoints between groups by analysis of variance. Multiple comparisons were made using Bonferroni and the Fisher protected least significant difference tests for corrected significance levels. Pearson correlation coefficients were calculated to determine whether specific endpoints (ie, NEP activity, respiratory permeability and plasma extravasation) showed a dose dependent effect. All tests were two-sided, and $P < 0.05$ was considered significant.

RESULTS AND INTERPRETATION

Exposure System

Dr Witten collaborated with an experienced engineering group at the University of Wisconsin to set up a diesel engine exposure system. Preceding the animal exposures, the investigators evaluated a number of engine operation modes for emissions of gases, metals, and particulate matter. They reported that an increase in the equivalence ratio* coincided with an increase in emission of sulfates and elemental carbon, a decrease in median particle number concentration, and a decrease in organic carbon. Organic carbon dominated at light engine loads, while elemental carbon became the dominant component of diesel particulate matter above medium loads. Higher levels of the trace metals calcium, iron and magnesium were observed at high engine loads. Elemental carbon and sulfate emissions increased with a change in engine speed from 1200 to 1800 rpm. Median particle size and particle concentrations of lead, calcium, and iron increased with increases in engine speed.

In engine mode 6, the engine operating condition used for animal exposure, elemental carbon was the dominant component, while sulfates and organic carbon were present in small amounts (Figure 9 of the Investigators' Report). For the lower concentration of DE (LDE), the averaged particle concentration was 35.3 ± 4.9 µg/m^3, which was substantially lower than the target of 65 µg/m^3. For the higher concentration of DE (HDE), the averaged particle concentration was 632.9 µg/m^3 ± 47.6, close to the target of 650 µg/m^3. Particle number and weighted size distributions for mode 6 are shown in Figure 10 of the Investigators' Report. Trace metal emissions, including sodium, magnesium, manganese, and lead were the same for LDE and HDE exposure conditions, whereas a 50% decrease in other trace metals, such as calcium, iron, and chromium was observed for LDE compared to HDE exposure (Table 7 of the Investigators' Report).

* The *equivalence ratio* is the actual air/fuel ratio divided by the theoretical air/fuel ratio at which perfect combustion would occur (ie, when all fuel would burn using all available oxygen). See Table 3 of the Investigators' Report for equivalence ratios for each CARB mode.

Biological Endpoints

The key findings are shown in the Critique Table. In brief, the investigators observed the following findings in the lungs of saline-treated, diesel exhaust–exposed rats:

- Higher plasma leakage and respiratory permeability than in air-exposed rats.
- Higher levels of alveolar edema, recruitment of inflammatory cells and mast cells; evidence of alveolar macrophages containing diesel particles; evidence of sloughing (cells detaching from airway epithelium).
- Consistently lower NEP activity compared to air-exposed rats.
- SP protein levels were lower in HDE-exposed rats than in air-exposed rats, but β-PPT-I mRNA (ie, gene) levels were not changed.
- NK1 receptor expression was inconsistent. A complicating factor was that the engine room control animals differed from animals kept undisturbed in the animal facilities.
- Higher levels of IL-1β and TNF-α, but not IL-6, IL-10 or IL-12.

In capsaicin-treated rats exposed to diesel exhaust, the investigators found the following differences compared to saline-treated rats exposed to diesel exhaust:

- SP and CGRP were not detectable, indicating depletion or obliteration of C fibers.
- Half the number of observed diesel-laden alveolar macrophages.
- No significant differences in plasma extravasation or levels of SP, NK1 receptor density, and NEP activity.
- A significantly lower level of TNF-α and IL-12 mRNA in HDE-exposed capsaicin-treated rats compared to saline-treated HDE-exposed rats.

The investigators found evidence of neurogenic inflammation in cigarette smoke–exposed rats compared to air-exposed controls, as shown by greater plasma extravasation, higher levels of β-PPT-I mRNA, lower NEP activity, and higher levels of IL-1β mRNA and IL-12 protein. In capsaicin-treated cigarette smoke–exposed rats some of these effects were reversed, for example β-PPT-I mRNA levels and NEP activity were the same as in saline-treated, air-exposed rats. The results were similar to those after HDE exposure, with a trend for larger effects after cigarette smoke exposure.

Critique Table. Key Findings in Lungs of Rats Exposed to Diesel Exhaust or Cigarette Smoke[a]

	Saline Compared to Air[b]			Capsaicin Compared to Saline[c]		
Parameter	LDE	HDE	CS	LDE	HDE	CS
Plasma extravasation	↑	↑	↑	=	=	=
Respiratory permeability	—	↑	↑	=	=	=
SP						
mRNA	—	—	↑	=	=	L*
Protein	—	↓	↓	ND	ND	ND
NK1 Receptor						
mRNA	↓	—	↓	=	=	=
Density	↓	—	—	=	=	=
NEP						
Activity	↓	↓	↓	=	=	H*
IL-1β						
mRNA	↑	↑	↑	=	=	=
Protein	—	—	—	=	=	H
IL-12						
mRNA	—	—	↓	=	L	H*
Protein	—	—	↑	=	=	H
TNF-α						
mRNA	—	↑	—	H	L*	H
Protein	—	—	—	=	=	=
Inflammatory cells[d]	—	↑	ND	=	=	ND
Mast cells	—	↑	ND	=	=	ND

[a] *Exposure concentration:* LDE, 35 μg/m^3; HDE, 650 μg/m^3; and CS, 400 μg/m^3.

[b] *Comparison with air-exposed rats:* — no significant difference; ↑ significantly higher; ↓ significantly lower ($P < 0.05$). ND, not detectable.

[c] *Comparison with saline-treated rats:* = no significant difference; H, significantly higher; L, significantly lower; ($P < 0.05$). ND, not detectable. *Asterisks indicate that capsaicin treatment countered diesel exhaust or cigarette smoke induced inflammation.

[d] Including macrophages, neutrophils, and basophils.

DISCUSSION

The authors are among the first to investigate neurogenic inflammation in the lungs of rats after to diesel exhaust. They employed an online diesel exhaust system to generate exposure conditions relevant to actual human exposure. Witten and colleagues observed some inflammatory responses in the lungs of diesel-exposed saline-treated rats.

Capsaicin-treated rats showed an inflammatory response similar to the saline-treated rats, however, suggesting that C fibers are unlikely to be involved in the inflammatory response after diesel exhaust.

After exposure of rats to both concentrations of diesel exhaust, the authors observed consistently higher levels of plasma extravasation and lower activity of NEP, which breaks down SP. The results for SP and NK1 receptors, key markers of neurogenic inflammation, were less consistent. Specifically, decreased levels of SP observed in this study are in contrast with studies reporting increased levels of SP after exposure to irritants such as SO_2 and ozone (Killingsworth et al 1996; Krishna et al 1997). They are also difficult to reconcile with the lower levels of NEP observed in the current study. The authors' speculation, that increased SP production after diesel exhaust exposure could have been followed by depletion of SP stores and the observed lower levels, seems unlikely. Other possibilities are that the results may have been complicated by neuropeptide release from the airway ganglia (or mast cells or eosinophils) or that the capsaicin treatment in adult rats was less effective compared to neonatal treatment. Dr Witten had originally proposed to treat neonatal rats, which is the more commonly used approach to deplete C fibers. It is possible that the capsaicin treatment in adult rats was not as effective or long-lasting. In addition, adult capsaicin treatment requires anesthesia, which could have interfered with the neuronal phenomena studied.

The absence of detectable SP and the lack of SP and CGRP immunoreactivity in the lungs in the Witten study suggest that C fibers may have been depleted successfully, but differences in biological responses between capsaicin-treated and saline-treated rats were negligible. These results argue against mediation of inflammatory response to diesel exhaust by C fibers. Capsaicin treatment was more effective in preventing the inflammatory responses to cigarette smoke (Critique Table), confirming that C fibers are involved in neurogenic inflammation after exposure to cigarette smoke (Lundberg et al 1991; Kuo and Lu 1995; Joad et al 1996; Bonham et al 2001).

Although lower levels of NEP activity and higher plasma extravasation in response to diesel exhaust exposure suggest the involvement of neurogenic inflammation, other pathways may have contributed as well. For instance, plasma extravasation may also be induced by mast cell mediators (Germonpre et al 1995). In addition, the majority of inflammatory changes in lung tissue observed by Witten and colleagues were difficult to quantify. Limited additional support for an inflammatory response was provided by measurement of cytokine levels. IL-1β mRNA levels increased consistently after diesel exhaust exposure, but TNF-α mRNA levels did not show consistent changes and mRNA or protein levels of IL-6, IL-10, and IL-12 did not change significantly. These results are consistent with findings by Yang and colleagues that rat alveolar macrophages showed increased release of IL-1 but not TNF-α after exposure to diesel exhaust particles (Yang et al 1997). In addition, Veronesi and colleagues (2002) found that exposure of bronchial epithelial cells to diesel exhaust particles did not alter the levels of IL-6, in contrast with cells exposed to other sources of particulate matter. Several oil fly ashes and woodstove emissions did show increased IL-6 levels. The results are in contrast with a study in human volunteers exposed for 2 hours to diesel exhaust at 100 $\mu g/m^3$, which reported increased levels of IL-6 in lung lavage fluid (Holgate et al 2003).

Several other studies investigated neurogenic inflammation in response to ozone, SO_2, hydrogen sulfide or cigarette smoke (Prior et al 1990; Jimba et al 1995; Kuo and Lu 1995; Takebayashi et al 1998; Long et al 1999; Vesely et al 1999). In these studies, capsaicin-treated animals experienced greater inflammatory responses and tissue necrosis than saline-treated animals, suggesting that neuropeptides and related mediators may have a protective effect by limiting tissue damage after air pollutant exposure. The short-term exposures in those studies may have induced initial beneficial effects of neuropeptide release but did not produce the detrimental effects of prolonged stimulation of neurogenic inflammatory pathways. In their study, Witten and colleagues exposed rats for 3 weeks, considerably longer than the exposure periods in the other studies. The investigators speculated that the exposure period was too long to observe the protective effects of neuropeptides. Because they did observe a difference between saline-treated and capsaicin-treated rats exposed to cigarette smoke for 7 days, it remains possible that they might have observed an effect in capsaicin-treated animals exposed to diesel exhaust for a period shorter than 3 weeks. On the other hand, chronic low level exposure to cigarette smoke may contribute to neurogenic inflammation (Mutoh et al 1999).

Whether the particulate or gaseous components of diesel exhaust are involved in the observed inflammatory responses remains to be determined. Rudell and colleagues (1996) exposed human subjects to unfiltered or filtered diesel exhaust, which contained 46% fewer particles. Filtering did not decrease adverse effects on lung function, suggesting that gaseous components may have contributed to the effects. Similarly, Lai and Kou (1998) reported increased C-fiber activity in the lung after exposure to the gaseous phase of wood smoke (with the particles removed). On the other hand, a comprehensive review by Veronesi and Oortgiesen (2001) promoted the role of particulate

matter as a initiator of neurogenic inflammation through activation of capsaicin-sensitive receptors and described a possible mechanism of receptor activation precipitated by particulate surface charge. Both particles and gases likely contribute to the inflammatory responses.

In addition to particle levels, Witten and colleagues reported levels of gaseous pollutants for HDE exposures, including oxides of nitrogen (3.69 ppm), NO_2 (0.1 ppm), carbon monoxide (2.95 ppm) and carbon dioxide (5.19 ppm). Gaseous pollutants such as NO_2 have been shown to affect lung function and inflammation at relatively low concentrations (eg, 2.0 ppm [Devlin et al 1999] and 0.27 ppm [Barck et al 2002]), suggesting that the gases may have contributed to some of the observed effects in the Witten study. Although Witten and colleagues did not describe the composition of sidestream cigarette smoke in their report, other studies employing cigarette smoke reported total suspended particle concentrations of ~100 $\mu g/m^3$, carbon monoxide levels in the range of 6 to 7 ppm, and nicotine levels between 220 and 450 $\mu g/m^3$ (Ji et al 1998; Mutoh et al 1999). The Witten study also investigated several engine operating conditions and their effect on diesel engine exhaust components. They found that changes in engine load and speed produced shifts in the levels of elemental carbon, organic carbon, sulfate and trace metals. Changing engine operating conditions caused a shift in particle size range, while mass loading remained the same. The investigators found some differences in particle composition between the LDE and HDE exposures, but what their contribution may have been to the inflammatory effects remains unclear. Further research will be needed to identify which components of the diesel exhaust mixture may contribute to the inflammatory effects.

SUMMARY

The authors are among the first to investigate neurogenic inflammation in the lungs of rats exposed to whole diesel exhaust. After exposure to both concentrations of diesel exhaust, the authors observed consistently higher levels of plasma leakage and lower activity of the enzyme NEP. Changes in levels of SP and its receptor NK1 were less consistent, however, and few changes were observed in cytokine levels. These results confirm previous findings of mild inflammatory responses after exposure to diesel exhaust.

The role of neurogenic inflammation remains unclear, however. Neurogenic inflammation has been convincingly demonstrated after exposure to ozone, SO_2, hydrogen sulfide, cigarette smoke, and wood smoke. In those studies, inflammatory responses were eliminated after animals had been treated neonatally with capsaicin. In the Witten study, rats were treated with capsaicin as young adults, which caused a complete absence of SP in lung tissue but had little effect on the inflammatory response to diesel exhaust. Thus, the results do not support a role for C fibers in the airway inflammatory response to diesel exhaust. The results of the current study also may have been complicated by neuropeptide release from sources other than C fibers (such as the airway ganglia or mast cells and eosinophils). The investigators did find evidence for neurogenic inflammation after exposure to cigarette smoke, which was, in part, reversed by capsaicin treatment.

When testing emissions at different engine operating conditions, the investigators found that elemental carbon dominated at medium to heavy loads, while organic carbon dominated emissions at lighter loads. Levels of sulfate, calcium, iron, magnesium, and particle numbers differed among operating conditions. They found some differences in particle composition between the lower and higher levels of diesel exhaust during the animal exposures, but their contribution to the inflammatory effects, if any, remains unclear. Additional research will be needed to investigate further the inflammatory mechanisms and the role of C fibers in airway responses to diesel exhaust and to identify which components of the diesel exhaust mixture may contribute to the inflammatory effects.

ACKNOWLEDGMENTS

The Health Review Committee thanks the ad hoc reviewers for their help in evaluating the scientific merit of the Investigators' Report. The Committee is also grateful to Maria Costantini for her oversight of the study, to Annemoon van Erp and Joann Sordillo for their assistance in preparing its Commentary, to Sally Edwards and Mary K Brennan for science editing of the Investigators' Report, and to Melissa R Harke and Jenny Lamont for their roles in publishing this Report.

REFERENCES

American Thoracic Society. 1996. Health effects of outdoor air pollution. Am J Respir Crit Care Med 153:3–50.

Barck C, Sandstrom T, Lundahl J, Hallden G, Svartengren M, Strand V, Rak S, Bylin G. 2002. Ambient level of NO_2 augments the inflammatory response to inhaled allergen in asthmatics. Respir Med 96:907–917.

Barnes PJ. 2001. Neurogenic inflammation in the airways. Respir Physiol 125:145–154.

Bonham AC, Chen CY, Mutoh T, Joad JP. 2001. Lung C-fiber CNS reflex: Role in the respiratory consequences of extended environmental tobacco smoke exposure in young guinea pigs. Environ Health Perspect 109(Suppl 4):573–578.

Devlin RB, Horstman DP, Gerrity TR, Becker S, Madden MC, Biscardi F, Hatch GE, Koren HS. 1999. Inflammatory response in humans exposed to 2.0 ppm nitrogen dioxide. Inhalation Toxicol 11:89–109.

Di Maria GU, Bellofiore S, Geppetti P. 1998. Regulation of airway neurogenic inflammation by neutral endopeptidase. Eur Respir J 12:1454–1462.

Diaz-Sanchez D, Tsien A, Casillas A, Dotson AR, Saxon A. 1996. Enhanced nasal cytokine production in human beings after in vivo challenge with diesel exhaust particles. J Allergy Clin Immunol 98:114–123.

Dockery DW, Pope CA III. 1994. Acute respiratory effects of particulate air pollution. Annu Rev Public Health 15:107–132.

Environmental Protection Agency (US). 2002. Health Assessment Document for Diesel Engine Exhaust. EPA/600/8-90/057F. National Center for Environmental Assessment, Office of Research and Development, Washington DC.

Frossard N, Advenier C. 1991. Tachykinin receptors and the airways. Life Sci 49:1941–1953.

Germonpre PR, Joos GF, Everaert E, Kips JC, Pauwels RA. 1995. Characterization of neurogenic inflammation in the airways of two highly inbred rat strains. Am J Respir Crit Care Med 152:1796–1804.

Goldsmith CA, Imrich A, Danaee H, Ning YY, Kobzik L. 1998. Analysis of air pollution particulate-mediated oxidant stress in alveolar macrophages. J Toxicol Environ Health A 54:529–545.

Health Effects Institute. 2001. Airborne Particles and Health: HEI Epidemiologic Evidence. HEI Perspectives. Health Effects Institute, Cambridge MA.

Hislop AA, Wharton J, Allen KM, Polak JM, Haworth SG. 1990. Immunohistochemical localization of peptide-containing nerves in human airways: Age-related changes. Am J Respir Cell Mol Biol 3:191–198.

Holgate ST, Sandström T, Frew AJ, Stenfors N, Nördenhall C, Salvi S, Blomberg A, Helleday R, Södenberg M. 2003. Part I: Healthy and asthmatic subjects exposed to diesel exhaust. In: Health Effects of Acute Exposure to Air Pollution. Research Report 112. Health Effects Institute, Boston MA.

Jancso G, Kiraly E, Such G, Joo F, Nagy A. 1987. Neurotoxic effect of capsaicin in mammals. Acta Physiol Hung 69:295–313.

Jancso N, Jancso-Gabor A, Szolcsanyi J. 1967. Direct evidence for neurogenic inflammation and its prevention by denervation and by pretreatment with capsaicin. Br J Pharmacol 31:138–151.

Ji CM, Royce FH, Truong U, Plopper CG, Singh G, Pinkerton KE. 1998. Maternal exposure to environmental tobacco smoke alters Clara cell secretory protein expression in fetal rat lung. Am J Physiol Lung Cell Mol Physiol 275:L870–L876.

Jimba M, Skornik WA, Killingsworth CR, Long NC, Brain JD, Shore SA. 1995. Role of C fibers in physiological responses to ozone in rats. J Appl Physiol 78:1757–1763.

Joad JP, Avadhanam KP, Watt KC, Kott KS, Bric JM, Pinkerton KE. 1996. Effects of extended sidestream smoke exposure on components of the C-fiber axon reflex. Toxicology 112:195–203.

Joos GF, Germonpre PR, Pauwels RA. 2000. Role of tachykinins in asthma. Allergy 55:321–337.

Killingsworth CR, Paulauskis JD, Shore SA. 1996. Substance P content and preprotachykinin gene-I mRNA expression in a rat model of chronic bronchitis. Am J Respir Cell Mol Biol 14:334–340.

Krishna MT, Chauhan AJ, Frew AJ, Holgate ST. 1998. Toxicological mechanisms underlying oxidant pollutant-induced airway injury. Rev Environ Health 13:59–71.

Krishna MT, Springall D, Meng QH, Withers N, Macleod D, Biscione G, Frew A, Polak J, Holgate S. 1997. Effects of ozone on epithelium and sensory nerves in the bronchial mucosa of healthy humans. Am J Respir Crit Care Med 156:943–950.

Kuo HP, Lu LC. 1995. Sensory neuropeptides modulate cigarette smoke-induced decrease in neutral endopeptidase activity in guinea pig airways. Life Sci 57:2187–2196.

Lai CJ, Kou YR. 1998. Stimulation of vagal pulmonary C fibers by inhaled wood smoke in rats. J Appl Physiol 84:30–36.

Lei YH, Barnes PJ, Rogers DF. 1995. Mechanisms and modulation of airway plasma exudation after direct inhalation of cigarette smoke. Am J Respir Crit Care Med 151:1752–1762.

Lilly CM, Drazen JM, Shore SA. 1993. Peptidase modulation of airway effects of neuropeptides. Proc Soc Exp Biol Med 203:388–404.

Long NC, Abraham J, Kobzik L, Weller EA, Murthy GGK, Shore SA. 1999. Respiratory tract inflammation during the

induction of chronic bronchitis in rats: Role of C-fibres. Eur Respir J 14:46–56.

Lotz M, Vaughan JH, Carson DA. 1988. Effect of neuropeptides on production of inflammatory cytokines by human monocytes. Science 241:1218–1221.

Lucchini RE, Springall DR, Chitano P, Fabbri LM, Polak JM, Mapp CE. 1996. In vivo exposure to nitrogen dioxide (NO_2) induces a decrease in calcitonin gene-related peptide (CGRP) and tachykinin immunoreactivity in guinea-pig peripheral airways. Eur Respir J 9:1847–1851.

Lundberg JM. 1995. Tachykinins, sensory nerves, and asthma: An overview. Can J Physiol Pharmacol 73:908–914.

Lundberg JM, Alving K, Karlsson JA, Matran R, Nilsson G. 1991. Sensory neuropeptide involvement in animal models of airway irritation and of allergen-evoked asthma. Am Rev Respir Dis 143:1429–1430; discussion 1430–1431.

Lundberg JM, Martling CR, Lundblad L. 1988. Cigarette smoke-induced irritation in the airways in relation to peptide-containing, capsaicin-sensitive sensory neurons. Klin Wochenschr 66(Suppl 11):151–160.

Mapp CE, Chitano P, Fabbri LM, Patacchini R, Santicioli P, Geppetti P, Maggi CA. 1990. Evidence that toluene diisocyanate activates the efferent function of capsaicin-sensitive primary afferents. Eur J Pharmacol 180:113–118.

McDonald DM, Mitchell RA, Gabella G, Haskell A. 1988. Neurogenic inflammation in the rat trachea. II. Identity and distribution of nerves mediating the increase in vascular permeability. J Neurocytol 17:605–628.

Mutoh T, Bonham AC, Kott KS, Joad JP. 1999. Chronic exposure to sidestream tobacco smoke augments lung C-fiber responsiveness in young guinea pigs. J Appl Physiol 87:757–768.

Nikula KJ, Avila KJ, Griffith WC, Mauderly JL. 1997. Lung tissue responses and sites of particle retention differ between rats and cynomolgus monkeys exposed chronically to diesel exhaust and coal dust. Fundam Appl Toxicol 37:37–53.

Peden DB. 1996. Effect of air pollution in asthma and respiratory allergy. Otolaryngol Head Neck Surg 114:242–247.

Peden DB. 2002. Influences on the development of allergy and asthma. Toxicology 181–182:323–328.

Prior M, Green F, Lopez A, Balu A, De Sanctis GT, Fick G. 1990. Capsaicin pretreatment modifies hydrogen sulphide-induced pulmonary injury in rats. Toxicol Pathol 18:279–288.

Reslerova M, Loutzenhiser R. 1998. Renal microvascular actions of calcitonin gene-related peptide. Am J Physiol Renal Physiol 274:F1078–F1085.

Robledo RF, Witten ML. 1999. NK1-receptor activation prevents hydrocarbon-induced lung injury in mice. Am J Physiol Lung Cell Mol Physiol 276:L229–L238.

Rudell B, Ledin MC, Hammarstrom U, Stjernberg N, Lundback B, Sandstrom T. 1996. Effects on symptoms and lung function in humans experimentally exposed to diesel exhaust. Occup Environ Med 53:658–662.

Russell LC, Burchiel KJ. 1984. Neurophysiological effects of capsaicin. Brain Res 320:165–176.

Samet JM, Zeger SL, Dominici F, Curriero F, Coursac I, Dockery DW, Schwartz J, Zanobetti A. 2000. The National Morbidity, Mortality, and Air Pollution Study, Part II: Morbidity and Mortality from Air Pollution in the United States. Research Report 94. Health Effects Institute, Cambridge MA.

Solway J, Leff AR. 1991. Sensory neuropeptides and airway function. J Appl Physiol 71:2077–2087.

Takebayashi T, Abraham J, Murthy GGK, Lilly C, Rodger I, Shore SA. 1998. Role of tachykinins in airway responses to ozone in rats. J Appl Physiol 85:442–450.

Veronesi B, de Haar C, Roy J, Oortgiesen M. 2002. Particulate matter inflammation and receptor sensitivity are target cell specific. Inhalation Toxicol 14:159–183.

Veronesi B, Oortgiesen M. 2001. Neurogenic inflammation and particulate matter (PM) air pollutants. Neurotoxicology 22:795–810.

Veronesi B, Oortgiesen M, Carter JD, Devlin RB. 1999. Particulate matter initiates inflammatory cytokine release by activation of capsaicin and acid receptors in a human bronchial epithelial cell line. Toxicol Appl Pharmacol 154:106–115.

Veronesi B, Oortgiesen M, Roy J, Carter JD, Simon SA, Gavett SH. 2000. Vanilloid (capsaicin) receptors influence inflammatory sensitivity in response to particulate matter. Toxicol Appl Pharmacol 169:66–76.

Vesely KR, Hyde DM, Stovall MY, Harkema JR, Green JF, Schelegle ES. 1999. Capsaicin-sensitive C-fiber-mediated protective responses in ozone inhalation in rats. J Appl Physiol 86:951–962.

Wang AL, Blackford TL, Lee LY. 1996. Vagal bronchopulmonary C-fibers and acute ventilatory response to inhaled irritants. Respir Physiol 104:231–239.

Yang HM, Ma JYC, Castranova V, Ma JKH. 1997. Effects of diesel exhaust particles on the release of interleukin-1 and tumor necrosis factor-alpha from rat alveolar macrophages. Exp Lung Res 23:269–284.

RELATED HEI PUBLICATIONS: PARTICULATE MATTER AND DIESEL EXHAUST

Number	Title	Principal Investigator	Date*
Research Reports			
120	Effects of Concentrated Ambient Particles on Normal and Hypersecretory Airways in Rats	JR Harkema	2004
118	Controlled Exposures of Healthy and Asthmatic Volunteers to Concentrated Ambient Particles in Metropolitan Los Angeles	H Gong Jr	2003
117	Peroxides and Macrophages in Toxicity of Fine Particulate Matter	DL Laskin	2003
111	Effect of Concentrated Ambient Particulate Matter on Blood Coagulation Parameters in Rats	C Nadziejko	2002
110	Particle Characteristics Responsible for Effects on Human Lung Epithelial Cells	AE Aust	2002
107	Emissions from Diesel and Gasoline Engines Measured in Highway Tunnels		
	Part I. Real-World Particulate Matter and Gaseous Emissions from Motor Vehicles in a Highway Tunnel	AW Gertler	2002
	Part II. Airborne Carbonyls from Motor Vehicle Emissions in Two Highway Tunnels	D Grosjean	2002
106	Effects of Combined Ozone and Air Pollution Particle Exposure in Mice	L Kobzik	2001
105	Pathogenomic Mechanisms for Particulate Matter Induction of Acute Lung Injury and Inflammation in Mice	GD Leikauf	2001
104	Inhalation Toxicology of Urban Ambient Particulate Matter: Acute Cardiovascular Effects in Rats	R Vincent	2001
96	Acute Pulmonary Effects of Ultrafine Particles in Rats and Mice	G Oberdörster	2000
91	Mechanisms of Morbidity and Mortality from Exposure to Ambient Air Particles	JJ Godleski	2000
76	Characterization of Fuel and Aftertreatment Device Effects on Diesel Emissions	ST Bagley	1996
68	Pulmonary Toxicity of Inhaled Diesel Exhaust and Carbon Black in Chronically Exposed Rats		
	Part I. Neoplastic and Nonneoplastic Lung Lesions	JL Mauderly	1994
	Part II. DNA Damage	K Randerath	1995
	Part III. Examination of Possible Target Genes	SA Belinsky	1995
40	Retention Modeling of Diesel Exhaust Particles in Rats and Humans	CP Yu	1991
33	Markers of Exposure to Diesel Exhaust in Railroad Workers	MB Schenker	1990
Special Reports			
	Research Directions to Improve Estimates of Human Exposure and Risk from Diesel Exhaust		2002
	Diesel Emissions and Lung Cancer: Epidemiology and Quantitative Risk Assessment		1999
	Diesel Exhaust: A Critical Analysis of Emissions, Exposure and Health Effects		1995

Continued

** Reports published since 1990.*
Copies of these reports can be obtained from the Health Effects Institute and many are available at www.healtheffects.org.

RELATED HEI PUBLICATIONS: PARTICULATE MATTER AND DIESEL EXHAUST

Number	Title	Principal Investigator	Date*
HEI Communications			
10	Improving Estimates of Diesel and Other Emissions for Epidemiologic Studies		2003
9	Evaluation of Human Health Risk from Cerium Added to Diesel Fuel		2001
8	The Health Effects of Fine Particles: Key Questions and the 2003 Review (Report of the Joint Meeting of the EC and HEI)		1999
7	Diesel Workshop: Building a Research Strategy to Improve Risk Assessment		1999
5	Formation and Characterization of Particles: Report of the 1996 HEI Workshop		1996
HEI Research Program Summaries			
	Research on Diesel Exhaust and Other Particles		2003
	Research on Diesel Exhaust		1999
	Research on Particulate Matter		1999
HEI Perspectives			
	Understanding the Health Effects of Components of the Particulate Matter Mix: Progress and Next Steps		2002
	Airborne Particles and Health: HEI Epidemiologic Evidence		2001

** Reports published since 1990.*
Copies of these reports can be obtained from the Health Effects Institute and many are available at www.healtheffects.org.

HEALTH
EFFECTS
INSTITUTE

Charlestown Navy Yard
120 Second Avenue
Boston MA 02129-4533 USA
+1-617-886-9330
www.healtheffects.org

RESEARCH
REPORT

Number 128
January 2005